CHAPTER 4

Electric-Dipole Spin Resonances

E.I. RASHBA

L.D. Landau Institute for Theoretical Physics of the USSR Academy of Sciences
117940 GSP-1 Moscow, ul. Kosygina 2, USSR

and

V.I. SHEKA

Institute of Semiconductors of the Academy of Sciences of the Ukranian SSR
252028 Kiev, prospekt Nauki 45, USSR

Landau Level Spectroscopy
Edited by
G. Landwehr and E.I. Rashba

Contents

1. Introduction

Resonance phenomena, which offer a powerful tool of studying intricate properties of condensed matter, have for a long time been divided into electric and magnetic resonances. Electron cyclotron resonance (CR), for instance, belongs to the class of electric resonances, whereas electron paramagnetic resonance (EPR) belongs to the class of magnetic resonance phenomena. Electric resonances are excited by the electric vector of an electromagnetic wave, and electrons experience a change in their orbital state but not in their spin state.

Naturally, the classification of the motion in terms of the coordinate and spin degrees of freedom, which in fact provides the grounds for such a simplified description, is possible only in the absence of spin–orbit (SO) interaction. The subject of this paper is an electron resonance of a more general type, excited due to SO interaction. The characteristic features of this resonance, called combined resonance (COR), are: (*i*) the electric mechanism of its excitation, and (*ii*) change of the spin quantum state, when the quantum numbers corresponding to the orbital motion either remain unchanged or are changing. In the former case the resonance occurs at the spin frequency of an electron and is called electric-dipole spin resonance (EDSR), or electric-dipole-excited electron-spin resonance (EDE-ESR). In the latter case it occurs at combinational frequencies, that is, linear combinations of orbital and spin frequencies. We shall call this the electric-dipole combinational frequency resonance. If the mechanism of its excitation is not specified, or if the emphasis is on the frequency of the resonance rather than on the mechanism of its excitation, we shall use the terms spin resonance (SR) or combinational frequency resonance (CFR).

At present COR, first predicted by Rashba (1960, 1961), is being experimentally discovered and studied for various crystals with different types of symmetry. It has been observed in 3D systems, i.e. in bulk, in 2D systems (on heterojunctions and inversion layers), in 1D systems (on dislocations) and in 0D systems (on impurity centres). Now COR is regularly used to investigate the band structure of semiconductors. The extensive use of the method is accounted for by: (*i*) the relatively high intensity of COR (which may exceed the EPR intensity by several orders of magnitude), (*ii*) the presence, as a rule, of several COR bands in the spectrum, and (*iii*) the fairly specific angular dependence of their intensity.

Now it is necessary to clarify, first, what the source is of the high COR intensity, and, second, why for more than 15 years after the discovery of EPR by Zavoisky (1945) and its extensive experimental investigation, COR was not observed. It is convenient to start this discussion by taking band electrons as an example.

In the absence of SO interaction, an electron put in a constant homogeneous magnetic field $\boldsymbol{H}$, performs two independent motions associated with orbital and

spin degrees of freedom. The first motion is cyclotron rotation with a frequency

$$\omega_c = eH/m^*c, \tag{1.1}$$

where m^* is the effective mass, and e and c are universal constants. A characteristic spatial scale corresponding to this motion is the magnetic length

$$r_H = (c\hbar/eH)^{1/2}. \tag{1.2}$$

Accordingly, the minimal electric-dipole moment corresponding to a transition between neighbouring quantum states under the influence of an a.c. electric field is $p_c \approx er_H$. The frequency ω_s of spin transitions is determined by the equation $\hbar\omega_s = |g|\mu_B H$, where g is the g-factor of an electron in a crystal and $\mu_B = e\hbar/2m_0c$ is the Bohr magneton, and m_0 is the mass of the electron in a vacuum. Putting $g \sim 2$, we can estimate the magnetic-dipole moment of the transition displayed in EPR as $\mu_s \sim e\lambda\!\!\!^{-}$. Here $\lambda\!\!\!^{-}$ is the Compton electron wavelength: $\lambda\!\!\!^{-} \approx 4 \times 10^{-11}$ cm. Therefore, if the values of $\tilde{E}$ and $\tilde{H}$ (the amplitudes of the electric and magnetic fields, respectively) are comparable, the ratio of the CR and EPR intensities is of the order of $I_{CR}/I_{EPR} \sim (r_H/\lambda\!\!\!^{-})^2$. For typical values of H, $r_H \sim 10^{-5}$–10^{-6} cm. This allows us to estimate the value of the ratio of the intensities; typically, $I_{CR}/I_{EPR} \sim 10^{10}$.

So, CR is many orders of magnitude stronger than EPR. This property is inherent in all electric resonances. For instance, for paraelectric resonance, r_H must be replaced by the characteristic atomic quantity, namely, the Bohr radius $r_B = \hbar^2/m_0e^2 = 0.5 \times 10^{-8}$ cm, and therefore the ratio of the intensities is $I_{PER}/I_{EPR} \sim (r_B/\lambda\!\!\!^{-})^2 \sim 10^4$. Since electric resonances are much stronger than magnetic resonances, one can expect that even weak SO interaction leading to the coupling of orbital and spin motions will cause intensive electric excitation of SR. Besides, for band electrons the coupling of orbital and spin motions makes it possible for the combinational frequencies $\omega = n\omega_c \pm \omega_s$ (where n is an integer) to appear in the spectrum. The intensity of the transition at these frequencies, i.e., the intensity of the electric-dipole CFR, is generally of the same order of magnitude as the EDSR intensity. Jointly they form the COR spectrum*. Usually it is convenient to observe the COR spectrum in cyclotron-resonance inactive (CRI) polarizations, since there is no strong CR background.

Now let us clarify why COR may be absent or, more exactly, very weak. Let us start with a free electron in a vacuum. The Thomas SO interaction energy is

$$\mathscr{H}_{so} = (\mu_B/2m_0c)\boldsymbol{\sigma}(\boldsymbol{E} \times \boldsymbol{p}). \tag{1.3}$$

*Very often only the electric-dipole CFR bands are ascribed to COR. However, we shall use the term COR in the sense defined above, in conformity with the original work (Rashba 1960) and with subsequent reviews (Rashba 1964a, 1979). Thus by COR we understand the entire family of electric-dipole spin resonances.

Here $\boldsymbol{\sigma}$ are Pauli matrices, $\boldsymbol{E}$ is the electric field and $\boldsymbol{p}$ is the momentum operator. If $\boldsymbol{E}$ is regarded as an a.c. electric field $\tilde{\boldsymbol{E}}$ with the frequency ω_s and $\boldsymbol{v} = \boldsymbol{p}/m_0$ is taken as the velocity of the electron, then $\mathscr{H}_{so} = \frac{1}{2}\mu_B \boldsymbol{\sigma}(\boldsymbol{E} \times \boldsymbol{v}/c)$. Comparing this expression with the Zeeman energy $\mu_B H$, and assuming $\tilde{E} = \tilde{H}$, we see that $I_{EDSR}/I_{EPR} \sim (v/c)^2$. In the nonrelativistic limit $(v/c)^2 \ll 1$ and EDSR is much weaker than EPR. This result is absolutely clear since up to the 'Thomas 1/2' the energy $\mathscr{H}_{so}$ coincides with the Zeeman energy in the effective magnetic field $\tilde{H}_{eff} = (v/c)\tilde{E}$ which acts on the electron in the reference system where the electron rests. Therefore the SO interaction is required to be sufficiently strong. In crystals, SO interaction is strong due to the fact that the field E in (1.3) is a static electric field of the crystal lattice which is particularly strong near nuclei and the operator $\boldsymbol{p}$ acts not on the smooth functions of the effective mass approximation (EMA) but on the Bloch functions:

$$\psi_{nk}(\boldsymbol{r}) = u_{nk}(\boldsymbol{r}) \exp(i\boldsymbol{k}\boldsymbol{r}), \tag{1.4}$$

the periodic factor $u_{nk}(\boldsymbol{r})$ rapidly varies near nuclei. As a result, the SO interaction becomes stronger with increasing charges of the nuclei of the atoms constituting the crystal. In typical semiconductors the SO splitting of the valence band is $\Delta \sim 0.1$–1 eV and it may compete with the forbidden gap width E_G. Thus the g-factor and other parameters of the electron are strongly renormalized as compared to the parameters of an electron in a vacuum. For example, the g-factor may change substantially and may have an anomalous sign (Yafet 1963). As a result, the spin of the electron somehow transforms into its 'quasispin'. Then due to the difference between $\mu^* = g\mu_B/2$ and μ_B the EPR intensity varies: at larger values of $|g|$ it may be much higher than for an electron in vacuum. But the COR intensity is determined not by the renormalized value of the g-factor but by specific terms in the EMA Hamiltonian which simultaneously involve the Pauli matrices (quasispin) and the quasimomentum operator $\boldsymbol{k}$ (orbit). The structure of these terms and, consequently, the COR intensity is determined by the symmetry of the crystal. This problem is discussed in section 2 and subsequent sections. On the whole, the higher the symmetry of the group G_k of the wave vector in the point of $\boldsymbol{k}$-space corresponding to the band extremum, and the larger the E_G, the lower the COR intensity. Naturally, the intensity decreases with a decreasing charge of the nucleus.

Despite the aforementioned restrictions the COR intensity for band carriers in many crystals is so high that it is impossible to observe EPR against the background of the COR intensity. However it significantly decreases in cases where electrons become bound in donor states. It follows from the Kramers theorem (see section 10) that in this case the intensity involves the factor $(\hbar\omega_s/\mathscr{E}_I)^2$, where $\mathscr{E}_I$ is the ionization potential of a donor. This factor can be very small if the field $\boldsymbol{H}$ is weak.

Sticking to the subject of this volume, we shall consider only COR of band carriers in the Landau levels and also electrons bound to shallow impurity

centres where $\mathscr{E}_1$ is comparable with $\hbar\omega_c$ and $\hbar\omega_s$. But it should be noted that EDSR is possible also for low-symmetry deep centres. For them, the EDSR intensity is determined not by the band spectrum of the semiconductor but by the structure of the electron shell of an impurity ion and by the local symmetry of the crystal field. On the whole, it is noticeably lower than for band electrons and for large-radius centres. EDSR for small-radius centres was predicted by Bloembergen (1961) and experimentally observed by Ludwig and Ham (1962). The survey by Roitsin (1971) and two monographs by Mims (1976) and by Glinchuk et al. (1981) are devoted to electric effects in the radiospectroscopy of deep centres.

The foregoing arguments shed some light upon why EDSR was not observed and identified experimentally until the conditions of its high intensity had been found theoretically.

The COR mechanism for free carriers we have discussed is totally due to the SO interaction entering in the Hamiltonian for a free carrier in a perfect crystal. According to this approach the presence of impurities or defects, which cause binding of carriers in shallow levels, diminishes the COR intensity. The theory based on this concept was developed in the early sixties and preceded the experiment: its results were summarized in a survey by Rashba (1964a). The diverse experimental data obtained since then are in agreement with the theory, and have permitted a number of new parameters of the energy spectrum of carriers to be found. Later theoretical works were aimed at describing the experimental results quantitatively within the framework of the original concept.

However, there is one other line of thinking in COR physics. Originating from experimental results rather than from theoretical ideas, its essence is the existence of specific COR mechanisms, caused by defects or impurities. As a result, in materials with a high concentration of imperfections, COR may prove to be considerably stronger than in high-quality samples. The paper by Bell (1962) on EDSR in strongly doped n-type InSb was the first to point to the existence of such mechanisms, and the problem was first recognized and formulated by Mel'nikov and Rashba (1971). For the moment, the problem remains somewhat obscure. That is why there is no doubt that future work on COR theory must be concentrated on this problem. One can expect the problem to attract the attention of experimentalists since it opens up new possibilities for studying disordered systems.

In terms of macroscopic electrodynamics, COR belongs to magnetoelectric phenomena, first reported by Curie (1894) and reviewed by O'Dell (1970) for magnetic materials. From the viewpoint of the microscopic mechanism the most significant feature of COR is the strong coupling of electron spins to the a.c. electric field in a broad class of crystals. By now different manifestations of this coupling have been found. This coupling, in particular, is responsible for spin-flip Raman scattering, discussed in chapter 5 by Häfele.

2. Basic formalism of the theory

The COR theory is based on the theory of the band spectrum of an electron in crystals and on the effective mass approximation. These concepts have been thoroughly developed and they were reviewed, for instance, in the paper by Blount (1962) and in the book by Bir and Pikus (1972), which we recommend to the reader.

In practical COR calculations for specific semiconductors one should proceed from the band structure of the semiconductor determined by: (*i*) symmetry properties and, (*ii*) by numerical values of the energy spectrum parameters. For example, for semiconductors with a narrow forbidden gap of the InSb-type it is often convenient to make use of a multiband Kane model (1957). However, (*i*) to elucidate the principal mechanisms of the COR phenomenon and, (*ii*) to do it from the same point of view conformably to different systems, it will be more convenient to use a two-branch (i.e. one-band) model wherever possible. By this term we understand two branches of the energy spectrum differing only in the spin state of an electron (or a hole). These branches of the spectrum in crystals with the inversion centre merge into one band in the entire $\boldsymbol{k}$-space (Elliott 1954) and in crystals without the inversion centre they stick together in a high-symmetry point and split in its vicinity. Numerical parameters of the two-branch model can be expressed via parameters of a more general model (Addendum B).

In the framework of the two-branch model, the most general approach to describe COR in a semiconductor, subjected to external fields (electric and magnetic), is as follows. The Hamiltonian $\mathscr{H}$ for an electron and the operator $\hat{\boldsymbol{r}}$ of its coordinate can be derived by means of the method of invariants (Bir and Pikus 1972) which employs only general symmetry requirements:

$$\mathscr{H} = \mathscr{H}_0 + e\varphi(\hat{\boldsymbol{r}}) + \mathscr{H}_{so}, \tag{2.1}$$

$$\mathscr{H}_{so} = \sum_j \sigma_j f_j(\hat{\boldsymbol{k}}), \tag{2.2}$$

$$\hat{\boldsymbol{r}} = \mathrm{i}\nabla_k + \sum_j \sigma_j X_j(\hat{\boldsymbol{k}}), \tag{2.3}$$

where σ_j are Pauli matrices and $\hat{\boldsymbol{k}}$ is the operator of the magnetic field quasimomentum

$$\hat{\boldsymbol{k}} = -\mathrm{i}\nabla_r - (e/c\hbar)\boldsymbol{A}(\boldsymbol{r}), \tag{2.4}$$

$\boldsymbol{A}(\boldsymbol{r})$ and $\varphi(\boldsymbol{r})$ are the vector and scalar potentials, respectively. The functions f_i and $\boldsymbol{X}_i$ are polynomials over powers of $\hat{k}_j$, being the Cartesian coordinates of the $\hat{\boldsymbol{k}}$ vector. These polynomials are such that $\mathscr{H}$ and $\hat{\boldsymbol{r}}$ possess the necessary transformation properties with respect to G_k, i.e., the group of $\boldsymbol{k}$, the wave vector near which an expansion in powers of k_j is performed. $\mathscr{H}$ must be a scalar

quantity and $\hat{\boldsymbol{r}}$ is a vector quantity with respect to spatial transformations. Both $\mathscr{H}$ and $\hat{\boldsymbol{r}}$ must be real operators, i.e., must retain their sign at time reversal $t \to -t$. The functions f_i and $\boldsymbol{X}_i$ include both symmetrized and antisymmetrized combinations of $\hat{k}_j$. In virtue of the commutation condition

$$[\hat{k}_j, \hat{k}_{j'}] = \mathrm{i}\frac{e}{c\hbar} H_{j''}, \tag{2.5}$$

where j, j' and j'' constitute cyclic permutations (e.g., if $j = 2$ or $j = y$, then $j' = 3$, $j'' = 1$, or $j' = z, j'' = x$), the antisymmetrized terms can be expressed via H_j. The $\varphi(\boldsymbol{r})$ potential can be regarded as, for instance, the one created by impurities. It is assumed that this potential is smooth. In the higher EMA order alongside $\varphi(\boldsymbol{r})$ there emerges a gradient $\boldsymbol{E} = -\nabla\varphi$ in H. The corresponding term in $\mathscr{H}$ is analogous to the SO interaction (1.3) for a Dirac electron (eigenfunctions of the operator $\mathscr{H}$ are two-component spinors).

If the a.c. electric field $\tilde{\boldsymbol{E}}$ exciting resonance transitions is described by the vector-potential $\tilde{\boldsymbol{A}}$, the interaction Hamiltonian is

$$\tilde{\mathscr{H}}_e = -(e/c)\hat{\boldsymbol{v}}\tilde{\boldsymbol{A}}, \tag{2.6}$$

where the velocity operator is determined by a commutator

$$\boldsymbol{v} = \frac{\mathrm{i}}{\hbar}[\mathscr{H}, \hat{\boldsymbol{r}}]. \tag{2.7}$$

From eqs. (2.1)–(2.3) and (2.7) it follows that

$$\boldsymbol{v} = \hbar^{-1}\nabla_k \mathscr{H} + \boldsymbol{\Omega}(\hat{\boldsymbol{k}}), \tag{2.8}$$

where $\boldsymbol{\Omega}(\hat{\boldsymbol{k}})$ is the polynomial over $\hat{\boldsymbol{k}}$. Note that the $\boldsymbol{X}_j(\hat{\boldsymbol{k}})$ operators become important only when the terms of the order k^4 or higher are taken into account in $f_j(\hat{\boldsymbol{k}})$.

A complicated structure of the $\hat{\boldsymbol{r}}$ operators in eq. (2.3) results from projecting the multiband Hamiltonian of the $\boldsymbol{kp}$ approximation (Luttinger and Kohn 1955) onto the conduction band (or valence band). Similar terms also exist in the Dirac problem. The Dirac Hamiltonian may be treated as a multiband Hamiltonian, simultaneously incorporating dynamics of differently charged particles (electrons and positrons, or, in terms of the solid state theory, electrons and holes). From this point of view interband matrix elements must correlate as $c\hat{\boldsymbol{p}} = c\hbar\hat{\boldsymbol{k}} \Rightarrow P\hat{\boldsymbol{k}}$ and the 'forbidden gap' as $2m_0c^2 \Rightarrow E_G$. In the $1/c^2$ approximation

$$\hat{\boldsymbol{r}} = \boldsymbol{r} + \frac{\hbar}{4m_0c^2}(\boldsymbol{\sigma} \times \hat{\boldsymbol{p}}) \Rightarrow \mathrm{i}\nabla_k + \frac{P^2}{E_G^2}(\boldsymbol{\sigma} \times \hat{\boldsymbol{k}}). \tag{2.9}$$

For semiconductors the coefficient entering in the SO term, is much larger than the appropriate coefficient in a vacuum, as has been pointed out in section 1.

The interaction of an electron with an electromagnetic wave can be described

not only by the vector but also by the scalar potential $\tilde{\varphi}(\hat{\boldsymbol{r}}) = -e\tilde{\boldsymbol{E}}\hat{\boldsymbol{r}}$. Then the COR intensity is expressed via matrix elements of the $\hat{r}$ operator. Due to the relation

$$\langle \mathrm{f}|\hat{\boldsymbol{v}}|\mathrm{i}\rangle = \mathrm{i}\omega_{\mathrm{fi}}\langle \mathrm{f}|\hat{\boldsymbol{r}}|\mathrm{i}\rangle \tag{2.10}$$

(ω_{fi} is the transition frequency), straightforwardly following from (2.7), the results obtained by either method coincide. It is worth stressing that the matrix elements $\langle \mathrm{f}|\hat{\boldsymbol{r}}|\mathrm{i}\rangle$ depend not only on $\boldsymbol{X}_j$ but also on $\mathscr{H}_{\mathrm{so}}$. This is because the wave functions of the i and f states are also $\mathscr{H}_{\mathrm{so}}$-dependent, this dependence being quite relevant (Rashba and Sheka 1961a, c).

To compare the EDSR and EPR intensities, it is necessary to calculate matrix elements of the interaction responsible for EPR. They are determined by the magnetic component of the electromagnetic field. The corresponding perturbation operator equals

$$\tilde{\mathscr{H}}_{\mathrm{m}} = \tilde{\boldsymbol{H}} \cdot \nabla_{\boldsymbol{H}}\mathscr{H} = \mathrm{curl}\ \tilde{\boldsymbol{A}} \cdot \nabla_{\boldsymbol{H}}\mathscr{H}. \tag{2.11}$$

Differentiation in (2.11) should be performed only with respect to $\boldsymbol{H}$ entering explicitly in $\mathscr{H}$ but not with respect to $\boldsymbol{H}$ entering through the vector-potential $\boldsymbol{A}(\boldsymbol{H})$, since the appropriate terms are already taken into account in (2.6).

Experiments typically use two types of mutual orientation of the unit vector $\boldsymbol{e}$ of the electric field of an electromagnetic wave, of its wave vector $\boldsymbol{q}$ and of the constant magnetic field $\boldsymbol{H}$: the Faraday geometry ($\boldsymbol{q} \parallel \boldsymbol{H}, \boldsymbol{e} \perp \boldsymbol{H}$) with two circular polarizations of $\boldsymbol{e}$ (transverse resonance), and the longitudinal Voigt geometry ($\boldsymbol{q} \perp \boldsymbol{H}, \boldsymbol{e} \parallel \boldsymbol{H}$) (longitudinal resonance). This choice of polarizations is also handy for constructing the theory. Therefore, apart from the original reference system A, associated with the crystallographic axes, it is useful to introduce another reference system A′, associated with the magnetic field in such a manner that $Z \parallel \boldsymbol{H}$ (Addendum A). In the A system the Cartesian basis is employed and the vectors $\boldsymbol{r}$, $\boldsymbol{k}$ and $\boldsymbol{v}$ are denoted by lowercase letters and their coordinates are numbered by Latin indices ($i, j = 1, 2, 3$). In the A′ system the vectors are denoted by capital letters. Their components are chosen in the circular basis

$$\boldsymbol{V} = (V_-, V_Z, V_+) = (V_{\bar{1}}, V_0, V_1), \tag{2.12}$$

and similarly $\boldsymbol{R}$ and $\boldsymbol{K}$. In (2.12)

$$V_\pm = (V_X \pm \mathrm{i}V_Y)/\sqrt{2}. \tag{2.13}$$

In the circular basis the coordinates are numbered by Greek indices $\alpha, \beta = \bar{1}, 0, 1$ or $-1, 0, 1$.

The direction of the Z-axis will be chosen from the condition $eH_Z > 0$ with the sign of the charge e taken into account. According to the conditions (2.5) K_Z is a c-number and the other components obey the commutation rule

$$[\hat{K}_-, \hat{K}_+] = eH/c\hbar \equiv k_H^2, \qquad k_H = r_H^{-1}. \tag{2.14}$$

If we single out the dimensional factor k_H from $\hat{K}$, the result can be represented by step-up and step-down operators a^+ and a as

$$\hat{\boldsymbol{K}} = k_H \boldsymbol{a}, \qquad \boldsymbol{a} = (a, \xi, a^+), \qquad aa^+ - a^+a = 1, \qquad \xi = k_H^{-1} K_Z. \tag{2.15}$$

In the circular basis the commutators of $\hat{\boldsymbol{K}}$ and $\boldsymbol{R}$ are written down as

$$[\hat{K}_\alpha, R_\beta] = -\mathrm{i}\delta_{\alpha\beta}. \tag{2.16}$$

So far we have dealt with purely technical aspects of the problem relevant to the formalism of calculations. In conclusion to this section we shall make an attempt to discuss the problem in physical terms. This will enable us to understand qualitatively certain COR mechanisms. Of course, such considerations are no substitute for a consistent analysis of the Hamiltonian (2.2) or for a more sophisticated Hamiltonian describing the multiband model.

There is a qualitative distinction between band structures of crystals with an inversion centre and crystals without one. In this section it has already been noted that in crystals without an inversion centre the spectrum is degenerate only at certain points of the $\boldsymbol{k}$-space, but in the vicinity of these points the degeneracy is lifted and the spectrum splits into two branches corresponding to different spin states of the electron. This splitting is due to the Hamiltonian (2.2) where f_j are linear or cubic in k (cf. sections 5 and 6). Since such terms in $\mathscr{H}_{so}$ are inherent in crystals without an inversion centre, the COR excitation mechanism caused by them is termed the inversion asymmetry mechanism. As a rule, it is fairly efficient.

In crystals with an inversion centre, $f_j \propto H$. This is indispensable for ensuring twofold degeneracy of bands for all $\boldsymbol{k}$. But the presence of the H factor diminishes $\mathscr{H}_{so}$, and it may have an observable value only if the forbidden gap E_G entering in the denominator of f_j is narrow. Under these conditions the region, where the dependence of f_j on $\boldsymbol{k}$ is quadratic, will be very narrow; this is why the COR mechanism associated with a small value of E_G is often termed the nonparabolicity mechanism (see section 8). Sometimes under these conditions a major role is played by the large value of the $\boldsymbol{X}_j(\boldsymbol{k})$ functions, a possibility made clear from (2.9) (see also section 9).

Above we have covered the two mechanisms which can be most clearly specified. But in realistic situations, especially when one is dealing with degenerate valence bands, to distinguish and interpret individually the contributions of different perturbations (in particular, of those responsible for warping) is practically impossible.

3. *COR theory in the Zeeman limit*

An exact analytical solution of the problem for an electron in a homogeneous magnetic field $\boldsymbol{H}$ can be derived only for a few specific cases even for the two-

branch model. Yet, the most interesting situation occurs when the Zeeman splitting dominates over SO splitting (Zeeman limit). It can be studied in the general form at $\varphi(\boldsymbol{r}) = 0$. In this case an expansion is performed in the parameter

$$\gamma(\bar{k}) \approx \langle \mathscr{H}_{so}^2 \rangle^{1/2} / \hbar\omega_{min} \ll 1, \tag{3.1}$$

where $\omega_{min} = \min\{\omega_c, \omega_s, n\omega_c - \omega_s\}$, n is an integer. Here $\bar{k}$ is a characteristic value of the quasimomentum; for instance, for a band electron it is determined by formula (3.4). The criterion (3.1) means that the mean energy of SO interaction is small compared to the spacing between magnetic quantization levels. Depending on the power l of the quasimomentum $\hat{\boldsymbol{k}}$ entering in $\mathscr{H}_{so}$, the criterion (3.1) is fulfilled in strong ($l = 1$) or weak ($l \geqslant 3$) fields.

Represent the polynomials $f_j(\hat{\boldsymbol{k}})$ as

$$f_j(\hat{\boldsymbol{k}}) = \delta_l \sum_{\{i\}} F^{(j)}_{i_1 i_2 \ldots i_l} \hat{k}_{i_1} \hat{k}_{i_2} \ldots \hat{k}_{i_l}, \tag{3.2}$$

where δ_l is the SO coupling constant. The matrix elements $F^{(j)}_{\{i\}} \sim 1$ are determined by the symmetry a system possesses. In the systems studied the number of factors $l \leqslant 4$. Keeping in mind (3.2), one gets

$$\gamma(\bar{k}) \approx \delta_l \langle \hat{\boldsymbol{k}}^2 \rangle^{l/2} / \hbar\omega_{min}, \tag{3.3}$$

where $\langle \hat{\boldsymbol{k}}^2 \rangle$ can be estimated as

$$\langle \hbar^2 \hat{\boldsymbol{k}}^2 / 2m^* \rangle \approx \max\{\eta, T, \hbar\omega_c\}, \tag{3.4}$$

where η is the Fermi energy, and T is the temperature.

In the field of an electromagnetic wave with the vector potential $\tilde{\boldsymbol{A}} = \tilde{A}_0 \boldsymbol{e} \cos\{\boldsymbol{qr} - \omega t\}$ the total perturbation (see (2.6) and (2.11)) is

$$\tilde{\mathscr{H}} = \tilde{\mathscr{H}}_e + \tilde{\mathscr{H}}_m \equiv -\frac{e}{c}(\boldsymbol{u}\tilde{\boldsymbol{A}})$$

$$= -\tilde{A}_0 \operatorname{Re}\left\{\left[\frac{e}{c}(\boldsymbol{ve}) + i\frac{g\mu_B}{2}\boldsymbol{e}(\boldsymbol{\sigma} \times \boldsymbol{q})\right] \exp[i(\boldsymbol{qr} - \omega t)]\right\}. \tag{3.5}$$

The operators $\boldsymbol{u}$ differ from $\boldsymbol{v}$ because they include the paramagnetic contribution (2.11) responsible for EPR.

As will be shown in section 7, taking into account both terms constituting $\tilde{\mathscr{H}}$ and their interference may prove to be important (in particular, in n-type InSb) but at the first stage we shall retain only the term $\mathscr{H}_e$, because it is usually considerably larger than the second. Calculation of matrix elements can be conveniently performed using eigenfunctions of $\mathscr{H}_0$, therefore in $\mathscr{H}$ one should eliminate $\mathscr{H}_{so}$ by the unitary transformation

$$\mathscr{H} \Rightarrow e^{\hat{T}} \mathscr{H} e^{-\hat{T}}. \tag{3.6}$$

$\mathscr{H}_{so}$ in the leading order of the perturbation theory can be treated as

nondiagonal*. All the operators ($\boldsymbol{r}$, $\boldsymbol{v}$, etc.) are transformed in a similar manner. In the $\mathscr{H}_{so}$-linear approximation the $\hat{T}$ operator is proportional to $\mathscr{H}_{so}$ and

$$\mathscr{H}_{so}(\hat{\boldsymbol{k}}) + [\hat{T}, \mathscr{H}_0] = 0, \tag{3.7a}$$

$$\hat{T} = -\mathrm{i}\int_0^\infty \mathscr{H}_{so}(\hat{\boldsymbol{k}}(t))\,\mathrm{d}t, \tag{3.7b}$$

$$\hat{\boldsymbol{k}}(t) = \exp(\mathrm{i}\mathscr{H}_0 t)\,\hat{\boldsymbol{k}}\exp(-\mathrm{i}\mathscr{H}_0 t). \tag{3.7c}$$

Transforming (2.7) analogously to (3.6) and expanding the transformed (2.7) in $\hat{T}$, we get

$$\boldsymbol{v} = \frac{\mathrm{i}}{\hbar}[\mathscr{H}_0, \hat{\boldsymbol{r}}], \tag{3.8a}$$

where

$$\hat{\boldsymbol{r}} = \mathrm{e}^{\hat{T}}\boldsymbol{r}\mathrm{e}^{-\hat{T}} \approx \boldsymbol{r} + [\hat{T}, \boldsymbol{r}] \equiv \boldsymbol{r} + \boldsymbol{r}_{so}. \tag{3.8b}$$

In the two-branch approximation under a quadratic dispersion law $\mathscr{H}_0$ equals

$$\mathscr{H}_0 = \frac{\hbar^2\hat{\boldsymbol{k}}^2}{2m^*} + \tfrac{1}{2}g\mu_B(\boldsymbol{\sigma}\boldsymbol{H}). \tag{3.9}$$

Here we confine ourselves to the spherically symmetric Hamiltonian $\mathscr{H}_0$, although the theory can also be developed for an anisotropic mass and g-factor (Rashba and Sheka 1961c). An isotropic Hamiltonian is attractive also because the transformation properties of $\boldsymbol{r}$ and $\boldsymbol{v}$ do not depend on the specific form of the Hamiltonian under the transformation A → A′. That is why angular diagrams of matrix elements are universal. For example, they do not alter when nonparabolicity of bands is taken into account, or when an electron is bound to a spherically symmetric impurity centre, etc.

Symmetry properties manifest themselves most explicitly if we take the A′ system and choose the circular basis in it (section 2). Rotation of the vectors from the A reference system to the A′ reference system is realized by the matrices $\boldsymbol{B}$, whose explicit form is given in Addendum A:

$$\hat{\boldsymbol{k}} = \boldsymbol{B}\hat{\boldsymbol{K}} = k_H\boldsymbol{B}\boldsymbol{a}, \qquad \hat{\boldsymbol{r}} = \boldsymbol{B}\hat{\boldsymbol{R}}. \tag{3.10}$$

The vectors $\boldsymbol{k}$ and $\boldsymbol{r}$ are defined by the Cartesian coordinates in A, whereas the vectors $\boldsymbol{K}$ and $\boldsymbol{R}$ are defined by the circular coordinates in A′ (section 2). To diagonalize the Zeeman energy $(\boldsymbol{\sigma}\boldsymbol{H})$ it is necessary simultaneously with the transformation $\boldsymbol{B}$ of the $\boldsymbol{H}$ vector to perform unitary transformation of Pauli

*The generalization of transformation (3.6) for the Hamiltonian involving the coupling of an electron to an electromagnetic wave has been done by Kalashnikov (1974), who formulated the COR theory with explicit gauge invariance.

matrices. This transformation matrix $\boldsymbol{S}(\theta, \phi)$ belongs to the $D_{1/2}$ rotation group representation. Here θ and ϕ are the polar and azimuthal angles, respectively. This transformation results in

$$\boldsymbol{S}\sigma_i\boldsymbol{S}^{-1} = \sum_\alpha B_{i\alpha}\sigma_\alpha, \qquad i = (1, 2, 3), \qquad \alpha = (\bar{1}, 0, 1). \tag{3.11}$$

The circular components σ_α of the $\boldsymbol{\sigma}$ vector are defined according to the general rule (2.12). It is natural that $\hat{\boldsymbol{k}}$, $\boldsymbol{H}$ and $\boldsymbol{\sigma}$ are equally transformed at rotations.

In the new reference system in conformity with (2.15)

$$H_0 = \hbar\omega_c(a^+a + \tfrac{1}{2} + \tfrac{1}{2}\beta^*\sigma_z + \tfrac{1}{2}\xi^2). \tag{3.12}$$

The eigenfunctions of H_0 are oscillator functions ψ_N and their eigenvalues equal

$$\mathscr{E}_{N\sigma\xi} = \hbar\omega_c(N + \tfrac{1}{2} + \tfrac{1}{2}\sigma\beta^* + \tfrac{1}{2}\xi^2),$$
$$\beta^* = g\mu_B H/\hbar\omega_c = gm^*/2m_0, \qquad \sigma = \pm 1, \quad N = 0, 1, \ldots. \tag{3.13}$$

Here $\hbar\omega_c$ is the cyclotron energy (1.1) and $\hbar\omega_s = |\beta^*|\hbar\omega_c$ is the energy of a purely spin transition.

Let us make use of the equality

$$\hat{k}_\alpha(t) = \hat{k}_\alpha \exp(i\alpha\hbar\omega_c t). \tag{3.14}$$

The matrix element of $\hat{T}$ on spin functions is

$$\langle\downarrow|\hat{T}|\uparrow\rangle = \delta_l\frac{\sqrt{2}}{\hbar\omega_c}\sum_{j(\bar{i})\{\alpha\}} B_{j\bar{l}}\frac{F^{(j)}_{i_1\ldots i_l}B_{i_1\alpha_1}\ldots B_{i_l\alpha_l}}{\alpha_1 + \ldots + \alpha_l - \beta^*}\hat{K}_{\alpha_1}\ldots\hat{K}_{\alpha_l}. \tag{3.15}$$

Commutation of $\hat{T}$ with $\hat{R}_\tau$ in (3.8b) reduces to the differentiation with respect to $\hat{K}_{\bar{\tau}}$ due to (2.16). Passing from matrix elements of the coordinate to those of the velocity, for the COR matrix element we get

$$\langle N'\downarrow|V_\tau|N\uparrow\rangle = \delta_l\frac{2^{1/2}}{\hbar}\frac{N' - N - \beta^*}{N' - N - \beta^* - \tau}\sum_{j(\bar{i})\{\alpha\}} B_{j\bar{l}}F^{(j)}_{(i)}B_{i_1\alpha_1}\ldots B_{i_l\alpha_l}$$
$$\times\left\langle N'\left|\frac{\partial}{\partial\hat{K}_{\bar{\tau}}}(\hat{K}_{\alpha_1}\ldots\hat{K}_{\alpha_l})\right|N\right\rangle. \tag{3.16}$$

Similar formulas have been applied to n-type InSn and n-type CdS crystals (Rashba and Sheka 1961a, c).

In conclusion let us roughly estimate the characteristic scale of matrix elements of the $\hat{\boldsymbol{r}}$ and $\boldsymbol{v}$ operators, responsible for COR. For this purpose it is convenient to start with formula (3.8b) for $\boldsymbol{r}_{so}$ and to use (3.1), (3.7b) and (3.8a), bearing in mind that the characteristic value of $\bar{r}$ is $\bar{k}^{-1}$. As a result, for COR matrix elements we obtain

$$r_{COR} \sim \gamma(\bar{k})\bar{r}, \qquad v_{COR} \sim r_{COR}\omega_s. \tag{3.17}$$

In sections 5–9 we shall consider COR for free carriers mainly in those systems for which we have reliable experimental data. However, in the next section we shall formulate preliminarily a general approach to define the selection rules and to calculate the angular dependence of COR intensities.

4. *Angular indicatrices and selection rules*

The COR intensity corresponding to each individual transition can be calculated on the basis of the scheme described in section 3. Then we can find the angular indicatrix of the transition, i.e., the dependence of the intensity of the transition on the orientation of $\boldsymbol{H}$ and $\boldsymbol{e}$. Nevertheless, independent calculation for each transition, in a number of cases rather time-consuming, is not necessary. Actually there is usually a relatively small number of different types of angular indicatrices. The correspondence of a transition to a certain definite indicatrix $\Omega(\boldsymbol{H}, \boldsymbol{e})$ is determined by symmetry properties; later in this section we shall discuss the principles according to which transitions can be classified.

For interpreting experimental data, it is very important and also nontrivial to examine the problems concerning the selection rules for different transitions and also the problems of their absolute intensities. These subjects have been discussed in numerous papers; for example, mainly applicable to narrow-gap semiconductors of a sphalerite lattice, a most detailed analysis in terms of the generalized Kane model (1957) has been carried out by Zawadzki and Wlasak (1976), Weiler et al. (1978), Braun and Rössler (1985) and Wlasak (1986).

Both of the above-formulated problems are closely related to each other, so that to solve them it is possible to develop a general approach. This approach uses the notion of angular quasimomentum (AQM), which will be introduced in this section. Treatment of the problem in terms of this notion is pretty general and fairly practical. It implies that the high-symmetry Hamiltonian $\mathscr{H}_0$ of the zero approximation, describing an electron in a magnetic field by means of a certain multiband model, makes it possible to introduce an AQM quantum number m. Then all transitions $m \to m'$ with a given value of $\Delta m = m' - m$ have identical indicatrices, determined exclusively by the form of the perturbation operator $\mathscr{H}'$ and by the polarization of radiation. In virtue of the universality of the Ω functions, they can be calculated in an explicit form for simple models (e.g., for the 2×2 instead of the 8×8 scheme). The problem of the selection rules is also solved in a general form. For each $\mathscr{H}'$ and each individual polarization there is a maximal $(\Delta m)_{\max}$ such that at $|\Delta m| > (\Delta m)_{\max}$ the transition is forbidden for any arbitrary orientation of $\boldsymbol{H}$. At $|\Delta m| \leqslant (\Delta m)_{\max}$ the transition is forbidden only in the zeroes of the corresponding Ω function.

The only problem which cannot be solved in a general form concerns numerical values of the coefficients at the functions Ω. These coefficients must be

expressed via matrix elements of $\mathscr{H}$ (e.g., via the constants entering in the generalized Kane Hamiltonian), and this can be done only by straightforward calculation, which is sometimes rather cumbersome.

The simplest way to define the selection rules which have been exploited in some early works is to calculate the contributions of $\mathscr{H}_{so}$ into the velocity operator $\boldsymbol{v}_{so} = i[\mathscr{H}_{so}, \boldsymbol{r}]/\hbar$ and subsequently calculate matrix elements of $\boldsymbol{v}_{so}$ by eigenfunctions of the operator $\mathscr{H}_0$. It is obvious that the number of operator factors in $\boldsymbol{v}_{so}$ will always be smaller by unity than in $\mathscr{H}_{so}$. The structure of $\boldsymbol{v}_{so}$ must be compared with the structure of the operator $\boldsymbol{v}$, determined by formulas (3.8) incorporating the perturbation of eigenfunctions of $\mathscr{H}_0$, produced by $\mathscr{H}_{so}$ (Rashba and Sheka 1961a,c). According to (3.8) operator structures of $\boldsymbol{v}$ and $\boldsymbol{r}_{so}$ coincide and their matrix elements differ by the factor equalling the transition frequency (with an accuracy up to i). Therefore the problem is reduced to comparing the operator structure of $\boldsymbol{v}_{so}$ with the operator structure of $\boldsymbol{v}$ or of $\boldsymbol{r}_{so}$. Since (3.14) holds for a simple band, in this case matrix elements of $\hat{T}$ and $\mathscr{H}_{so}$ differ only by the denominator in (3.15), then $\boldsymbol{v}_{so}$ and $\boldsymbol{r}_{so}$ have similar operator structures. Yet, in a more general form of $\mathscr{H}_0$, terms in $\boldsymbol{r}_{so}$ emerge with a larger number of operator factors than in $\boldsymbol{v}_{so}$ and owing to these terms, the originally forbidden transitions become allowed.

Let us start with the symmetry arguments leading to the classification of indicatrices $\Omega(\boldsymbol{H}, \boldsymbol{e})$. Consider the most interesting case of cubic crystals with a direct gap at $\boldsymbol{k} = 0$. From the total Hamiltonian $\mathscr{H}$ of the system, single out the zero approximation Hamiltonian $\mathscr{H}_0$, describing a spherically symmetric system in a magnetic field. In all other aspects, it is arbitrary. In particular, it may have arbitrary dimensionality; for instance, for a 'quasi-Ge' band structure it may be an 8×8 Hamiltonian. All other terms in $\mathscr{H}$ will be treated as perturbation $\mathscr{H}'$. It includes the anisotropic part of the $\mathscr{H}_{so}$ operator. Both $\mathscr{H}$ and $\mathscr{H}_0$ depend on coordinates exclusively through the operators $\hat{K}_+$ and $\hat{K}_-$. The operator $\mathscr{H}_0$ is constructed as a spherical invariant (and $\mathscr{H}$ as a cubic invariant), involving the product of basis matrices, multiplied by the product of the operators $\hat{k}_i$. Since $\mathscr{H}_0$ is spherically symmetric, its multicomponent eigenfunctions Ψ_m can be classified according to the angular momentum m. The operators $\hat{K}_+$ and $\hat{K}_-$, acting in the A′ system, respectively, raise and lower the projection m of the angular momentum of the Ψ_m function by unity (i.e., $\hat{K}_\alpha \Psi_m \in \{\Psi_{m+\alpha}\}$). On the other hand, when the commutation properties (2.14) are taken into account, the $\hat{K}_\alpha$ operators can be regarded as step-up and step-down operators for an auxiliary oscillator, changing the value of its quantum number N by α (cf. (2.15)). This allows us to establish the correlation between the angular momentum m and the quantum number N of the auxiliary oscillator by representing certain components of the multicomponent wave function Ψ_m in terms of Landau oscillator eigenfunctions. For instance, in the Kane model the wave function corresponding to the projection m (m is a half-integer) of the total

angular momentum onto $\boldsymbol{H}$ is written as

$$\Psi_m = \begin{vmatrix} C_1\psi_{m-1/2} \\ C_2\psi_{m+1/2} \\ C_3\psi_{m-3/2} \\ C_4\psi_{m-1/2} \\ C_5\psi_{m+1/2} \\ C_6\psi_{m+3/2} \\ C_7\psi_{m-1/2} \\ C_8\psi_{m+1/2} \end{vmatrix} \tag{4.1}$$

(Addendum B). The arrangement of bands in the Kane model is illustrated in fig. 1. This chart clarifies the principle according to which the components of Ψ_m

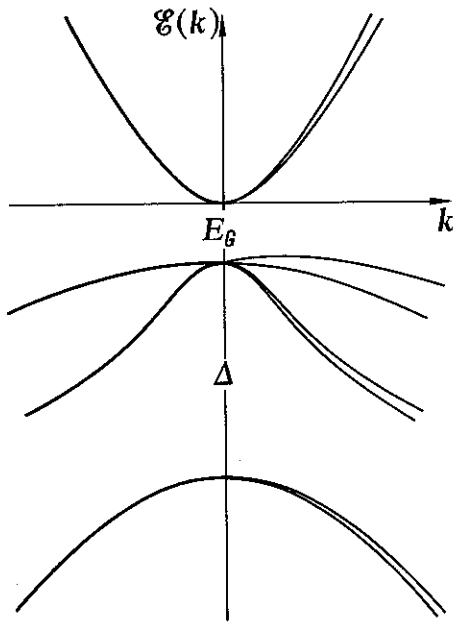

Fig. 1. Arrangement of bands in direct-gap cubic semiconductors, described by the Kane model (1957). E_G is the width of the forbidden band, and Δ is the SO splitting. On the top is the conduction band; in the middle the valence band, consisting of light hole and heavy hole bands; at the bottom is the split-off band. The figure applies to the $A_{III}B_V$-type of semiconductors. The weak splitting of the bands (emphasizing their twofold degeneracy) is due to the absence of an inversion centre. On the left-hand side, the splitting is neglected; on the right-hand side, the splitting is shown but its magnitude is exaggerated.

are constructed; the two upper components correspond to the conduction band (spin 1/2), the next four components correspond to the valence band (spin 3/2), and the two lower components correspond to the split-off band (spin 1/2).

Although in the preceding paragraph m is referred to as the angular momentum of the Ψ_m function, strictly speaking this is not so and m should really be called the angular quasimomentum (AQM). A genuine angular momentum is determined by the action of the operator $\hat{J}_Z$ on the wave function; $\hat{J}_Z$ being the projection of the total angular momentum onto the direction of $\boldsymbol{H}$. Having only operators $\hat{K}_+$ and $\hat{K}_-$, one cannot construct the operator $\hat{J}_Z$, which is evident if the simplest Hamiltonian (3.9) is taken as an example. That is why it is impossible to define the respective quantum number. Nevertheless, to find angular diagrams it is not necessary to correlate m with the genuine momentum. The functions $\Omega(\boldsymbol{H}, \boldsymbol{e})$ are completely determined (within the scope of the approximation stipulated at the end of this section) by a change in the m number which coincides with a change of the genuine angular momentum. It is noteworthy that the angular momentum can be introduced only in the axial gauge of $\boldsymbol{A}$. Nevertheless m retains the meaning of AQM in an arbitrary gauge, which is clear from its close relationship with the quantum number N.

In the Kane model a set of eight functions Ψ_m of the type (4.1), differing from each other by numerical coefficients C_i, corresponds to each value of m. For particles (electrons, holes) positioned at the edge of the band, the coefficients C_i, corresponding to this band, are large. This property makes it possible to single out the functions describing electron and hole states from the complete set. Both transitions inside the set ($\Delta m = 0$) and transitions between different sets ($\Delta m \neq 0$) are possible. Among these transitions there are intraband and interband transitions. For all the systems investigated so far, the form of indicatrices is universal in the sense that it is exclusively Δm-dependent. However, matrix elements determining the indicatrices were found in the first order in $\mathscr{H}_{so}$; involving only the terms containing some of the lowest powers of k. The explicit meaning of this restriction depends on an individual form of the Hamiltonian. For the Kane model the appropriate analysis is carried out in Addendum B. For a more general five-band (fourteen-branch) Hermann–Weisbuch model (1977), which describes GaAs and a number of other $A_{III}B_V$ compounds very well, the AQM notion retains its validity for a spherically symmetric approximation (it is broken due to interaction of two p-bands) (Rössler 1984, Zawadzki et al. 1985). There are grounds for hoping that the universality of the $\Omega(\boldsymbol{H}, \boldsymbol{e})$ functions will turn out to be a general property, although no proof of this has yet been found.

Above we have discussed transitions between quantum states of band carriers. But a similar problem also arises for carriers bound in local centres (Sheka and Zaslavskaya 1969). Here the angular indicatrix of the transition is also determined completely by the value of Δm. It is natural that in a given case m is the projection of the genuine angular momentum. Actually the impurity centre Hamiltonian includes the $\boldsymbol{r}$-dependent potential energy operator. Thus compo-

nents of the operator $\boldsymbol{r}$ are added to the $\hat{K}_\pm$ operators, so the total number of the operators of our theory increases. As a result, the operator $\hat{J}_Z$ is also an operator of this theory.

Now consider modifications which have to be introduced into the selection rules due to the second term of (3.8b). For this purpose, consider the 'quasi-Ge' valence band; but in order to treat the problem analytically, impose specific restrictions upon coefficients of the Hamiltonian.

(*i*) Assume that the band is spherically symmetric, i.e., the Luttinger parameters obey the condition $\gamma_2 = \gamma_3$ (Luttinger 1956). Then from the very beginning it is convenient to work in the A′ system, where $Z \| \boldsymbol{H}$ (section 2).

(*ii*) Assume that $K_Z = 0$.

(*iii*) Assume that the numerical value of the g-factor is such that

$$\mathscr{H}_0 = aA(\hat{\boldsymbol{K}}) + bB(\hat{\boldsymbol{K}}),$$

$$a = (\hbar^2/2m_0)(\gamma_1 + 5\gamma_2/2), \qquad b = -(\hbar^2/2m_0)\gamma_2, \tag{4.2}$$

where

$$A(\hat{\boldsymbol{K}}) = \hat{\boldsymbol{K}}^2 + 2k_H^2 \hat{J}_Z,$$

$$B(\hat{\boldsymbol{K}}) = (\hat{\boldsymbol{J}}\hat{\boldsymbol{K}})^2 - \tfrac{1}{4}\,\mathrm{tr}\{(\hat{\boldsymbol{J}}\hat{\boldsymbol{K}})^2\} - 2k_H^2 \hat{J}_Z. \tag{4.3}$$

The operator $A(\hat{\boldsymbol{K}})$ commutates with $B(\hat{\boldsymbol{K}})$ and with $(\hat{\boldsymbol{J}}\hat{\boldsymbol{K}})$. In the A′ system the eigenfunctions Ψ_m are the four middle lines of (4.1).

As was stated at the beginning of this section, our strategy should be to compare operator structures of $\boldsymbol{v}_{so}$ and $\boldsymbol{r}_{so}$. Since $\mathscr{H}_{so}$ in formula (3.7b) depends on the operator $\hat{\boldsymbol{K}}(t)$, let us start by calculating it. Transform the operator $\exp(\mathrm{i}\mathscr{H}_0 t)$ entering in (3.7c)

$$\exp(\mathrm{i}\mathscr{H}_0 t) = \exp(\mathrm{i}aAt)\{\cos(bCt) + \mathrm{i}BC^{-1}\sin(bCt)\}. \tag{4.4}$$

The operator, introduced here,

$$C(\hat{\boldsymbol{K}}) = \{[A(\hat{\boldsymbol{K}})]^2 + \tfrac{9}{4}k_H^2\}^{1/2}, \tag{4.5}$$

is proportional to a diagonal 4×4 matrix in the Ψ_m basis. At the derivation of (4.4) we have used commutativity of A and B as well as the identity $B^2 = C^2$, valid at $K_Z = 0$. From (3.7c) and (4.4) it follows that $\hat{K}_\alpha(t)$ have the following structure:

$$\hat{K}_\alpha(t) = \hat{K}_\alpha \varphi_\alpha^{(1)}(\hat{\boldsymbol{K}}^2, t) + [B(\hat{\boldsymbol{K}}), \hat{K}_\alpha]\varphi_\alpha^{(2)}(\hat{\boldsymbol{K}}^2, t). \tag{4.6}$$

We shall not need the explicit form of the φ functions. According to (3.8b) the next step is to calculate the commutator $[\hat{T}, \boldsymbol{r}]$. Since $\mathscr{H}_{so}$ is a polynomial over $\hat{K}_\alpha$, calculation of $[\hat{T}, \boldsymbol{r}]$ is based on calculation of the commutators $[\hat{K}_\alpha(t), \boldsymbol{r}]$. From (4.6) and (2.16) it follows that

$$[\hat{K}_\alpha(t), R_\tau] = \delta_{\alpha\tau}\chi_\alpha^{(1)}(\hat{\boldsymbol{K}}^2, t) + \hat{K}_\alpha \hat{K}_\tau \chi_\alpha^{(2)}(\hat{\boldsymbol{K}}^2, t). \tag{4.7}$$

Formula (4.7) enables us, using (3.7b) and (3.8b), to calculate $\boldsymbol{r}_{so}$. Moreover, to follow through this procedure to the end is not necessary. The basic result is already contained in (4.7). Analyzing this formula, one should bear in mind that $\hat{\boldsymbol{K}}^2 = \hat{K}_\beta \hat{K}_{\bar{\beta}}$, entering in the arguments of $\chi_\alpha^{(1)}$ and $\chi_\alpha^{(2)}$ does not alter m at the action upon the Ψ_m functions. Therefore $\hat{\boldsymbol{K}}^2$ can be ignored. That is why only the operators entering in (4.7) as coefficients of the χ functions are important. In fact, the first of them almost coincides with the commutator $[\hat{K}_\alpha, R_\tau]$ (see (2.16)), which is employed in the course of the calculation of $\boldsymbol{v}_{so}$. It is this coefficient that is responsible for the reduction in the number of operator factors in $\boldsymbol{v}_{so}$ by unity in comparison to those in $\mathscr{H}_{so}$. In contrast, the second term in (4.7) raises the number of operator factors by unity. Due to this, the effect of the operators $\boldsymbol{v}_{so}$ and $\boldsymbol{r}$ is essentially different. The raise in the number of factors gives rise to the appearance of extra bands. Since there is no small parameter in the Hamiltonian (4.2), the intensities of these extra bands and the other bands are comparable. Calculation for InSb of the effect of inversion asymmetry (Addendum B) and of warping (Sheka and Zaslavskaya 1969) shows that the indicatrices of the 'original' bands, generated by the $\boldsymbol{v}_{so}$ operator, are not altered due to the second term in (4.7). The indicatrices of the extra bands are contained in the set of the indicatrices for the 'original' bands.

This scheme is handy for finding out general properties of the V_τ operators and the selection rules. Concrete calculations can be conveniently performed if the explicit form of all operators in the basis of the $\mathscr{H}_0$ operator eigenfunctions is used in (3.7).

To determine the indicatrix, corresponding to a given change in AQM Δm and to a given polarization τ (formula (2.12)), let us make use of (B.23). The explicit relation between the $\Psi_m^{(t)}$ and $\Psi_{m+\alpha}^{(t)}$ functions in (B.23) is irrelevant, only the difference between the subscripts being of importance. Therefore it stands to reason to make this formula more abstract by introducing 'step operators': step-up ($\alpha > 0$), step-down ($\alpha < 0$) and step-zero ($\alpha = 0$) operators acting on m. Symbolically they are defined as

$$\hbar_\alpha \Psi_m \Rightarrow \bar{\Psi}_{m+\alpha}. \tag{4.8}$$

Now (B.22) can be rewritten in the operator form

$$\mathscr{H}' = \sum_\alpha \mathscr{B}_{-\alpha}^{(l)}(\theta, \phi)\hbar_\alpha, \tag{4.9}$$

the superscript l is defined by formula (3.2). An analogue of (4.9) for the velocity, expressed via the step operators υ_α, defined similarly to (4.8), has the form

$$V_\tau = \sum_\alpha \mathscr{B}_{-\alpha}^{(l)}(\theta, \phi)\upsilon_{\alpha+\tau}. \tag{4.10}$$

Formulas (4.9) and (4.10) contain the rule for determining the angular

indicatrices of the transitions, induced by small (and, as a rule, not spherically symmetric) perturbation $\mathscr{H}'$:

(*i*) the operator $\mathscr{H}'$ should be expanded in the step operators in comformity with (4.8) in the A′ system $(Z\|\boldsymbol{H})$. This expansion determines the coefficients $\mathscr{B}_\alpha^{(l)}$;

(*ii*) the expansion of the velocity in the step operators is determined by formula (4.9) where the coefficients are $\mathscr{B}_\alpha^{(l)}$;

(*iii*) the AQM values m and m' should be ascribed to the initial and final states, respectively;

(*iv*) the transition $m \to m'$ in the polarization τ is described by a matrix element, proportional to $\mathscr{B}_{-\alpha}(\theta, \phi)$ with $\alpha = m' - m - \tau$ and the intensity of the transition is determined by the indicatrix

$$\Omega_\alpha^{(l)}(\theta, \phi) = \Omega_{|\alpha|}^{(l)}(\theta, \phi) = |\mathscr{B}_{-\alpha}^{(l)}(\theta, \phi)|^2, \qquad \alpha = m' - m - \tau. \tag{4.11}$$

The $\Omega^{(l)}(\theta, \phi)$ functions are invariants of a group of the crystalline class and, consequently, their number is infinite. The rank of invariants grows with increasing power l in the expansion of $\mathscr{H}'$ in $\hat{\boldsymbol{k}}$. The choice of the set of the same-rank invariants should be made separately for a chosen $\mathscr{H}'$. The Ω functions, given in sections 5 and 6, may serve as an example.

5. *Three-dimensional spectrum with linear terms in the dispersion law*

It is convenient to start the application of the COR theory to concrete dispersion laws from the case when $\mathscr{H}_{so}$ is linear in k, i.e., when the expansion of $f_i(\boldsymbol{k})$ in (2.2) starts with k. Of particular interest is the Hamiltonian describing carriers in the vicinity of the $\boldsymbol{k} = 0$ point in noncentrosymmetric crystals having a symmetry axis of the order no lower than the third. Examples of this are wurtzite-type crystals (Rashba and Sheka 1959, Casella 1960, Balkanski and Cloizeaux 1960) as well as sphalerite-type crystals uniaxially strained in the symmetric crystallographic directions (Bir and Pikus 1972). To construct the EMA Hamiltonian it is important to bear in mind that carriers are described by the spinor rotation group representation $D_{1/2}$ corresponding to the angular momentum $J = 1/2$. For this representation Pauli matrices are transformed as components of the pseudovector $\boldsymbol{\sigma}$, odd with respect to time reversal. Writing down $\mathscr{H}$ as a sum of invariants, we get

$$\mathscr{H} = \mathscr{H}_0 + \mathscr{H}_{so}, \tag{5.1}$$

$$\mathscr{H}_0 = \frac{\hbar^2 \hat{\boldsymbol{k}}^2}{2m^*} + \tfrac{1}{2} g \mu_B (\boldsymbol{\sigma H}) \equiv H_L + H_Z, \tag{5.2}$$

$$\mathscr{H}_{so} = \delta_1 (\boldsymbol{\sigma} \times \hat{\boldsymbol{k}}) \boldsymbol{c}, \tag{5.3}$$

$\boldsymbol{c}$ is a unit vector directed along the symmetry axis. For simplicity it is assumed in (5.2) that m^* and the g-factor are isotropic. This allows us to discuss the results in terms of the general approach developed in section 4. Besides, this model is realistic for strained $A_{III}B_V$ crystals and also for a number of hexagonal $A_{II}B_{VI}$ crystals.

At $\boldsymbol{H}=0$ the energy spectrum has two branches

$$\mathscr{E}^{\pm}(\boldsymbol{k}) = \hbar^2\boldsymbol{k}^2/2m^* \pm \delta_1 k_\perp,$$
$$k_\perp = (k_x^2 + k_y^2)^{1/2}, \qquad z \| c. \tag{5.4}$$

The minimum of energy $\mathscr{E}_{\min}$ is achieved on a circumference (on the loop of extrema) of the radius $k_0 = m^*\delta_1/\hbar^2$,

$$\mathscr{E}_{\min} = -\Delta_1, \qquad \Delta_1 = m^*\delta_1^2/2\hbar^2. \tag{5.5}$$

The velocity operator $\boldsymbol{u}$, describing all resonance transitions, equals

$$\boldsymbol{u} = \hbar\boldsymbol{k}/m^* + \delta_1(\boldsymbol{c} - i\boldsymbol{q}') \times \boldsymbol{\sigma}/\hbar. \tag{5.6}$$

Here

$$\boldsymbol{q}' = \hbar^2\beta^* q/2m^*\delta_1, \qquad q' \sim a_B q/(\delta_1)_{\text{a.u.}}, \tag{5.7}$$

where a_B is the Bohr radius, and the index a.u. means that the quantity it is attached to is expressed in atomic units. In (5.6) the first term describes CR, the second term COR, and the third one EPR. At $\boldsymbol{q} \| \boldsymbol{c}$ the second and third terms differ from each other only by a numerical factor, therefore all parameters (e.g., width and shape of bands) coincide in COR and EPR and their intensities are related to each other as

$$I_{\text{EPR}}/I_{\text{CR}} = (q')^2. \tag{5.8}$$

This ratio increases with increasing q, i.e., with the increasing frequency at which the resonance is observed. Maximal frequencies at which measurements are carried out now correspond to wavelengths $\lambda \approx 100$ μm, i.e., $q \approx 2 \times 10^3$ cm^{-1} in a crystal. At the values $\delta_1 \sim (10^{-2}$–$10^{-3})$ a.u., typical of $A_{II}B_{VI}$ crystals (Romestain et al. 1977, Dobrowolska et al. 1982, Ivchenko and Sel'kin 1979, Pevtsov and Sel'kin 1983) $q' \lesssim 10^{-3}$. Consequently, COR must dominate over EPR.

At $\boldsymbol{H} \| \boldsymbol{c}$ the problem is solved exactly (Rashba 1960, 1961). The eigenfunctions are

$$\Psi_m = \begin{vmatrix} C_{N1}\psi_{N-1} \\ C_{N2}\psi_N \end{vmatrix}, \qquad N = m + \tfrac{1}{2}. \tag{5.9}$$

Here C_{Ni} are the coefficients and ψ_N are the eigenfunctions of the Landau

oscillator. For all $N > 0$ there are two solutions with the energies:

$$\mathscr{E}_{N\sigma}(k_z) = \hbar\omega_c\left\{N \pm \sigma\left[\tfrac{1}{4}(1-\beta^*)^2 + \frac{4\Delta_1}{\hbar\omega_c}N\right]^{1/2}\right\} + \frac{\hbar^2 k_z^2}{2m^*}. \tag{5.10}$$

The index $\sigma = \pm 1$ numbers the branches of the spectrum. For $N = 0$ there is only one solution with $C_{01} = 0$ and the energy

$$\mathscr{E}_0(k_z) = \tfrac{1}{2}\hbar\omega_c(1-\beta^*) + \hbar^2 k_z^2/2m^*. \tag{5.11}$$

At the Zeeman limit, $S = \sigma/2$ acquires the meaning of a spin quantum number. In this case (5.10) is simplified, and after the levels are renumbered, the spectrum ((5.10) and (5.11)) at $0 < \beta^* < 1$ is written as

$$\mathscr{E}_{NS}(k_z) = (N + \tfrac{1}{2})\hbar\omega_c \pm S\hbar\omega_s + \hbar^2 k_z^2/2m^*. \tag{5.12}$$

This spectrum is depicted in fig. 2, which also gives a scheme of transitions in CRA polarization. This scheme illustrates the universality of the selection rule $\Delta m = 1$ for all types of resonances. At moderate magnetic fields, when $\hbar\omega_c \sim \hbar\omega_s \sim \Delta_1$, the arrangement of the levels is much more sophisticated. Nevertheless it is possible to check that the selection rule $\Delta m = 1$ also holds for this case.

Using the explicit form of the coefficients C_{Nl} one can calculate intensities for all bands. Then an interesting peculiarity shows up; at the Zeeman limit the intensity of the CFR band, corresponding to the CFR transition and depicted in fig. 2 by the dashed line, vanishes. At $N \sim 1$ it is by the factor $\sim(\Delta_1/\hbar\omega_c)$ weaker than the intensity of the EDSR band. This disappearance of the CFR band, allowed by the selection rules, is at first glance in contradiction with the general assertions of section 4 and Addendum B. However, this seeming contradiction is accounted for by the fact that these statements were made for a spherically symmetric Hamiltonian $\mathscr{H}$ of a general form (in the case under consideration in

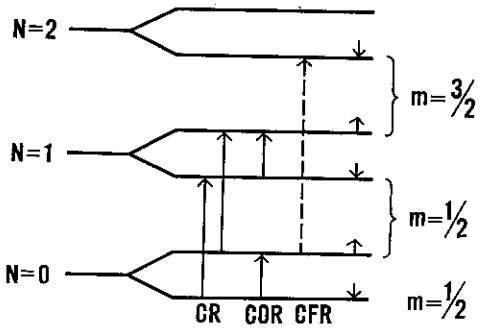

Fig. 2. Arrangement of electron energy levels, their classification in terms of the N and m quantum numbers, and quantum transitions allowed in the Faraday geometry (CRA polarization), $H \| c$. The figure applies to the case when $\omega_c > \omega_s$, $g > 0$. The short arrows on the right-hand side of the figure indicate spin orientations.

the $\boldsymbol{H} \| c$ geometry axial symmetry is sufficient). At the same time $\mathscr{H}_L$ from (5.2) possesses a specific property: it is quadratic in $\hat{\boldsymbol{k}}$. If we take into account the nonparabolicity of $\mathscr{H}_0$, i.e., introduce into it an additional term ensuring anharmonicity

$$\mathscr{H}_a = \hbar\omega_a(\hat{\boldsymbol{k}}^2/k_H^2)^2, \tag{5.13}$$

then the 'accidentally' forbidden transition becomes allowed. The same is true if we take into consideration the anharmonic correction to $\mathscr{H}_{so}$. The calculation is analogous to the one given in section 4 for the valence band. It shows that in the presence of $\mathscr{H}_a$ there emerges a new contribution to the velocity operator

$$v_+ = \mathrm{i}\frac{\delta_1}{\hbar}\frac{8\omega_a(2-\beta^*)}{\omega_c(1-\beta^*)^2}(\hat{k}_+/k_H)^2\sigma_-, \tag{5.14}$$

ensuring nonzero intensity of the transition $N\uparrow \to (N+2)\downarrow$.

Thus, any violation of the harmonicity of the zero approximation Hamiltonian by incorporating (5.3) or (5.13) into it, allows the transition $2\omega_c - \omega_s$. Then the matrix element of the velocity acquires a small factor of the order $\Delta_1/\hbar\omega_c$ or ω_a/ω_c, respectively.

In the Zeeman limit (section 3) it is possible to find the angular dependence of matrix elements of the velocity (5.6) in a tilted field $\boldsymbol{H}$, for instance, employing (3.16). In this case only $F_2^{(1)} = 1$ and $F_1^{(2)} = -1$ are nonzero, while V_τ do not involve the $\hat{K}_\alpha$ operators and therefore are diagonal relative to the Landau quantum number. Bearing in mind the properties of the $\boldsymbol{B}$ matrix (Addendum A), we have ($\theta = \widehat{c\boldsymbol{H}}$)

$$\langle N\uparrow|V_+|N\downarrow\rangle = -\mathrm{i}2^{1/2}\frac{\delta_1}{\hbar}\frac{\beta^*}{1-\beta^*}\cos\theta,$$

$$\langle N\uparrow|V_-|N\downarrow\rangle = 0, \qquad \langle N\uparrow|V_Z|N\downarrow\rangle = -\frac{\delta_1}{\hbar}\sin\theta \tag{5.15}$$

(Rashba and Sheka 1961c). Thus, only EDSR is allowed and CFR is absent. Equation (5.15) has recently been rederived by La Rocca et al. (1988a, b).

It is of interest to compare this result with the general selection rules formulated in section 4 and to compare the angular indicatrices. We shall do so to demonstrate the potential of the general method, using a simple model. For the case under study, results can also be obtained in a different way; but in complicated cases (e.g., degenerate valence band) to describe the angular indicatrices by straightforward calculation is an extremely cumbersome procedure. At the same time the procedure discussed in section 4 directly yields angular dependences, and the problem is only to bring them into proper correlation with electronic transitions.

The SO contribution to the velocity is determined by formula (4.10). To derive the appropriate expressions for the problem we are investigating, let us start

with $\mathscr{H}_{so}$ (5.3), which in the A' system (Addendum A) can be written analogously to (4.9)

$$\mathscr{H}_{so} = \sum_{\alpha=-1}^{1} \ell_{-\alpha} h_{\alpha}. \tag{5.16}$$

Here $\ell_\alpha \equiv \mathscr{B}_\alpha^{(1)}$ equal

$$\ell_0 = \cos\theta, \qquad \ell_1 = \ell_{-1}^* = -i2^{-1/2}\sin\theta, \tag{5.17}$$

$$h_\alpha = i\delta_1(\boldsymbol{\sigma}\times\hat{\boldsymbol{K}})_\alpha = i\delta_1(\sigma_{\alpha'}\hat{K}_{\alpha''} - \sigma_{\alpha''}\hat{K}_{\alpha'}). \tag{5.18}$$

The subscripts α, α' and α'' constitute a cyclic permutation from $\bar{1}$, 0, 1, and properties of h_α as step operators are verified by inspection. The explicit form of $v_{\alpha+\tau}$ can be found only provided the explicit form of the $\mathscr{H}_{so}$ operator is used. Properties of $v_{\alpha+\tau}$ as step operators are dependent on their subscript. Table 1, relating the polarization of a transient and AQM change with the angular indicatrix $\Omega_\alpha = |\ell_\alpha|^2$ uses these properties.

There is complete agreement between (5.15) and table 1 for transitions occurring at the frequency ω_s, yet all other transitions illustrated in table 1 are absent for the Hamiltonian ((5.1)–(5.3)) in the Zeeman limit. From (5.14) it is clear that incorporation of the anharmonism (5.13) allows the transition $2\omega_c - \omega_s$ but only in the polarization $\tau = 1$. The transition $\omega_c + \omega_s$ also becomes allowed. The transition $\omega_c - \omega_s$ becomes allowed but only at $\tau = 0, 1$. Angular indicatrices of these transitions are in agreement with table 1. We should stress that in contrast to 'extra' transitions in the valence band (section 4), the matrix elements for both of these 'extra' bands are small over the parameter ω_a/ω_c.

The example considered illustrates how the generalization of the Hamiltonian $\mathscr{H}_0$ promotes the appearance in the absorption spectrum of the bands which should exist according to the general theory but do not exist at a specific form of $\mathscr{H}_0$ (formula (5.2)).

Table 1
Allowed transitions and their angular indicatrices

τ	Δm				
	2	1	0	−1	−2
$\bar{1}$	–	–	Ω_1	Ω_0	Ω_1
0	–	Ω_1	Ω_0	Ω_1	–
1	Ω_1	Ω_0	Ω_1	–	–
Frequencies	$\omega_c + \omega_s$	ω_s $2\omega_c - \omega_s$	$\omega_c - \omega_s$ $\omega_s - \omega_c$	$-2\omega_c + \omega_s$ $-\omega_s$	$-\omega_c - \omega_s$

The table gives indicatrices Ω_τ for all polarizations τ at possible AQM changes $\Delta m = m' - m$. At larger values of $|\Delta m|$ no transitions occur. The dashes mark forbidden transitions. The bottom lines give transition frequencies (positive for absorption, negative for emission). The table holds for the case $g > 0$.

In principle, the band $3\omega_c - \omega_s$ must also be present since for this band $\Delta m = 2$ (i.e. the maximal Δm of table 1). However when we choose $\mathscr{H}_{so}$ in the form (5.3), this band is missing. The reason is that the generalization of $\mathscr{H}_0$ results in the appearance in the velocity operator of the term, containing a higher power of k than in $\mathscr{H}_{so}$, the power being larger only by unity (section 4). From this fact it follows that the maximal change of N (N in the Zeeman limit has the meaning of the Landau quantum number) in the case we're dealing with here equals $|\Delta N| = 2$. Therefore the band $3\omega_c - \omega_s$ to which $\Delta N = 3$ corresponds is forbidden by virtue of the selection rules with respect to N.

Above we have assumed that m^* and the g-factor are spherically symmetric (see (5.2)). But in the general case in crystals with the preferred axis $\boldsymbol{c}$ the tensors of the effective mass and of the g-factor are anisotropic. In this case EDSR angular diagrams are noticeably more complicated compared to (5.15) (Rashba and Sheka 1961c).

The most convincing experiments on EDSR, caused by k-linear terms, were carried out on n-type InSb samples subjected to uniaxial strain. Bir and Pikus (1961) were the first to notice the existence of such terms. If we take into account only the deformation potential C_2 (see table 2, Addendum B), the term in $\mathscr{H}$ emerging due to the strain is

$$\mathscr{H}_\varepsilon = \tfrac{2}{3} P C_2 \left(\frac{1}{E_G} - \frac{1}{E_G + \Delta} \right) [\sigma_x (\hat{k}_z \varepsilon_{zx} - \hat{k}_y \varepsilon_{yx}) + \text{c.p.}]. \tag{5.19}$$

A distinctive feature of this Hamiltonian is that it becomes zero when the stress X is acting along [001], despite the fact that the restrictions imposed by symmetry alone do not require that $\mathscr{H}_\varepsilon = 0$ in this case. Kriechbaum et al. (1983) experimentally discovered that for $X \| [001]$ EDSR is very weak, and therefore they concluded that the most important role is that of the C_2 potential. Their main measurements were done for $X \| [110]$. In these conditions $\mathscr{H}_{so}$ is described by (5.3) with $\boldsymbol{c} \| [110]$ and $\delta_1 \propto \varepsilon_{xy}$. These experiments were made in the Faraday geometry ($\boldsymbol{q} \| \boldsymbol{H}$) with linearly polarized (or nonpolarized) light. $\boldsymbol{H} \| [112]$ was tilted with respect to the symmetry axis. In these conditions the transition is allowed and its intensity is X^2-proportional. This dependence was observed in experiments at $X \lesssim 1$ kbar. A quadratic dependence at small X testifies to the fact that EDSR excited by k-linear terms is much stronger than that excited by k^3 terms.

An experiment, somewhat complicated as a result of the technique employed but equivalent in physical essence, was performed by Jagannath and Aggarwal (1985). They studied the generation at the frequency ω_3, using the mixing of two laser beams with frequencies ω_1 and ω_2 such that $\omega_3 = \omega_1 - \omega_2$. The generation exhibits a strong resonance at $\omega_3 = \omega_s$. Its intensity is proportional to the EDSR intensity. Therefore the three-wave process employed provides an independent method for studying EDSR. Uniaxially strained n-type InSb crystals with $X \| \boldsymbol{H} \| [111]$ were used. In this case there also arises the Hamiltonian (5.3) with $\delta_1 \propto X$; $\boldsymbol{H}$ being oriented along the symmetry axis. The results are collected in

fig. 3. The band observed at $X=0$ is ascribed to a magnetic-dipole transition because in the geometry which was used, an electric-dipole transition is forbidden for both the inversion asymmetry mechanism (section 6) and the nonparabolicity mechanism (section 9). At $X\neq 0$ there occurs radiation with $\tilde{\boldsymbol{E}}\perp\boldsymbol{H}$ in agreement with (5.15). Its frequency is shifted depending on the stress, which is accounted for by the g-factor dependence on X, and its intensity rapidly increases with the stress. As is obvious from fig. 4, the dependence of the intensity on the stress complies with the law X^2 in conformity with the theory.

The situation for p-type InSb subjected to uniaxial stress is much more intricate due to band degeneracy. The effect of k-linear terms, induced by the stress, is partially masked by the k-linear terms contribution entering in the valence band Hamiltonian at $X=0$. Besides, contributions coming from k-odd terms and from the strong nonparabolicity induced by the strain (section 8), are competing with each other. A thorough analysis of the experimental data (Ranvaud et al. 1979) pointing to the existence of a few COR bands was made on the basis of the calculations by Trebin et al. (1979).

Unfortunately there are practically no experimental data on COR caused by k-linear terms in uniaxial free crystals. An interesting object for investigation is

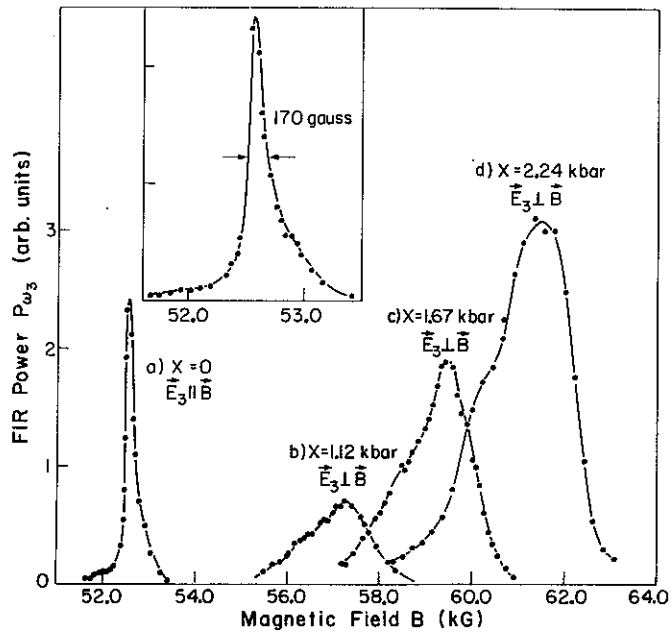

Fig. 3. Far-infrared power as a function of magnetic field (denoted as $\boldsymbol{B}$) for n-type InSb ($n_e = 5 \times 10^{15}$ cm^{-3}) at 1.8 K in the $X\|\boldsymbol{B}\|[111]$ geometry. Polarization of the emitted radiation (denoted as $\boldsymbol{E}_3$) is shown. (a) $X=0$, the asymmetric shape of the curve is illustrated in the same inset. (b)–(d) The electric-dipole emission due to k-linear terms of the Hamiltonian for different values of X (Jagannath and Aggarwal 1985).

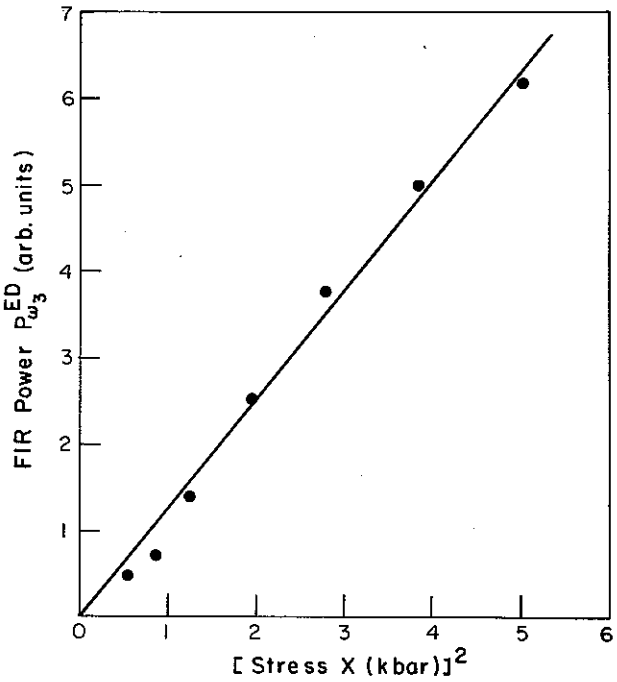

Fig. 4. Far-infrared power as a function of X^2. The solid line is the least squares fit to the data shown by dots (Jagannath and Aggarwal 1985).

$Pb_{1-x}Ge_xTe$ crystals experiencing a structural phase transition $O_h \rightarrow C_{3v}$. In their cubic modification (at $T > T_c$) these crystals have a band structure typical of Pb salts (section 8). Electron and hole bands have four extrema, positioned in the L points. After the phase transition ($T < T_c$) the symmetry axis is directed along [111]. As a result, three extrema remain equivalent to each other but are positioned in very low symmetry points ($G_k = C_s$), whereas the fourth extremum is on the symmetry axis ($G_k = D_{3d}$). This situation is reminiscent of Bi (see section 8) but with the difference that there is no inversion centre in the lattice having the symmetry C_{3v}, and therefore the bands for arbitrary $\boldsymbol{k}$ are not degenerate. Thus, k-linear terms appear in the spectrum. EDSR was observed by Fantner et al. (1980) at $x = 0.01$. Calculations by Bangert (1981) show that EDSR becomes considerably stronger at transition to the rhombohedral phase.

6. *Inversion asymmetry mechanism for n-type InSb bands*

In crystals with sphalerite symmetry the expansion $f_i(\boldsymbol{k})$ starts with k^3. The COR theory for this case was formulated by Rashba and Sheka (1961a). Here, like

in the systems described in section 5, the spinor representation $D_{1/2}$ is acting. In the reference system formed by the crystallographic axes, apart from the pseudovector of the T_d group constituted by Pauli matrices, there is another pseudovector whose components are

$$\kappa_j(\hat{k}) = \hat{k}_{j'}\hat{k}_j\hat{k}_{j'} - \hat{k}_{j''}\hat{k}_j\hat{k}_{j''}, \tag{6.1}$$

where j, j' and j'' form a cyclic permutation. This notation already implies noncommatativity of the operators $\hat{k}_j$ (2.5). The electron Hamiltonian equals

$$\mathscr{H} = \hbar^2\hat{\boldsymbol{k}}^2/2m^* + \tfrac{1}{2}g\mu_B(\sigma\boldsymbol{H}) + \delta_3(\boldsymbol{\sigma\kappa}). \tag{6.2}$$

Before calculating the explicit form of the matrix element of the velocity by means of the formulas from section 3, let us find out, using the rules of section 4, possible transitions and their intensity indicatrices. The Hamiltonian (6.2) is approximate and can be derived from the Kane Hamiltonian by projecting it onto the conduction band (see (B.1), (B.2) and (B.4)). In the two-branch approximation, eigenvalues of the Hamiltonian $\mathscr{H}_0$ can be chosen as

$$\Psi^{(+)}_{N+1/2} = \begin{vmatrix} \psi_N \\ 0 \end{vmatrix} \equiv |N\uparrow\rangle \Rightarrow |N+\tfrac{1}{2}\rangle,$$

$$\Psi^{(-)}_{N-1/2} = \begin{vmatrix} 0 \\ \psi_N \end{vmatrix} \equiv |N\downarrow\rangle \Rightarrow |N-\tfrac{1}{2}\rangle, \tag{6.3}$$

The arrows here mark transformation to the notation in terms of the AQM formalism.

The notation in terms of the Landau oscillator eigenfunctions ψ_N is convenient since it clearly points to possible transitions between Landau levels. On the other hand, a general analysis is conducted in terms of AQM m, which in accordance with (6.3) can be easily brought into correlation with N:

$$m = N + \tfrac{1}{2} \quad \text{(for spin-up)},$$
$$m = N - \tfrac{1}{2} \quad \text{(for spin-down)}. \tag{6.4}$$

The probability of a spin-flip transition $+ \to -$ with a change in the Landau levels $N \to N'$ is determined by the velocity matrix element

$$\langle\downarrow N'|V_\tau|N\uparrow\rangle \Rightarrow \langle N' - \tfrac{1}{2}|V_\tau|N + \tfrac{1}{2}\rangle \equiv \langle m'|V_\tau|m\rangle. \tag{6.5}$$

In this form the matrix element of V_τ is defined in the basis of the functions with a given AQM, and therefore the rules of section 4 are applicable to it. In particular, its angular dependence is determined by the coefficient $\mathscr{B}^{(3)}_{-\alpha}(\theta, \phi)$ with $\alpha = m' - m - \tau = N' - N - \tau - 1$. The intensity indicatrices in conformity

with (4.11) and (B.15) are

$$\Omega_\alpha = |\mathscr{B}_{-\alpha}(\theta, \phi)|^2 = |\mathscr{B}_\alpha(\theta, \phi)|^2 \tag{6.6}$$

(the superscript 3 is dropped). They are equal to

$$\Omega_0 = 9I_0, \qquad \Omega_2 = I_2 - 3I_0 - I_1,$$
$$\Omega_1 = 2I_1, \qquad \Omega_3 = \tfrac{9}{2}(I_1 + 8I_0). \tag{6.7}$$

Here I_0, I_1 and I_2 are cubic harmonics

$$I_0 = h_x^2 h_y^2 h_z^2,$$
$$I_1 = h_x^2(h_y^2 - h_z^2) + h_y^2(h_z^2 - h_x^2) + h_z^2(h_x^2 - h_y^2),$$
$$I_2 = h_x^6 + h_y^6 + h_z^6, \tag{6.8}$$

and $h_i = H_i/H$. Formulas (6.7) and (6.8) follow from (B.11)–(B.14).

Possible COR transitions in n-type InSb are given in fig. 5. The general analysis also indicates a possibility of transitions with $|\Delta m| = |\Delta N| \leqslant 4$. In fact, $|\tau| \leqslant 1$ and in (B.23) $|\alpha| \leqslant 3$. Transitions with $|\Delta N| > 2$ are possible only as long as the dispersion law is nonparabolic (cf. section 5). Therefore in the conduction band these transitions are weakened (but in the valence band there are no restrictions for their intensity (cf. section 4)). Thus, for the Hamiltonian (6.2) spin-flip processes can be accompanied by transitions with $\Delta N = 0, \pm 1, \pm 2$ only. They occur at frequencies $\omega_s = \omega_c|\beta^*|$, $\omega_c(1 \pm \beta^*)$ and $\omega_c(2 \pm \beta^*)$, if as usual $|\beta^*| < 1$. In contrast to CR and EPR, COR is, as a rule, observable in all three polarizations. The COR intensity is strongly anisotropic whereas the CR and EPR anisotropy is weak and is caused by effects not considered above (warping, etc.).

Let us now calculate the matrix elements of the velocity. If the mean energy of an electron is of the order $\hbar\omega_c$ (3.4) and $(m^*\delta_3)_{a.u.} \approx 1$ (this holds for n-type InSb, see section 7), the condition $\gamma \ll 1$ (3.1) is fulfilled even in strong magnetic fields $H \approx 5 \times 10^4$ G. Thus, one can make use of the results of section 3.

The nonzero coefficients $F^{(j)}_{\{i\}}$ equal

$$F^{(j)}_{j'jj'} = 1, \qquad F^{(j)}_{j''jj'} = -1. \tag{6.9}$$

Now use formula (3.16). The products of this formula have two operator factors applicable to the case under study and the matrix elements of the velocity are

$$\langle N'\downarrow|V_\tau|N\uparrow\rangle = 2^{1/2}k_H^2\frac{\delta_3}{\hbar}\frac{N' - N - \beta^*}{N' - N - \beta^* - \tau}\sum_{\beta\gamma} B_{(\tau\beta\gamma)}\langle N'|a_\beta a_\gamma|N\rangle. \tag{6.10}$$

The coefficients $B_{(\tau\beta\gamma)}$, which are symmetric with respect to all subscripts, are expressed via ternary products of the elements of the matrix $\boldsymbol{B}$ (Addendum A), $B_{(\bar{1}\bar{1}\bar{1})}$ being zero. Among the other coefficients there are only four independent

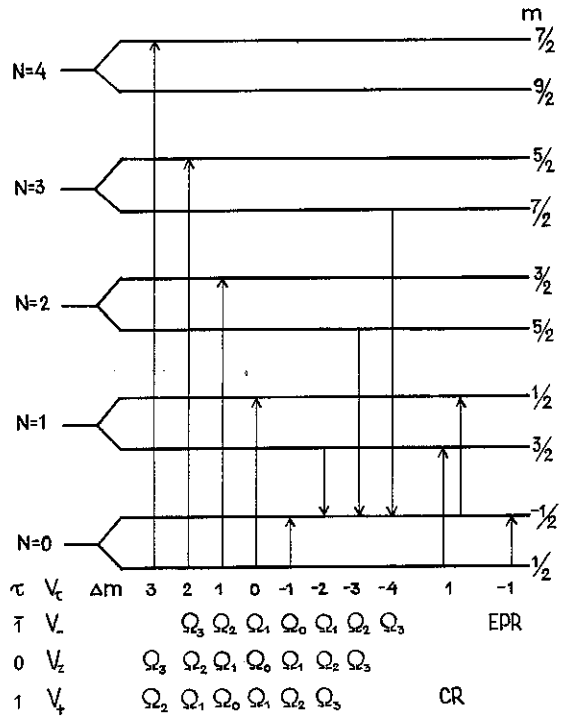

Fig. 5. Scheme of COR transitions in n-type InSb for the inversion asymmetry mechanism ($g < 0$). Under the transition the respective values of Δm and of the intensity indicatrix for all polarizations τ are given. The transitions with $\Delta N = 3$ and $\Delta N = 4$ are forbidden in the Zeeman limit for the Hamiltonian (6.2). Polarizations in which CR and EPR are excited are also indicated, their indicatrices being isotropic.

coefficients (Rashba and Sheka 1961a). The fact that there are just four of them is dictated by formula (B.23). $\mathscr{B}_\alpha(\theta, \phi)$, entering in (4.10) as factors at the corresponding step-operators, are expressed via these coefficients according to (B.16).

The theory predicted that the EDSR and CFR intensities would exceed that of EPR (Rashba and Sheka 1961a,b), and this was confirmed experimentally. The latest data show $\delta_3 = -56$ a.u. (section 7). The EDSR induced by k^3-terms was first discovered in n-type InSb by Dobrowolska et al. (1983) in the longitudinal $\boldsymbol{e} \| \boldsymbol{H}$ polarization (fig. 6). The angular dependence of the observed resonance intensity at a rotation of the specimen around the wave vector $\boldsymbol{q}$ at $\boldsymbol{q} \| [100]$ in agreement with the theory is perfectly described by the function Ω_1. This convincingly proves that k^3-terms, i.e., the inversion asymmetry mechanism, are responsible for the observed EDSR.

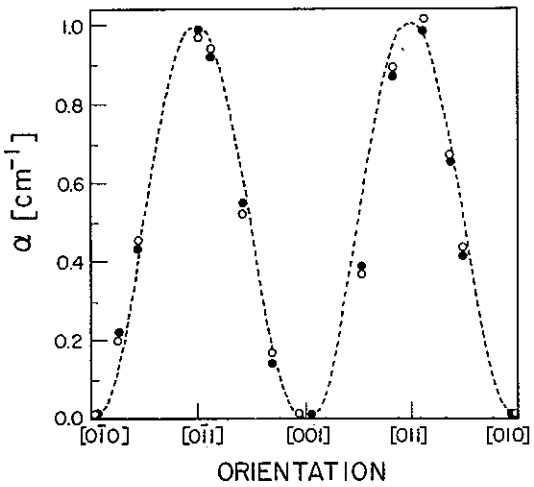

Fig. 6. EDSR intensity in n-type InSb as a function of the orientation of $\boldsymbol{H}$ in the (100) plane. Black and white dots indicate opposite orientations of the field. The dashed line is the theoretical dependence for this plane (Rashba and Sheka 1961a), normalized to the experimental data for $\boldsymbol{H} \parallel [011]$. The data were observed at 4.5 K at 118.8 μm on a sample with $n_e = 3.6 \times 10^{14}\,\mathrm{cm}^{-3}$, 4 mm thick (Dobrowolska et al. 1983).

7. *EDSR and EPR interference*

It follows from (3.5) that simultaneous excitation of EDSR and EPR is possible, but their interference occurs only if certain conditions are satisfied. The interference term in the absorption spectrum is proportional to the correlation function $\langle \tilde{\mathscr{H}}_e(t)\tilde{\mathscr{H}}_m(t)\rangle$. Statistical averaging in this function involves integration in K_Z. The integral is nonzero only if $\tilde{\mathscr{H}}_e$ and $\tilde{\mathscr{H}}_m$ have the same parity with respect to $\boldsymbol{k}$. Consequently, interference is possible only if there are terms which are odd with respect to $\boldsymbol{k}$ in $\mathscr{H}_{so}(\boldsymbol{k})$. The interference is strong if $\tilde{\mathscr{H}}_e$ and $\tilde{\mathscr{H}}_m$ do not strongly differ in magnitude. These two conditions are fulfilled in n-type InSb where $\mathscr{H}_{so} \propto k^3$ and the EPR intensity due to a large value of the g-factor ($g \approx -50$) is high. The theory was developed by Sheka and Khazan (1985), Chen et al. (1985b), and Gopalan et al. (1985) on the basis of the work by Rashba and Sheka (1961a).

The first COR experiments were carried out in the millimeter wavelength range, and therefore a natural way to distinguish between EDSR and EPR was to put a specimen into positions where either $\tilde{E}$ or $\tilde{H}$ reach their maximum (Bell 1962, McCombe et al. 1967). In observing the spin resonance in the infrared wavelength range ($\lambda \sim 100$ μm), as has been done in recent experiments, such spatial separation is of course impossible, so EPR occurs on the background of EDSR. This is what creates the possibility of their interference.

In the Faraday geometry, in neither of the circular polarizations is there interference: in one of them EPR is not excited, while in the other the difference in phases of the matrix elements of $\tilde{\mathscr{H}}_e(t)$ and $\tilde{\mathscr{H}}_m(t)$ equals $\pi/2$. In the longitudinal Voigt polarization ($\boldsymbol{q} \perp \boldsymbol{H} \| \tilde{\boldsymbol{E}}$) the SR intensity anisotropic part is proportional to (Sheka and Khazan 1985):

$$I_s(\boldsymbol{q}, \boldsymbol{h}) = \Omega_1(\boldsymbol{h}) - \frac{2\hbar\omega_s}{3\delta_3 k_H^3} \frac{q}{k_H} \sum_i \frac{q_i}{q} \kappa_i(\boldsymbol{h}). \tag{7.1}$$

The first term describes EDSR, the second EDSR and EPR interference. The isotropic term, responsible for EPR, is dropped. A similar result was obtained by Chen et al. (1985b). In the geometry of fig. 6 the interference term vanishes.

The second term in (7.1) is odd with respect to $\boldsymbol{q}$ and $\boldsymbol{H}$, therefore I_s varies at separate inversion of both $\boldsymbol{q}$ and $\boldsymbol{H}$, but remains unaltered at their simultaneous inversions, which is in essence the effect discovered by Dobrowolska et al. (1983). It is illustrated in fig. 7. Rotation of the specimen by 180° corresponds to the reversal of $\boldsymbol{q}$ or $\boldsymbol{H}$. The dependence of the spectrum on the sign of $\boldsymbol{q}$, i.e., a strong spatial dispersion, is at first glance quite unexpected at such a large wavelength of the light (~ 100 μm). This dispersion is caused by the EDSR and EPR interference (Dobrowolska et al. 1983). The influence of the interference upon the angular indicatrix is shown in fig. 8. It is noteworthy that the

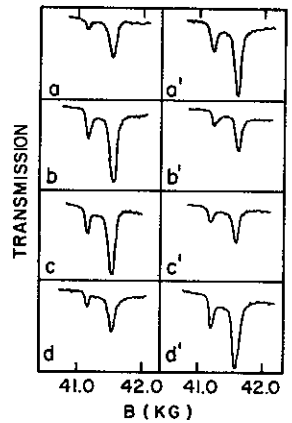

Fig. 7. Variation of the EDSR spectrum in n-type InSb at rotation of the sample, observed in the longitudinal Voigt geometry at 118.8 μm and 4.5 K with $n_e = 2.3 \times 10^{14}$ cm^{-3}. The sample faces are in the (110) plane. (a) EDSR for $\boldsymbol{H} \| [1\bar{1}0]$, $\boldsymbol{q} \| [110]$. (b) The sample has been rotated by 180° about $\boldsymbol{q}$ relative to (a). (c) The sample has been rotated by 180° about $\boldsymbol{H}$ relative to (a). (d) It has been rotated by 180° about $\boldsymbol{q} \times \boldsymbol{H}$ relative to (a). The sequence (a')–(d') corresponds to configurations (a)–(d), respectively, but with the magnetic field reversed. In each resonance doublet the higher-field, stronger line is the free-electron EDSR, and the weaker line is EDSR of donor-bound electrons (Dobrowolska et al. 1983).

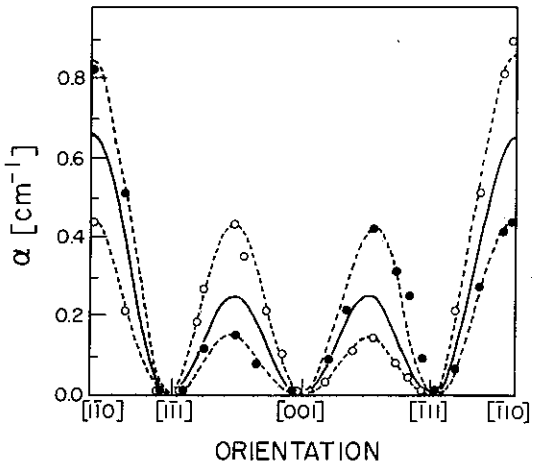

Fig. 8. EDSR intensity as a function of the orientation of $\boldsymbol{H}$ in the (110) plane for $\boldsymbol{q} \| [110]$ (longitudinal Voigt geometry). Black and white circles correspond to opposite signs of $\boldsymbol{H}$, respectively. The solid line is the theoretical angular dependence of EDSR (Rashba and Sheka 1961a). The dashed curves are guides for the eye, connecting experimental points (Dobrowolska et al. 1983).

interference is strong although the ratio of the EPR intensity to the EDSR intensity does not exceed 0.02.

It is very important that this interference opens up a unique possibility for finding not only the magnitude but also the sign of δ_3 from SR. To help us understand the situation it is essential that in the T_d group the [111] axis be polar, i.e., the directions [111] and $[\bar{1}\bar{1}\bar{1}]$ must be physically nonequivalent. The manifestation of this fact is that the opposite faces of a crystal are not equivalent. So, for a conventional choice of the direction [111] the face whose external normal is [111], consists of group III atoms, whereas the opposite face consists of group V atoms. Therefore these faces exhibit different behaviour when the sample is etched; this is how they were specified by Dobrowolska et al. (1983).

The choice of a reference system which is consistent with this definition of the (111) face is unambiguous. It is clear from the arrangement of surfacial atoms on this face (Gatos and Levine 1960) that if the origin is chosen at a site where a group III atom is positioned, then one of its nearest group V neighbours lies in the first octante. Therefore the sign of δ_3 has an absolute sense.

First Rashba and Sheka (1961b) estimated δ_3 as $|\delta_3| \approx 200$ a.u.; McCombe (1969) found the upper limit for $|\delta_3| \lesssim 50$ a.u., Sheka and Khazan (1985), by processing the data given in fig. 8, obtained $\delta_3 \approx -75$ a.u.; Chen et al. (1985b) and Gopalan et al. (1985), using the whole variety of experimental data, found that $|\delta_3| \approx 56$ a.u.; and Cardona et al. (1986a), after performing numerical calculations, concluded that $\delta_3 = 54 \pm 3$ a.u. The difference in sign is accounted

for by the choice of the opposite reference system. In their following paper, Cardona et al. (1986b) gave an experimental value of $\delta_3 = 56 \pm 3$ a.u.

8. COR in semiconductors with inversion centre

The COR mechanism considered in sections 5 and 6 is missing in crystals with an inversion centre. This mechanism is caused by the splitting of bands in the vicinity of the point $\boldsymbol{k} = 0$, described by formulas (2.2) and (3.2). In crystals with an inversion centre, all bands are twofold degenerate in the entire $\boldsymbol{k}$-space (Elliott 1954), therefore splitting of the kind which was discussed in sections 5 and 6 is absent. That is why we must take into account other COR mechanisms, usually induced by higher order terms in k in $\mathscr{H}_{so}$. Such terms can be constructed using the method of invariants. Some of these terms can be conveniently interpreted as the dependence of the g-factor on $\hat{\boldsymbol{k}}$.

The COR theory for crystals with the inversion centre was first formulated by Boiko (1962) for electrons in Si and Ge. In Si the minima of the band are located on the $\langle 001 \rangle$ axes in the general position points. In these points the wave vector group is $G_k = C_{4v}$. The situation is akin to the one in wurtzite (section 5) in the sense that EDSR is induced by k-linear terms in $\mathscr{H}_{so}$. However, an important difference is that in Si these terms are H-proportional. Therefore EDSR is much weaker than in wurtzite-type semiconductors. According to the estimates made by Boiko (1962), $I_{EDSR} \sim I_{EPR}$. EDSR must be present in all polarizations. In Ge the minima are on the boundary of the Brillouine zone in the $\langle 111 \rangle$ directions and $G_k = D_{3d}$. $\mathscr{H}_{so}$ is linear in H and quadratic in k. The operators $\boldsymbol{r}$ and $\boldsymbol{v}$ are linear in $\hat{\boldsymbol{k}}$. EDSR and the electric-dipole CFR must have comparable intensities, which according to Boiko's estimates (1962) may exceed the EPR intensity by one order at an electron concentration of $\sim 10^{14}\,\mathrm{cm}^{-3}$. With increasing concentration this ratio must increase. As far as we know, COR has not so far been observed for band electrons either in Ge or in Si.

The $\mathscr{H}_{so}$ dependence on $\boldsymbol{k}$ is particularly strong in the presence of narrow gaps in the spectrum. In this respect it is helpful to study p-type Ge subjected to uniaxial strain. The strain cancels out the fourfold degeneracy at the top of the valence band, the gap $2\varepsilon_0'$ in the spectrum being proportional to the stress T. On the basis of the Hamiltonian derived by Bir and Pikus (1959) the theory was constructed by Gurgenishvili (1963) for $\boldsymbol{H} \| T \|$ [001] and by Hensel (1968) for $\boldsymbol{H} \| T \|$ [111]. In the latter case, if $\varepsilon_0' \gg \eta$ (where η is the Fermi energy of holes) one can obtain an effective two-branch Hamiltonian $\mathscr{H}_{so}$ by mapping the 4×4 hole Hamiltonian onto a subspace with the angular momentum projection $\pm 1/2$, corresponding to the upper branch of the strained crystal spectrum:

$$\mathscr{H}_{so} \propto \frac{(\hbar\omega_c)^2}{\varepsilon_0'} \frac{K_Z}{k_H^2} (\hat{K}_- \sigma_+ + \hat{K}_+ \sigma_-). \tag{8.1}$$

Formula (8.1) is written in the reference system, associated with $\boldsymbol{H}$. It is clear from this formula that in the longitudinal $\tilde{\boldsymbol{E}} \| \boldsymbol{H}$ polarization there are only transitions with $\omega = \omega_c - \omega_s$. The experimental data obtained by Hensel (1968) are exhibited in fig. 9. The solid curves are a result of the exact diagonalization of the 4×4 Hamiltonian, which was indispensable since the spectrum of holes was noticeably nonequidistant. This is obvious from the great difference in the frequencies of transitions of the same type. The high precision of the experimental data and their thorough processing made it possible for the first time to find the g-factor of holes in Ge.

Schaber and Doezema (1979 a, b) observed EDSR in n-type PbTe in the Faraday geometry. PbTe is a narrow-gap direct semiconductor with a lattice of the NaCl-type. The extrema of the bands are located at the L points (on the boundary of the Brillouine zone). The isoenergetic surfaces are almost ellipsoid-like and differ only slightly for electrons and holes. It is natural to expect that in such a system the nonparabolicity mechanism will be dominating in EDSR (section 9). However, the authors assert that the EDSR intensity observed was

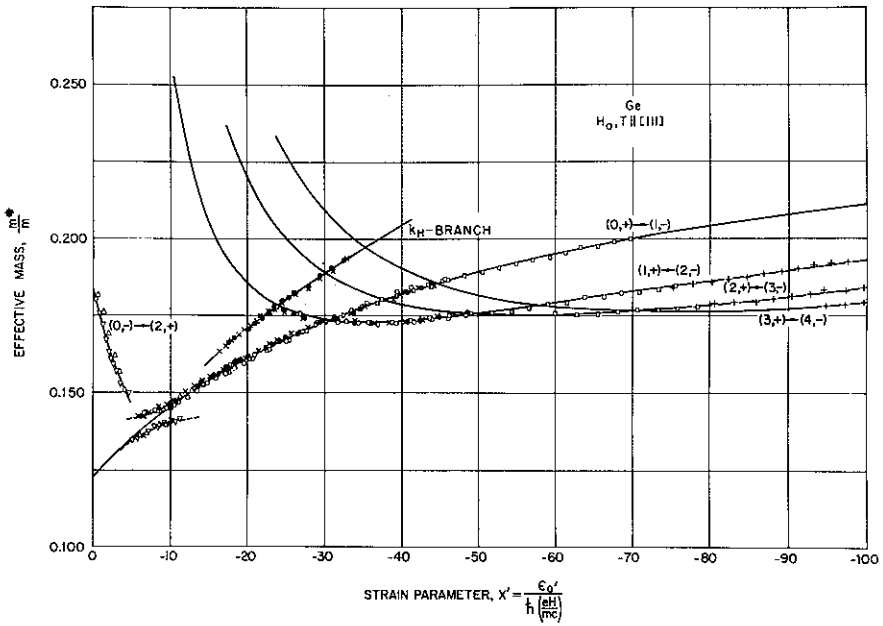

Fig. 9. Positions of COR bands for p-type Ge as a function of the dimensionless strain parameter x', $\boldsymbol{T}$, $\boldsymbol{H}$, $\tilde{\boldsymbol{E}} \| [111]$, the temperature is 1.2 K, $\upsilon = 52$ GHz. The resonance frequencies are expressed in terms of the 'effective mass' m^*; m is the electron mass in vacuum. Quantum numbers, corresponding to the strong strain limit (in contrast to the figure in the original paper, Hensel (1968)), label energy levels. The 'k_H-branch' is interpreted as a transition $(0, +) \rightarrow (1, -)$ for electrons with large values of K_Z.

much higher than implied by the theory. The dominating EDSR mechanism remains rather obscure.

Of great interest is the mechanism of spin transitions in Bi and Sb. Although there is an extensive literature on the electronic properties of these materials, the mechanism of spin transitions in them remains rather vague. The Bi lattice results from a parent cubic lattice due to a slight trigonal deformation. The result of this deformation is a semimetallic spectrum with three electron pockets and one hole pocket (Abrikosov and Fal'kovskii 1962). The electron pockets are positioned at the low symmetry points of the Brillouine zone and the hole pocket is located at the high symmetry point. Fermi surfaces of electrons and holes resemble strongly prolate ellipsoids; the presence of small masses in the spectrum indicates the existence of narrow gaps. The two-band Cohen–Blount model (1960) satisfactorily describes certain properties of electrons in Bi. However, the shape of the Fermi surface shows considerable deviation from this model (McClure and Choi 1977).

Observations of the resonance at the frequencies ω_s and $\omega_c \pm \omega_s$ on electrons in Bi and Sb were first reported by Smith et al. (1960). However, the assignment of bands proposed by them was later rejected. A new announcement of the observation of SR and CFR bands (the frequency $\omega_c - \omega_s$) was made by Burgiel and Hebel (1965). Due to nonparabolicity, they observed several bands of each type; their intensities were much lower than the CR intensity.

For electrons in Bi, the following competing mechanisms were discussed:

(*i*) due to the narrow gap, the nonparabolicity mechanism may be of importance. This theory was formulated by Wolff (1964) on the basis of the Cohen–Blount model, in close analogy with the theory of the Dirac electron in a magnetic field;

(*ii*) the influence of other adjacent bands is possible (Yafet 1963);

(*iii*) due to its low symmetry, the electron Hamiltonian must involve terms of the order Hk, which have a lower order in k than the nonparabolicity mechanism.

As far as we know, there are not yet sufficiently detailed experimental data to make it possible to find out the dominating COR mechanism for electrons.

Thanks to the study by Verdun and Drew (1976), the situation pertaining to holes in Bi is now much better understood. They showed that the theory based on the two-band Hamiltonian (Wolff 1964) cannot adequately describe the experimental results. The interpretation they proposed is based on the EMA Hamiltonian involving terms up to k^4. The coefficients attached to these terms were found from the calculations made by Golin (1968) and then corrected within the error-rate admissible for the theory, to get agreement with the experimental data. This procedure makes it possible to take into account the real band structure, including several adjacent bands. As a result, Verdun and Drew (1976) succeeded in describing versatile experimental data on EDSR and on the electric-dipole CFR in the Faraday and Voigt geometries, including

angular indicatrices of the position and of the intensity of the bands.

McCombe et al. (1974) reported that they observed in the far infrared spectrum of the n-type $Bi_{0.885}Sb_{0.115}$ alloy a band which they assigned as the electron EDSR with $\omega_s > \omega_c$.

9. *COR in narrow-gap and zero-gap semiconductors*

This section is devoted to COR in narrow-gap semiconductors of the InSb type and in zero-gap semiconductors of the HgTe type. It is natural that the theory for such semiconductors should be constructed on the basis of the Kane model (Addendum B). In the framework of this model, by introducing a relatively small number of parameters, one can describe a wide variety of electron properties of crystals, including the strong nonparabolicity effect induced by a small value of E_G. It is very important that the Kane model enables one to find Landau levels with high accuracy in the conduction and valence bands. It is possible to find a set of parameters entering the Hamiltonian if the theoretical positions of these levels optimally match the relevant experimental data. The Landau quantization theory for the Kane model was developed in papers by Bowers and Yafet (1959) and Lax et al. (1961). Pidgeon and Brown (1966) and Pidgeon and Groves (1969) proposed the formulation of the theory which is now used as standard. The most complete form of the 8×8 Hamiltonian, involving k-linear and k-quadratic terms, was proposed by Weiler et al. (1978). Numerical values of the ten parameters of this Hamiltonian for InSb are contained in the paper by Littler et al. (1983), where they also carried out comparisons with results obtained by other workers. The values of most parameters are now definitely known, although certain parameters still need some improvement (Chen et al. 1985a).

The theory of COR arising due to nonparabolicity mechanism, was put forward by Sheka (1964) for InSb and later by Kacman and Zawadzki (1976) for zero-gap semiconductors. In each of these papers the authors employed the simplest form of the 8×8 Hamiltonian which allowed an exact analytical solution for the problem to be found. In this form, of all the nondiagonal terms only the P-proportional terms are retained. Numerical calculations of COR intensities based on a more general form of the 8×8 Hamiltonian were initiated by Bell and Rogers (1966). Now such calculations have become conventional. It is noteworthy that in order to find the position of energy levels, which are experimentally measured with high precision, numerical calculations are indispensable, particularly for the valence band. Even for the conduction band such calculations are justified if we are dealing with such weak effects as the energy dependence of the g-factor anisotropy (Ogg 1966, Chen et al. 1985a). However, for calculating COR intensities, especially for transitions between electron levels, sufficient accuracy can be achieved in the framework of the two-branch model.

By transforming the 8 × 8 Hamiltonian into a 2 × 2 Hamiltonian it is possible not only to simplify the calculations but also to get an adequate idea of the physical mechanism of the resonance formation.

Transformation of the 8 × 8 Hamiltonian into a 2 × 2 Hamiltonian is realized by means of the standard projection procedure (cf. section 3). The k^3 term in $\mathscr{H}_{so}$ with the coefficient δ_3 (B.4) in the 2 × 2 Hamiltonian (6.2) stems from the Pk and Gk^2 terms of the original Hamiltonian. The role of the k^3 term in COR was considered in section 6. The next power term in the expansion containing $\boldsymbol{\sigma}$ originates from nondiagonal P-proportional elements of the 8 × 8 matrix. This term is

$$\mathscr{H}_{so} = -g\mu_B(\boldsymbol{\sigma}\boldsymbol{H})\frac{\hbar^2\boldsymbol{k}^2}{2m^*}\left(\frac{1}{E_G}+\frac{1}{E_G+\Delta}\right), \tag{9.1}$$

where m^* and g are determined by formulas (B.1) and (B.2). Since $H \propto k_H^2$, $\mathscr{H}_{so}$ must be regarded as a quantity of the order of k^4. If we compare formula (B.4) for δ_3 with (9.1), it becomes clear that the large factor gm_0/m^* enters in (9.1). Therefore although the k^3 terms in the EMA formalism are lower powers in comparison with the k^4 terms, the latter are comparable with them at relatively small values of k. This means that the k^4 terms are relatively large.

It is important to understand the physical meaning of $\mathscr{H}_{so}$ (9.1). The operator $\mathscr{H}_{so}$ is diagonal if taken between the eigenfunctions of the operator $\mathscr{H}_0$ (3.9). This can be regarded as a correction to the g-factor due to nonparabolicity (cf. (B.2)). Since $\mathscr{H}_{so}$ is diagonal, it cannot excite electric-dipole transitions, and in particular, it cannot excite COR. The term of the order of $(\boldsymbol{k}^2)^2$, also entering the Hamiltonian, does not cause spin transitions either. This term can be regarded as a correction to m^* due to nonparabolicity (cf. (B.1)). Thus the nonparabolicity terms in the 2 × 2 Hamiltonian, considered here, do not lead to COR.

Nevertheless, COR does occur but its origin is different. If the projection operation is performed by means of the Luttinger–Kohn procedure (1955), the matrix $\hat{T}$ is determined by formula (3.7a). The perturbation is the terms of the 8 × 8 operator containing P. The transformed operator of the coordinate $\hat{\boldsymbol{r}}$ is calculated according to (3.8b)

$$\hat{\boldsymbol{r}} = \exp(\hat{T})\boldsymbol{r}\exp(-\hat{T}) \approx \boldsymbol{r} + [\hat{T}, \boldsymbol{r}] + \tfrac{1}{2}[\hat{T}[\hat{T}, \boldsymbol{r}]] \equiv \boldsymbol{r} + \boldsymbol{r}_{so}. \tag{9.2}$$

Since $\boldsymbol{r}$ can be regarded as a diagonal operator (see the end of Addendum B) and $\boldsymbol{v}_{so}$ contains only interband terms (table 2), then $[\hat{T}, \boldsymbol{r}]$ does not contribute to the 2 × 2 operator. Calculation of the second commutator yields

$$\boldsymbol{r}_{so} = \frac{\hbar^2 g}{4m_0}\left(\frac{1}{E_G}+\frac{1}{E_G+\Delta}\right)(\boldsymbol{\sigma}\times\boldsymbol{k}). \tag{9.3}$$

This formula was derived by Yafet (1963). The SO contribution to the velocity stems from communication of (9.2) with $\mathscr{H}_0$. Thus, the COR mechanism, which

is conventionally called a 'nonparabolicity' mechanism, in this case is ensured not by the nonparabolicity terms in the Hamiltonian but by the SO contribution to the coordinate operator.

The relation (9.3) is spherically symmetric, and therefore the selection rules entail from the angular momentum conservation. Since in n-type InSb $g < 0$, EDSR is excited in the CRI polarization. For the same reason in n-type InSb in the longitudinal polarization a transition is excited at the frequency $\omega_c + \omega_s$, AQM at this transition remaining unaltered.

COR at the frequency $\omega_c + \omega_s$ in n-type InSb was discovered by McCombe et al. (1967). The experiments were carried out in the range 300–650 cm^{-1}, ensuring the fulfillment of the weak scattering criterion $\omega\tau \gg 1$ (where τ is the relaxation time). The experimental data collected in fig. 10 show that COR is observed in agreement with the theory only in the longitudinal Voigt polarization. In the conditions of the experiments conducted by McCombe et al. (1967) the nonparabolicity mechanism for the band $\omega_c + \omega_s$ is much more efficient than the inversion asymmetry mechanism. One can check this by using the value of δ_3 cited in section 6 and the formulas for the COR intensities for both mechanisms (Rashba and Sheka 1961a,b, Sheka 1964). Convincing arguments in favour of the dominating role of the nonparabolicity mechanism are given in the article by McCombe (1969). These arguments are based on the dependence of the intensity upon the orientation and magnitude of $\boldsymbol{H}$. The paper by McCombe et al. (1967) has been of major importance for COR studies, since the authors were the first to discover CFR, i.e., spin transitions induced by the a.c. electric field were observed in conditions satisfying the basic criterion of the theory $\omega\tau \gg 1$ (in an earlier paper of Bell (1962) EDSR was discovered in conditions where this

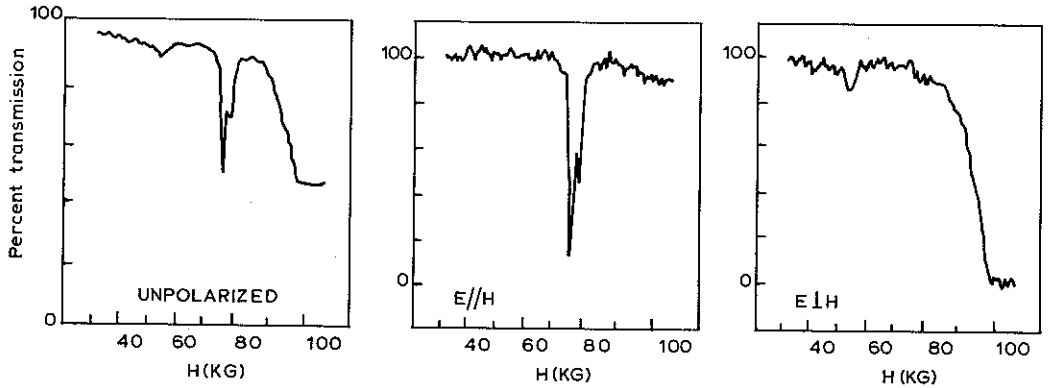

Fig. 10. Transmission spectra obtained at 500 cm^{-1} and 6 K for the 9.25 mm thick sample of InSb with carrier concentration $n_e = 2 \times 10^{14}$ cm^{-3} and carrier mobility 5×10^5 $cm^2/V\,s$ at 80 K. H is the magnetic field, and E is the a.c. electric field. The doublet structure of the transition reflects the presence of both free and localized electrons (McCombe et al. 1967).

criterion was violated; cf. section 13). In the same paper COR was used for determining the g-factor for the $N = 1$ level. The energy of a quantum absorbed in COR is

$$\hbar\omega_{\mathrm{COR}} = \hbar\omega_{\mathrm{c}} + \tfrac{1}{2}\mu_{\mathrm{B}}H[g(N+1, H) - g(N, H)]. \tag{9.4}$$

Since $\omega_{\mathrm{c}}(H)$ and $g(N = 0, H)$ were known from the data on CR and SR, it became possible for the first time to experimentally find $g(N = 1, H)$ from CFR. Since then COR has been systematically used to study g-factors (McCombe (1969), Appold et al. (1978) in InSb, Pascher (1981) in PbTe, etc.). Some time later McCombe and Kaplan (1968) observed in the CFR spectrum a distinct pinning in the region of the resonance $\omega_{\mathrm{c}} = \omega_{\mathrm{LO}}$, and were able to find the constant of the coupling of electrons to optic phonons (Johnson and Larsen 1966). Observation of the pinning in the CFR spectrum is more reliable than in the CR spectrum, because the frequency at which the measurements are performed is remote from the reststrahlen region.

It is clear from (9.3) that matrix elements of EDSR and CFR differ by the factor $K_z r_H \ll 1$. Consequently, $I_{\mathrm{EDSR}}/I_{\mathrm{CFR}} \sim (\hbar\omega_{\mathrm{c}})^{-1} \max\{\eta, T\} \ll 1$. This inequality was well fulfilled under the actual conditions of the experiment by McCombe et al. (1967). Therefore, EDSR was weak and was not observed. Later, McCombe (1969) reported the observation of this transition at $T = 80$ K, where the probability of transition, judging by the afore-given estimate, must be higher. The temperature dependence of the shape of this band was also investigated (McCombe and Wagner 1971). Temperature dependence was observed in the transverse CRI polarization and its origin is ascribed to the nonparabolicity mechanism.

COR in the valence band is much more difficult to interpret in great detail, but at the same time is much more informative for finding numerical values of the parameters. COR in the valence band was studied in p-type InSb by Littler et al. (1983) and fig. 11 presents the experimental data for the strongest COR bands. The best fit of the theory with the experiment made it possible to improve the values of a number of the parameters of the 8×8 Hamiltonian. The difference in position of the resonances at $\boldsymbol{H} \| [111]$ and at $\boldsymbol{H} \| [100]$ testified to the anisotropy of hole states.

In its electron properties, $Hg_{1-x}Cd_xTe$ with $x > 0.16$ is analogous to InSb (at $x < 0.16$ its band structure is inverted). However, E_{G} is much smaller than in InSb ($E_{\mathrm{G}} \approx 60$ meV at $x \approx 0.2$) and due to this the nonparabolicity mechanism is much stronger. McCombe et al. (1970a) discovered EDSR in this material in the CRI polarization. The g-factor changed from -200 to -100 with H increasing up to 50 kG, in agreement with the theory (Bowers and Yafet 1959). The resonance intensity fell with increasing H according to H^{-1} in agreement with the predictions of the theory based on the nonparabolicity mechanism, and its absolute value was also found in agreement with the theory (Sheka 1964). Some time later the same team (McCombe et al. 1970b) discovered and studied COR

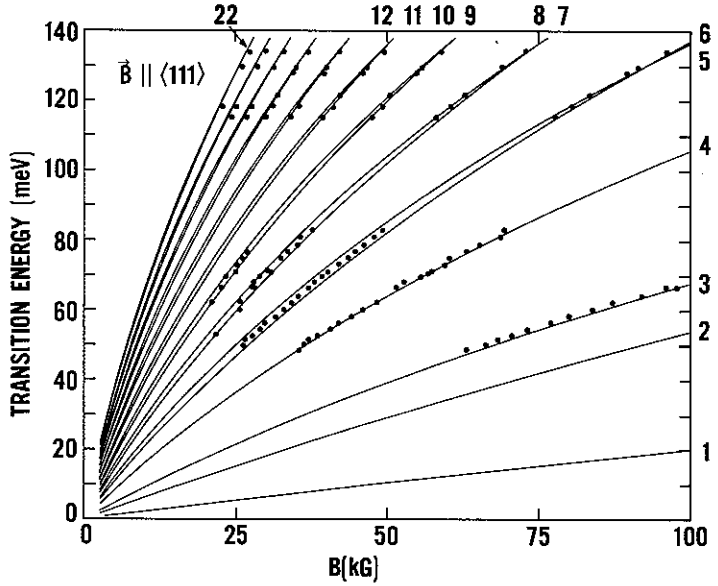

Fig. 11. COR transition energies, calculated from the 8×8 band model (solid lines) and the observed free-hole transitions (dots). B is the magnetic field. The numbers correspond to the following transition assignment: 1. $b^-(1) \rightarrow a^+(0)$; 2. $a^+(1) \rightarrow b^+(0)$, 3. $b^-(2) \rightarrow a^+(1)$; 4. $b^-(3) \rightarrow a^+(2)$; 5. $a^-(1) \rightarrow b^+(2)$; 6. $b^-(4) \rightarrow a^+(3)$; 7. $a^-(2) \rightarrow b^+(3)$; 8. $b^-(5) \rightarrow a^+(4)$; 9. $a^-(3) \rightarrow b^+(4)$; 10. $b^-(6) \rightarrow a^+(5)$; 11. $a^-(4) \rightarrow b^+(5)$; 12. $b^-(7) \rightarrow a^+(6)$; 13. $a^-(5) \rightarrow b^+(6)$; 14. $b^-(8) \rightarrow a^+(7)$; 15. $a^-(6) \rightarrow b^+(7)$; 16. $b^-(9) \rightarrow a^+(8)$; 17. $a^-(7) \rightarrow b^+(8)$; 18. $b^-(10) \rightarrow a^+(9)$; 19. $a^-(8) \rightarrow b^+(9)$; 20. $b^-(11) \rightarrow a^+(10)$; 21. $a^-(9) \rightarrow b^+(10)$; 22. $b^-(12) \rightarrow a^+(11)$. The designations are given as in the article by Weiler et al. (1978) (Littler et al. 1983).

in n-type $Hg_{1-x}Cd_xTe$ at the frequency $\omega_c + \omega_s$. This resonance was also excited by the nonparabolicity mechanism. COR in $Hg_{1-x}Cd_xTe$ was also observed by Golubev and Ivanov-Omskii (1977).

COR studies were also conducted in materials with the sphalerite lattice which has an inverted band structure. Pastor et al. (1981) investigated pure samples of HgSe with the electron concentration 4×10^{16} cm^{-3} at $T = 4$ K by measuring the transmission in the far infrared range. The EDSR band was discovered both in the longitudinal ($\tilde{E} \| H$) and transverse ($\tilde{E} \perp H$) polarizations. This unambiguously points to a considerable contribution of the inversion asymmetry mechanism. Actually, angular indicatrices are universal, i.e., independent of the dimensionality of the Hamiltonian (section 4) and therefore it is possible to employ the arguments given above for the 2×2 Hamiltonian. Approximately describing electrons by this Hamiltonian, Pastor et al. (1981) estimated the asymmetry coefficient as $\delta_3 \approx 300$ a.u. for the electron band. This value is 6 times as large as the one in InSb (section 7). COR bands were also

observed. The authors think that it is possible to explain the complexity of the observed bands by assuming that the contribution coming from the inversion asymmetry mechanism is large. Weiler (1982), after analyzing the experimental data obtained on HgSe, came to the conclusion that this mechanism is dominating for HgSe.

$Hg_{1-x}Mn_xTe$ with $x = 0.03$ was investigated by Witowski et al. (1982). This material is also a zero-gap semiconductor. EDSR was observed at $\tilde{\boldsymbol{E}} \perp \boldsymbol{H}$ and CFR was observed at the frequency $\omega_c + \omega_s$ at $\hat{\boldsymbol{E}} \parallel \boldsymbol{H}$. Both resonances were used for studying the dependence $\omega_s(T)$ in this semimagnetic semiconductor.

Tuchendler et al. (1973) studied properties of HgTe, which is also a zero-gap semiconductor, in the submillimeter frequency range. The experimental results were compared with the results of the calculation of the energy spectrum in the 8×8 model and its parameters were found on the basis of this analysis. In the Faraday geometry COR was observed at the frequency $\omega_c + \omega_s$.

In semimagnetic $Hg_{1-x}Mn_xTe$ with $x \approx 0.1$ a gap opens ($E_G \approx 50$ meV). This interesting system has not yet been sufficiently studied but observations of EDSR and CFR (Stepniewski and Grynberg 1985) as well as CFR involving spins of Mn ions (Stepniewski 1986) have been reported. (Concerning possible excitation mechanisms for the latter bands see the end of section 14.)

The energy spectrum of zero-gap semiconductors with the inverted band structure is modified in the presence of a slight tetragonal deformation. This situation, according to Bodnar (1978), is inherent in Cd_3As_2 and is described by the generalized Kane model. CFR transitions at the frequencies $\omega_c \pm \omega_s$ were observed by Thielemann et al. (1981) in the longitudinal Voigt geometry at $\boldsymbol{H} \parallel \boldsymbol{c}$, $\boldsymbol{c}$ is a unit vector along the tetragonal axis. The COR theory for this band structure was formulated by Singh and Wallace (1983).

10. COR on shallow local centres

We shall focus our attention here on large-radius impurity centres while sticking to our general concept, i.e., establishing a correlation between specific COR mechanisms and the respective terms of the EMA Hamiltonian. Here, as in the case of band carriers, EDSR and CFR are possible. In strong fields the orbital quantum number, changing in CFR, may be both a Landau level number with which the Coulomb spectrum of the centre is related, and a number of the level in this spectrum.

Let us start with EDSR. The first problem is whether the electron binding in the impurity centre affects the EDSR intensity. If it does, the effect should be especially strong in a weak field when $\hbar\omega_s \ll \mathscr{E}_I$, $\mathscr{E}_I$ is the ionization energy of the centre. Consider a situation typical of donors. If the band is degenerate with respect to the spin only, then in the limit $H \to 0$ there is only Kramers degeneracy in the ground state of the centre. The two spinor functions, belonging to the Kramers doublet, are Ψ and $K\Psi$, where K is the time reversal operator: $K\Psi = \sigma_y \Psi^*$. Writing out the matrix element of the coordinate $\boldsymbol{r}$ corresponding

to the electric-dipole transition between these states, and applying the operator K to this element, in accordance with the well-known rules (Wigner 1959), we get

$$(K\Psi, r\Psi) = (Kr\Psi, K^2\Psi) = -(Kr\Psi, \Psi) = -(K\Psi, r\Psi) = 0. \tag{10.1}$$

Here we have made use of the fact that the operator $\boldsymbol{r}$ is real and Hermitian, and also of the property $K^2 = -1$. Consequently, the matrix element vanishes in the zeroth order in H. In connection with (10.1) it is noteworthy that EDSR on band electrons, in contrast to the situation dwelt upon here, occurs between the states which are not Kramers conjugates. In the band, EDSR occurs between the states with opposite spin orientations but with the same value of the projection of the vector $\boldsymbol{k}$ onto $\boldsymbol{H}$. That is why constraints imposed by formula (10.1) are invalid for EDSR on band electrons.

Using this result, we can get estimates for r_{COR} and for v_{COR} by analogy with formula (3.17). Equation (10.1) shows that the transition is forbidden in the zeroth order, which gives rise to the appearance of the factor $\hbar\omega_s/\mathscr{E}_1$ in r_{COR}. The second small factor emerges when the mixing of levels induced by the SO interaction is taken into account. This factor is of the order $\delta_l k^l/\mathscr{E}_1$, where $k \sim R^{-1}$, and R is the radius of the electron state in the impurity centre. As a result, we get for the EDSR band (Rashba and Sheka 1964a)

$$r_{\mathrm{COR}} \sim (\hbar\omega_s/\mathscr{E}_1)(\delta_l R^{-l}/\mathscr{E}_1)R, \qquad v_{\mathrm{COR}} \sim r_{\mathrm{COR}}\omega_s. \tag{10.2}$$

The obtained estimate is correct if l is odd (as is the case for n-type CdS and n-type InSb). If l is even, it is necessary to introduce another small factor, since the transition is parity forbidden in the lowest order. Comparing (10.2) with (3.17) and putting in (3.17) $\bar{k} \sim r_H^{-1}$, we obtain the ratio of the EDSR matrix elements for bound and free electrons:

$$(r_{\mathrm{COR}})_{\mathrm{bound}}/(r_{\mathrm{COR}})_{\mathrm{free}} \sim (\hbar\omega_s/\mathscr{E}_1)^{(5-l)/2} \ll 1. \tag{10.3}$$

The inequality in (10.3) is valid, since in fact $l \leqslant 3$. Therefore the binding of carriers weakens the EDSR excited by the mechanisms induced by the SO coupling in the electron band.

Naturally, in the opposite limit of strong magnetic fields the difference in the intensity of the EDSR excitation on free and bound carriers vanishes.

The theory for an arbitrary ratio of $\hbar\omega_s$ to $\mathscr{E}_1$ was formulated in the paper by Rashba and Sheka (1964a) whose approach we shall follow below. The theory in this work was developed conformably to semiconductors with the extrema loop. In this case $\mathscr{H}_{so}$ is linear in k (see (5.3)). Since its value is usually small, it stands to reason to confine ourselves to the Zeeman limit $\mathscr{H}_{so} \ll \hbar\omega_s$.

The Hamiltonian $\mathscr{H}_0$ can be represented as

$$\mathscr{H}_0 = \mathscr{H}'_0 + \tfrac{1}{2}\hbar\omega_c L_H + \tfrac{1}{2}g\mu_B(\sigma H),$$

$$\mathscr{H}'_0 = -\frac{\hbar^2}{2m^*}\Delta - \frac{e^2}{\kappa_0 r} + \frac{m^*\omega_c^2}{8}\rho^2. \tag{10.4}$$

The eigenvalues of these operators are equal to $\mathscr{E}^{\pm}_{nm} = \mathscr{E}'_{n|m|} + \hbar\omega_c m/2 \pm \hbar\omega_s/2$ and $\mathscr{E}'_{n|m|}$, respectively. Here L_H is the projection of the angular momentum operator onto the direction of the magnetic field, $\boldsymbol{\rho}$ is the radius-vector in the plane, perpendicular to $\boldsymbol{H}$, and m is the magnetic quantum number. For simplicity, assume that m^* and g are isotropic. In this case to obtain the angular indicatrices of the longitudinal and transverse resonances, it is possible to make direct use of the results of sections 4 and 5.

Since $\mathscr{H}_0$ in (10.4) is axially symmetric and permits the introduction of the angular momentum m, all the results based on the symmetry arguments in section 5 are valid. Nevertheless, using table 1, one should bear in mind that the energy spectrum of the impurity centre is richer than the Landau spectrum of the band electron and that instead of $(m'-m)\omega_c \pm \omega_s$ there appear transition frequencies $(\mathscr{E}^{\pm}_{n'm'} - \mathscr{E}^{\mp}_{nm})/\hbar$. In the polarization τ the indicatrices Ω_α (4.11) with $\alpha = m' - m - \tau$ correspond to these transitions, and according to (5.17) $\Omega_1 \propto \cos^2\theta$ and $\Omega_0 \propto \sin^2\theta$. Experimental identification of the indicatrices must help to unambiguously assign the electric-dipole CFR bands. In particular, as in the case of free electrons, EDSR must be observed in the Faraday geometry in one of the circular polarizations (depending on the sign of the g-factor) and also in the longitudinal Voigt polarization.

The matrix element of the spin transition between the 'spin-down' and 'spin-up' states of the ground level, calculated in the first order of the perturbation theory in the parameter $\mathscr{H}_{so}/\hbar\omega_s$, is

$$\langle\uparrow|R_\tau|\downarrow\rangle = \delta_{\tau-1}\, 2^{1/2}(m^*\delta_1/\hbar^2)\hbar\omega_s \times \sum_{\substack{nm \\ n\neq 0}} \left\{ \frac{\langle 0|R^+_\tau|nm\rangle\langle nm|R_\tau|0\rangle}{\mathscr{E}'_0 - \mathscr{E}'_{n|m|} + \hbar\omega_\tau} + \frac{\langle 0|R_\tau|nm\rangle\langle nm|R^+_\tau|0\rangle}{\mathscr{E}'_0 - \mathscr{E}'_{n|m|} - \hbar\omega_\tau} \right\}. \tag{10.5}$$

Here $|nm\rangle$ are the eigenfunctions of the operator $\mathscr{H}'_0$ in the A′ system, corresponding to the quantum numbers n, m ($n=0$ is the ground state), $\hbar\omega_\tau = \hbar\omega_s - \hbar\omega_c\tau/2$, and the sign of ω_s in (10.5) coincides with the sign of the g-factor. The angular dependences of the matrix elements in (10.5) are identical to the ones of band electrons (formula (5.17)).

The presence of poles in (10.5) at

$$\hbar\omega_\tau = \mathscr{E}'_{n|m|} - \mathscr{E}'_0, \tag{10.6}$$

i.e., at the resonance of the spin transition frequency with the frequency of one of the allowed orbital transitions in the impurity centre, testifies to a strong dependence of the spin-flip transition intensity on H and to the existence of gigantic intensity resonances in it.

Infinite summation over n in (10.5) makes it difficult to get the results in the explicit form. Yet, it is possible to obtain them approximately if the sums in

(10.5) are interpreted as second-order corrections for certain auxillary Hamiltonians. Namely, they are for the transverse ($\tau = \pm 1$) resonance

$$\mathscr{H}_{\text{aux}} = \mathscr{H}'_0 - \hbar\omega_c L_Z + \varepsilon(R_1 + R_{\bar{1}}) \tag{10.7}$$

and for the longitudinal ($\tau = 0$) resonance

$$\mathscr{H}_{\text{aux}} = \mathscr{H}'_0 - \tfrac{1}{2}\hbar\omega_s \hat{\mathscr{J}} + \varepsilon R_0, \tag{10.8}$$

where $\hat{\mathscr{J}}$ is the operator of the spatial inversion. In both formulas the last term is perturbation. One can immediately check that the sum in (10.5) in either case can be obtained as the coefficient at ε^2 in the expression for the corresponding eigenvalue of the operator $\mathscr{H}_{\text{aux}}$. Determination of this coefficient by the eigenvalue of $\mathscr{H}_{\text{aux}}$, found by the variational method, is a handy means of calculating matrix elements (10.5).

Resonance growth of the EDSR intensity, predicted by Rashba and Sheka (1964a), was experimentally observed by Dobrowolska et al. (1982) for semimagnetic semiconductors. They are a unique object in which the resonance in the intensity can be observed in the region of relatively weak fields $\hbar\omega_c \ll \mathscr{E}_1$. Dobrowolska et al. (1982, 1984) used high-quality $Cd_{1-x}Mn_xSe$ crystals with $x = 0.1$ and 0.2. In these conditions the value of the g-factor is very large ($g \approx 100$). The experimental data are given in fig. 12. In the Faraday geometry, EDSR was observed in the CRA polarization and hence $g > 0$. The initial analysis of the experimental results was made on the basis of the Wolff (Dobrowolska et al. 1984) and Dietl (1983) theories for different versions of the two-level model. Later, Gopalan et al. (1986) carried out a new analysis of the experimental data. In fig. 12 the curve found by Gopalan et al. (1986) is plotted as well as the best fit obtained by us for the Hamiltonian (10.7) with a simple variational function (containing two exponents). The value we found for δ_1 is $|\delta_1| \approx 1.6 \times 10^{-3}$ a.u.

The EDSR mechanism studied above is entirely associated with k-linear terms in the dispersion law and is not specific for semimagnetic semiconductors. Yet in semimagnetic crystals there is a completely different SR mechanism, briefly described at the end of section 14.

The intensity of transitions at combinational frequencies for weak H has been calculated by Edelstein (1983).

The majority of experiments where COR was observed on donors were carried out in InSb in the conditions $\hbar\omega_c \gg \mathscr{E}_1$. Dickey and Larsen (1968) and McCombe and Kaplan (1968) observed that the resonance at the combinational frequency somewhat shifted with respect to $\omega_c + \omega_s$, due to the effect of the Coulomb field of the impurity. Another type of transition at combinational frequencies was observed by Kuchar et al. (1984). Although their proposed interpretation of the experimental data is rather tentative, there is no doubt that they observed combinations of ω_s with frequencies of the transitions within one Coulomb series. Analogous impurity CFR transitions had previously been

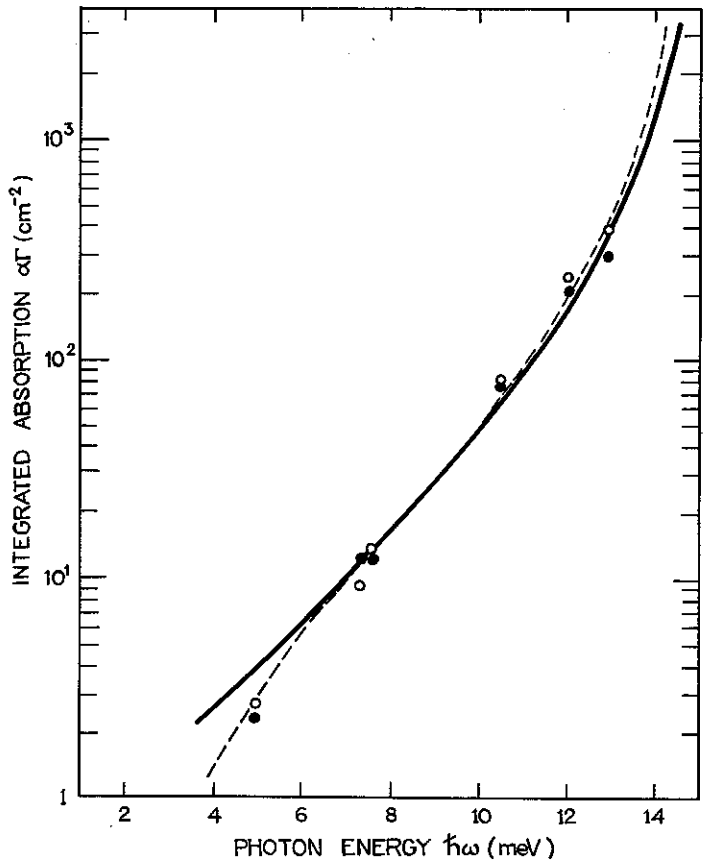

Fig. 12. Dependence of the EDSR intensity on the photon energy according to Dobrowolska et al. (1984). Here α is the absorption coefficient in the EDSR peak and Γ is the total resonance width at half maximum. Measurements were performed for the $Cd_{0.9}Mn_{0.1}Se$ crystal in the CRA polarization at $\boldsymbol{H} \| c$. Circles are experimental data (open circles, 4.7 K, black circles, 9.8 K). The solid line is the best fit with the Gopalan et al. (1986) theory, and the dashed curve shows the best fit with variational calculation.

reported by Lin-Chung and Henvis (1975) and Grisar et al. (1976) for frequencies associated with $\omega_c + \omega_s$ and $2\omega_c + \omega_s$ transitions respectively. EDSR was observed by McCombe and Wagner (1971) and later by other physicists. The EDSR band on bound electrons, observed by Dobrowolska et al. (1983) is shown in fig. 7; it is a bit shifted towards weak fields in comparison with the band corresponding to free electrons.

There are situations when the value of r_{COR} is much larger than the one ensuing from (10.2). For instance, the denominator can be much smaller than $\mathscr{E}_1$.

This is possible for a multivalley spectrum and also for COR on excited levels. Yet the most important case is the case of acceptors in crystals with degenerate bands (Rashba and Sheka 1964a, b).

By virtue of the degeneracy of hole bands in the Ge- and InSb-type of crystals, the ground state of the large-radius acceptors is fourfold degenerate. In the magnetic field it splits into levels with the angular momentum projections $m = \pm 1/2, \pm 3/2$. The levels with the same value of $|m|$ are Kramers conjugates. That is why for transitions between the levels with different values of $|m|$ the first factor in (10.2) is absent. The second small factor is also missing since the two-band spectrum corresponding to light and heavy holes implies strong SO interaction, the spacing between these bands of the spectrum at $k \sim R^{-1}$ noticeably exceeding $\mathscr{E}_I$. However, for EDSR to occur, it is necessary to introduce instead of these two factors a factor which is responsible for the absence of the central symmetry in the Hamiltonian of the impurity centre. In the hole Hamiltonian in crystals of the $A_{III}B_V$ type there is a nonrelativistic (and, consequently, large) term, proportional to $\hat{J}\boldsymbol{\kappa}(\hat{\boldsymbol{k}})$ (analogous to the $\boldsymbol{\sigma\kappa}$ term in formula (6.2)). The presence of this term enables one to construct the EDSR theory for acceptors within the framework of the EMA method. Employing the Kane model (Addendum B) for InSb one can obtain an estimate for the matrix element r_{EDSR} (Rashba and Sheka 1964b):

$$r_{EDSR} \sim \frac{PG}{E_G E_I} \langle x k^3 \rangle \sim 10^3 \text{ a.u.} \tag{10.9}$$

This is larger by three orders of magnitude than the estimate for the EPR characteristic length. The angular indicatrices of EDSR on acceptors, found by Rashba and Sheka (1964b), agree with the general rules formulated in section 4. Observation of SR is simplified in the presence of uniaxial strain, lifting up the degeneracy of the spectrum (Kohn 1957). In this case r_{EDSR} becomes smaller compared to (10.9) by the factor $(\hbar\omega_s/\Delta_\varepsilon)^2$, where Δ_ε is the splitting of hole bands caused by the strain (Bir et al. 1963). Even if this factor is taken into account, r_{EDSR} remains large enough for experimental observation of the resonance.

Much more intricate for the theory is the case of acceptors in Ge and Si (Bir et al. 1963). Crystals of this type possess the inversion centre and it is absent only in the site group of the impurity centre. Therefore the value of r_{EDSR} depends on how the potential changes on the scale of the lattice spacing a, and it is only possible to roughly estimate the orders of magnitude of EDSR. Since the site group is a tetrahedron group, the antisymmetric part of the potential can be modelled as the octupole potential and at a distance R it has the order of magnitude $\mathscr{E}_I(a/R)^3$. This leads to the estimate:

$$r_{EDSR} \sim (a/R)^3 R = (a/R)^2 a, \tag{10.10}$$

i.e., $r_{EDSR} \ll a$. At the same time, the thus estimated r_{ESDR} exceed λ for Ge and, particularly, for Si. Bir et al. (1963) obtained an estimate similar to (10.10), but

according to their data, due to the presence of the small numerical factors, $r_{EDSR} \sim \hat{\lambda}$ for Si and $r_{EDSR} \ll \hat{\lambda}$ for Ge.

So far no experimental results on EDSR on large-radius acceptors are available.

11. *Two-dimensional systems: heterojunctions and MOS structures*

Spin resonance was observed in the inversion n-type layers in the GaAs–$Al_xGa_{1-x}As$ heterojunctions. In such structures, the normal to the plane of the junction is along [001]. Under these conditions for a perfectly plane heterojunction the 2D symmetry group is C_{2v}, which is a subgroup of T_d. The symmetry planes are (110) and $(1\bar{1}0)$. For the GaAs band structure under these conditions the Hamiltonian of 2D electrons is anisotropic and involves two k-linear terms,

$$\mathscr{H}_{so} = \delta_1(\sigma_x k_y - \sigma_y k_x) + \delta_1'(\sigma_x k_x - \sigma_y k_y). \tag{11.1}$$

The presence of the independent constants δ_1 and δ_1' may be considered as the effect of the 'terminal layer'. The values of these constants are determined by whether GaAs in the heterojunction is terminated by a layer of Ga atoms or by a layer of As atoms. The other reason for appearance of two constants will be clarified in what follows. At present, there are no experimental data that show a difference in properties of the heterojunction in the [110] and $[1\bar{1}0]$ directions, so, it is reasonable when analyzing the experimental data to confine ourselves to the isotropic model. Since both invariants entering into eq. (11.1) are unitarily equivalent, one can set $\delta_1' = 0$, i.e., take the Hamiltonian of eq. (5.1) with $\boldsymbol{c} \parallel [001]$.

It is useful to discuss the question of which mechanisms generate δ_1 and δ_1'.

First, this is the SO interaction in the plane of the heterojunction in a layer with a width of the order of the lattice spacing. It contributes to both δ_1 and δ_1'. To estimate the magnitude of these terms, it is convenient to compare them with the k-linear terms in $A_{II}B_{VI}$ compounds. Since in both cases these terms have a common origin, one can expect that they will have the same order of magnitude. The only difference is that in the heterojunction the potential is strongly asymmetric, but the width of the heterojunction amounts to only 10% of the width of the electron channel and the maximum of the ϕ function is probably beyond the plane of the heterojunction. As a result, the real value of $\delta_1(\delta_1')$ can be a factor of about 10^2 smaller than its maximum value, obtained from first-principles atomic estimates. In crystals of the $A_{II}B_{VI}$ type with the wurtzite lattice, deviation of the nearest-neighbour coordination from the tetrahedral coordination amounts to 1%. However, it is this deviation that gives

rise to the appearance of the linear terms. Therefore, the small numerical factor has roughly the same order of magnitude as in the former case.

The second mechanism generates only δ_1', this contribution comes from the bulk k^3-terms of eq. (6.2). It can be obtained (Bychkov and Rashba 1985) from the estimate given by Aronov et al. (1983) for δ_3,

$$\delta_3 = \tfrac{1}{2}\alpha_c \hbar^3 (2m^* E_G)^{-1/2} \langle \hat{k}_z^2 \rangle, \tag{11.2}$$

where $\alpha_c \approx 0.06$ for GaAs and $\langle \ldots \rangle$ denotes the average value over the wave function of the electron confined in a channel. A reasonable estimate, $\langle \hat{k}_z^2 \rangle \approx (40\ \text{Å})^{-2}$, yields $\delta_1 \approx 10^{-10}$ eV cm. This contribution exists even for symmetric wells, and is not very sensitive to the behaviour of the potential near the interface. The third mechanism is that the k-odd terms with $\delta_1' = 0$ emerge due to the inhomogeneous electric field in the space-charge layer.

The interference of the second and the third contribution may result in anisotropy of $\mathscr{H}_{so}$. However, it is important only when both contributions have a comparable magnitude. We shall not consider the case of such an accidental coincidence. According to Malcher et al. (1986) the second contribution dominates over the third for electrons in GaAs–$Al_xGa_{1-x}As$ heterojunctions.

Stein et al. (1983) observed spin resonance in the GaAs–$Al_{0.3}Ga_{0.7}As$ heterostructures with carriers with high mobility ($\mu > 10^5\ \text{cm}^2/\text{V s}$) at $T \sim 1$ K. The resonance was detected by conductivity modulation of the specimen, its intensity was high. Bychkov and Rashba (1984) made an assumption that the observed SR is the EDSR caused by the k-linear term of eq. (5.3) [cf. the first term in eq. (11.1)] in the dispersion law, and proposed to find δ_1 from the dependence of the resonance frequency ν on H, which is shown in fig. 13. An important peculiarity is that $\nu(H)$ extrapolated from the region of high H always shows a nonzero offset ν_0 at $H = 0$. It follows from eq. (5.10) that for the $N = 1$ level in the region of strong H the resonance frequency is

$$\nu(H) = \nu_0 + \nu_Z(H),$$
$$\nu_0 \approx -(6\Delta_1/\pi\hbar)\ \text{sign}\ g, \qquad \nu_Z(H) = |g|\mu_B H/2\pi\hbar. \tag{11.3}$$

This linear dependence agrees with the experimental data shown in fig. 13. The sign of the offset, ν_0 is positive, indicates that $g < 0$ in agreement with other experimental data. The value of ν_0, determined for a non-illuminated specimen (2) from fig. 13 and eq. (11.3), gives $\Delta_1 \approx 2.5 \times 10^{-6}$ eV and $\delta_1 \approx 2 \times 10^{-3}$ a.u. Calculating I_{EDSR}/I_{EPR} according to eqs. (5.7)–(5.8) we get a value of about 10^7, i.e., EDSR strongly prevails over EPR. The value obtained for δ_1 coincides with the typical value of this coefficient in the bulk dispersion law for carriers in hexagonal crystals of the $A_{II}B_{VI}$ type (see section 5).

Despite the fact that the δ_1 found here has a reasonable magnitude, the approach which led to this result is open to criticism. Lommer et al. (1985) have shown that in GaAs–$Al_xGa_{1-x}As$ heterostructures a very important contri-

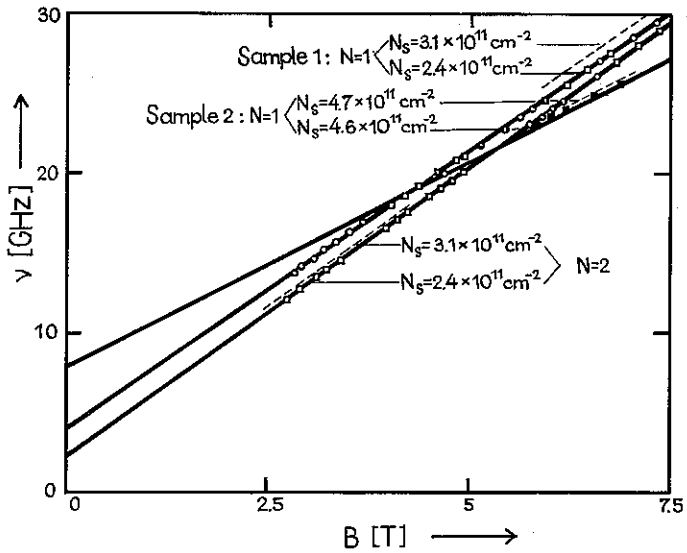

Fig. 13. Dependence of the SR frequency ν on H for two samples. N is the Landau quantum number. The carrier concentration N_s was altered by illuminating the sample. The dashed lines represent data obtained by another method of cooling the samples (Stein et al. 1983).

bution to the dependence $\nu = \nu(H)$ comes from the k-dependence of the g-factor, originating from the bulk k^4-nonparabolicity. This contribution alone is sufficient to describe experimental data satisfactorily, so it is impossible to find two independent constants from these data. The role of nonparabolicity enhances with increasing frequency ν, and in recent experiments by Dobers et al. (1988) on quantum wells at $\nu \sim 60$ GHz it played a dominant role. However, the most important statement (Bychkov and Rashba 1984) that the electro-dipole mechanism of the excitation of SR dominates in heterojunctions, seems undeniable, since the magnitude of $\delta_1 \approx 10^{-3}$–10^{-2} a.u. has been found afterwards in independent experiments, e.g., on Shubnikov–de Haas oscillations [on Si MOS structures (Dorozhkin and Ol'shanetskii 1987), and on $A_{III}B_V$ quantum wells (Luo et al. 1988, Das et al. 1989)]. This statement has been also confirmed in experiments by Störmer (1988).

Erhardt et al. (1986) investigated absorption spectra of p-layers in GaAs–AlGaAs heterojunctions in the submillimeter range of the spectrum in magnetic fields up to 25 T. They observed EDSR and electric-dipole CFR transitions. There is no adequate interpretation of the observed bands, especially those which were observed in fields higher than 20 T.

Därr et al. (1976) observed EDSR in the inversion n-layer on the (111) face of InSb. The resonance intensity considerably enhances with increasing angle θ

between the normal to the surface and H. They supposed that $\delta_1(\theta = 0) \approx 0$ but that this parameter rapidly increases with θ if taking into account a finite value of the parameter $\langle z^2 \rangle / r_H^2$, which is usually regarded to be small. The reason for $\delta_1(\theta = 0)$ being so small that minor correction terms are dominating, is, so far, unclear. However, this effect was confirmed by Merkt et al. (1986). These authors also observed an unusual dependence of the shape of the EDSR line on electron concentration in a channel. At a low electron concentration n_s ($n_s \approx 1.6 \times 10^{11}$ cm^{-2}) in the spectrum on the EDSR frequency one can observe a dip which, with increasing n_s, is continuously becoming a peak, distinctly seen already at $n_s \approx 2.8 \times 10^{11}$ cm^2. The unusual profile of the EDSR line is ascribed to the Fano-resonance occurring due to the fact that the EDSR line is observed on the background of a broad CR band.

12. One-dimensional systems: dislocations

Dislocations in crystals are extended defects which may produce the attractive potential for electrons. This potential localizes electrons in the plane perpendicular to the plane of the dislocation, but the motion of electrons along the dislocation remains free. As a result, one can expect that electrons trapped by the dislocation will exhibit 1D behaviour. The most convincing argument in favour of the existence of 1D energy bands for carriers bound to dislocations is apparently the discovery of the Ch-line; the Ch-line has been identified as an EDSR band for 1D carriers (Kveder et al. 1986).

The Ch-line was discovered by Kveder et al. (1984) on oriented dislocations in Si. Annealing led to the reconstruction of dislocations, which resulted in the disappearance of the original EPR signal corresponding to dangling bonds and in the appearance of a new SR signal, the Ch-line. The Ch-line is excited by the electric field $\tilde{E}$ parallel to the $[1\bar{1}0]$ direction coinciding with the direction of dislocations, and a slightly anisotropic g-factor, close to $g = 2$, corresponds to this line. The measurements were carried out at the frequency $\nu = 9.5$ GHz and the electric mechanism of the excitation was established by moving a specimen within the resonator: when the specimen was moved away from the antinode of $\tilde{E}$, the signal became 200 times weaker.

The dependence of the EDSR intensity on the orientation of the specimen (at a fixed reciprocal orientation of $\boldsymbol{H}$ and $\tilde{\boldsymbol{E}}$) appears to decisively prove that not point defects but electrons of the dislocation band are responsible for the Ch-line. The experimentally observed angular dependence can be accounted for by assuming the dislocations to have low symmetry, allowing for the invariant vector perpendicular to the dislocation axis. Let us bring these two directions into correlation with the unit vectors $\boldsymbol{b}$ and $\boldsymbol{l}$, respectively. The electron quasimomentum $\boldsymbol{k}$ can be oriented only along the straight line $\boldsymbol{l}$. The energy of the SO interaction and the respective contribution to the velocity can be written

as

$$\mathscr{H}_{so} = \delta_1(\hat{\boldsymbol{k}}\boldsymbol{l})(\boldsymbol{\sigma}(\boldsymbol{b}\times\boldsymbol{l})), \qquad \boldsymbol{v}_{so} = \frac{\delta_1}{\hbar}\boldsymbol{l}(\boldsymbol{\sigma}(\boldsymbol{b}\times\boldsymbol{l})). \tag{12.1}$$

These formulas are analogous to (5.3) and (5.6). The operator $\boldsymbol{v}_{so}$ completely describes the effect of the SO interaction since in 1D systems the operator $\hat{T}$ commutates with the spin-independent term in the velocity $\boldsymbol{v}$ (section 3). The matrix element describing the EDSR excited by the field $\tilde{\boldsymbol{E}}\|\boldsymbol{e}$, is proportional to

$$\langle\uparrow|\boldsymbol{v}_{so}\boldsymbol{e}|\downarrow\rangle = \frac{\delta_1}{\hbar}(\boldsymbol{e}\boldsymbol{l})\sum_i(\boldsymbol{b}\times\boldsymbol{l})_i B_{i1} = \frac{\delta_1}{\hbar}(\boldsymbol{e}\boldsymbol{l})B_{21}. \tag{12.2}$$

In deriving (12.2), we have here as elsewhere switched over from the A system (with the axes $x\|\boldsymbol{b}$, $y\|(\boldsymbol{b}\times\boldsymbol{l})$, $z\|\boldsymbol{l}$; fig. 14) to the A′ system. Using formula (A.5) for B_{21} in notations of fig. 14, we get the expression for the angular EDSR intensity dependence (Kveder et al. 1986):

$$I = I_0\cos^2\theta_{\tilde{E}}(1-\sin^2\theta\sin^2\phi). \tag{12.3}$$

Formula (12.3) holds if the g-factor is isotropic. Agreement of this dependence with the experimental data is illustrated by figs. 15a, b. They convincingly testify to the fact that the model based on the existence of the electron dislocation band is correct.

The estimate of the lower bound on δ_1, following from the experimentally found ratio $I_{EDSR}/I_{EPR} \gtrsim 200$ is $|\delta_1| \gtrsim 20\lambda\hbar \times 2\pi\hbar\nu \sim 10^{-14}$ eV cm. It is by a few orders smaller than in other cases (sections 5 and 11). The coefficient can be correlated with the effective force $\boldsymbol{F}$ or with the effective transverse electric field, $\boldsymbol{E}_{eff} = \boldsymbol{F}/e$, acting on the electron. A very rough estimate, which makes it possible to relate $\boldsymbol{F}\|\boldsymbol{b}$ and δ_1, would be $F \sim \delta_1/\lambda\hbar^2$. According to Kveder et al. (1986), who obtained the estimate in a somewhat different manner, $E_{eff} \gtrsim 10^7$–10^8 V/cm, i.e.,

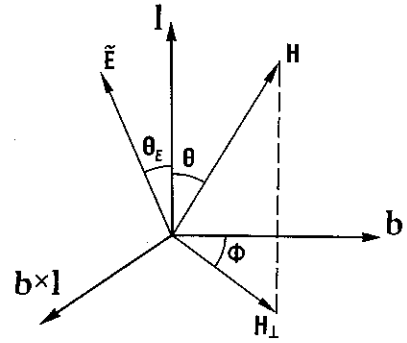

Fig. 14. Orientation of the d.c. magnetic field $\boldsymbol{H}$, of the a.c. electric field $\tilde{\boldsymbol{E}}$ and of the a.c. magnetic field $\tilde{\boldsymbol{H}}$ relative to the dislocation axis $\boldsymbol{l}$ and to the invariant vector $\boldsymbol{b}\perp\boldsymbol{l}$ (Kveder et al. 1986).

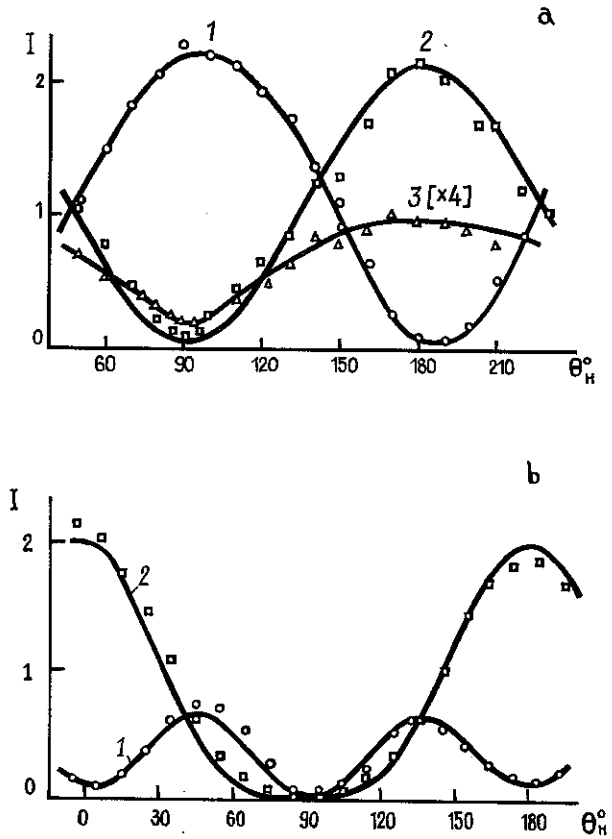

Fig. 15. Dependence of the EDSR intensity on the orientation of the sample: (a) $\varphi_H = 0$; (b) $\varphi_H = \pi/2$. Curves 1 in (a) and (b) correspond to $\tilde{E} \perp H$, $\tilde{E}$, H and l are in the same plane. Curve 2 and 3 correspond to $\tilde{E} \| H$. The solid line shows the theoretical results and the dots the experimental results. Curves 1 and 2 are obtained in the linear regime, and curve 3 at higher microwave power when the resonance is close to saturation (Kveder et al. 1986).

it has an atomic order of magnitude. Therefore it was concluded that the 1D band responsible for the Ch-line lies deeply in the forbidden gap.

A more detailed description of experimental data is given in the paper by Kveder et al. (1989) while the theory is given in the article by Koshelev et al. (1988).

Babich et al. (1988) discovered a few new EDSR bands, associated with dislocations in Si. The EDSR intensity exceeds the EPR intensity by two orders. The authors ascribe this to paramagnetic centres (1/2 spin) with the symmetry C_s, built in cores of dislocations which are components of the dislocation dipoles.

13. Shape of the EDSR band

The shape of the resonance curve for band carriers is determined by a number of factors. These include the scattering of carriers by phonons, the spread of resonance frequencies for carriers with different quantum numbers, and narrowing due to scattering (this mechanism for EPR in n-type InSb was described by Sugihara (1975)). Consequently, the theory must be developed to conform to concrete situations, and no theory of this kind for COR is available. That is why below we shall discuss only one aspect of this problem, which is important for understanding the main features of the spectrum and for treating the experimental data.

Figure 16 shows the CR and EDSR spectra in n-type InSb obtained by Bell (1962). In this work EDSR on free carriers was observed for the first time, and we shall come back to it in section 14. Here let us note only three things. First, the electric mechanism of SR excitation was unambiguously proved by moving within a waveguide a sample whose width amounted to 1/20 of the wavelength: the spin transition intensity increased when the sample was moved away from the microwave magnetic field antinode (i.e., the electric field node). Secondly, the EDSR band is much narrower than the CR band (by 2 orders). And thirdly, the CR band zero is only slightly shifted with respect to the origin ($H = 0$). This

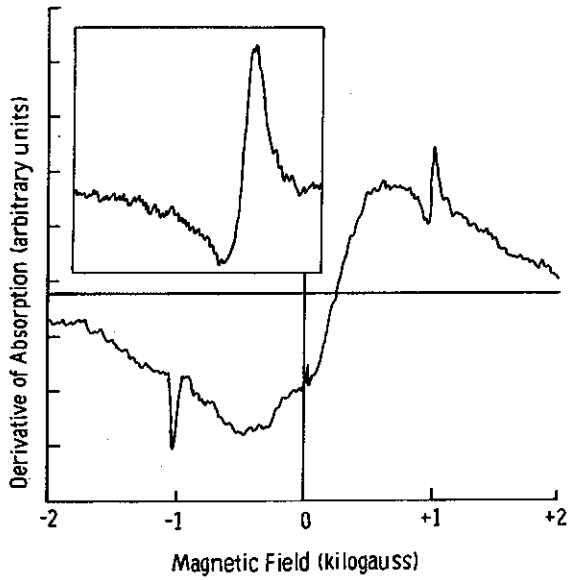

Fig. 16. CR (broad band) and EDSR (two narrow lines) spectra in n-type InSb. The inset shows the detailed shape of the spin line. Donor concentration is 9×10^{13} cm^{-3}. $T = 1.3$ K, frequency $\nu = 72$ GHz (Bell 1962).

means that $\omega\tau < 1$, where τ is the momentum relaxation time, and the Landau quantization is destroyed by scattering. On the other hand, the SR band is narrow. Therefore $\omega\tau_s \gg 1$, where τ_s is the spin relaxation time.

It is evident that at $\tau \ll \tau_s$ the CR band and all electric-dipole CFR bands will have the collisional width $\sim\tau^{-1}$. Under the conditions $\omega\tau < 1$ all electric-dipole CFR bands will fuse with the CR band and will not be observable on its mighty background. The situation is quite different for the EDSR band. Mel'nikov and Rashba (1971) showed that the EDSR band consists of a broad band of width $\sim\tau^{-1}$ and of a narrow line of width $\sim\tau_s^{-1}$ (if only the collisional mechanism of broadening is taken into account). Distribution of the intensity between them strongly depends on the dispersion law.

The integral intensity of each of the COR bands is practically independent of the scattering rate. If $\omega\tau$, $\omega\tau_s \gg 1$, all bands may be resolved and can be brought into correlation with the respective terms in the velocity operator. For each of the bands the real part of the diagonal components of the conductivity σ_{jj} can be written as

$$\sigma_{jj}(\omega) \propto \mathrm{Re}\int_0^\infty \mathrm{d}t\, \mathrm{e}^{\mathrm{i}\omega t}\langle[v_j(t), v_j]\rangle,$$
$$v_j(t) = \exp(\mathrm{i}\mathscr{H}t/\hbar)v_j \exp(-\mathrm{i}\mathscr{H}t/\hbar), \tag{13.1}$$

where $\langle\ldots\rangle$ denotes an average over the ensemble and $\mathscr{H}$ is the total Hamiltonian of the system. The integrated intensity of the absorption in each of the bands is expressed via matrix elements of the velocity at coinciding times:

$$\sigma_{jj} \propto \sum_{\mathscr{E}_n < \mathscr{E}_{n'}} (\rho_n - \rho_{n'})|(v_j)_{n'n}|^2. \tag{13.2}$$

Here ρ is the density matrix. Therefore as long as the perturbation operator responsible for the scattering of carriers does not affect the energy spectrum and matrix elements $(v_j)_{n'n}$, the integrated intensity of each band is τ-independent. Overlapping of bands does not bring about any major changes.

With regard to EDSR, the problem is how the overall intensity is distributed between the broad band and the narrow line. Let us base our consideration on the strong inequality $\tau \ll \tau_s$. Since the duration of the spin transition is of the order of τ_s, in the course of the spin transition an electron experiences a good deal of collisions (of the order $\tau_s/\tau \gg 1$), affecting its momentum but not its spin. We shall call them momentum collisions. From the considerations below it will ensue that they affect EDSR in a different manner than EPR.

If the g-factor is isotropic, the Hamiltonian for a perfect crystal is

$$\mathscr{H} = \mathscr{H}_0(\hat{\boldsymbol{K}}) + \tfrac{1}{2}g\mu_B(\boldsymbol{\sigma}\boldsymbol{H}) - \frac{e}{c}\boldsymbol{V}(\hat{\boldsymbol{K}})\tilde{\boldsymbol{A}}(t). \tag{13.3}$$

It is convenient to write down the velocity as $\boldsymbol{V} = \sigma_+ V_-(\hat{\boldsymbol{K}}) + \sigma_- V_+(\hat{\boldsymbol{K}})$

$+\sigma_z V_Z(\hat{\boldsymbol{K}})$. The Z-axis is directed along $\boldsymbol{H}$. Since $\tau_s \gg \tau$, the SO interaction is weak. Therefore one can assume that it is completely incorporated in $V(\hat{\boldsymbol{K}})$ by means of the appropriate canonical transformation (cf. section 3) and is missing in $\mathscr{H}_0$. Then at $\tilde{\boldsymbol{A}} = 0$ the eigenstates can be classified according to coordinate and spin quantum numbers, and it stands to reason that the collision integral should be divided into two parts, corresponding to momentum and spin collisions (W and W_s). If the $\tilde{\boldsymbol{A}}$-linear correction to the density matrix is written as $\rho'(t) = \rho(t) - \rho_0$, the equation for it in the interaction representation over $\mathscr{H}_0$ is

$$\hbar\frac{\partial\rho'}{\partial t} + \tfrac{1}{2}g\mu_B[\boldsymbol{\sigma H}, \rho'] + \hat{W}(\rho') + \hat{W}_s(\rho') = \mathrm{i}\frac{e}{c}[\boldsymbol{V}(t)\tilde{\boldsymbol{A}}(t), \rho_0]. \tag{13.4}$$

Here $\hat{W}$ and $\hat{W}_s$ are linearized collision integrals. Within the spin line the largest term is $\hat{W}$. Therefore $\rho'(t)$ should be sought in the condition $\hat{W}(\rho') = 0$. This is not difficult to do if we bear in mind that the equivalent condition $W(\rho(t)) = 0$ corresponds to the equilibrium distribution of electrons in an instantaneous magnetic field $\boldsymbol{H} + \tilde{\boldsymbol{H}}(t)$ with different chemical potentials $\eta_1(t)$ and $\eta_2(t)$ for the two spin orientations. A most general form of ρ' is

$$\rho'(\mathscr{E}, t) = \left\| \begin{array}{cc} (\eta_1 - \eta)\dfrac{\partial f(\mathscr{E}_1 - \eta)}{\partial\eta} & \gamma[f(\mathscr{E}_2 - \eta) - f(\mathscr{E}_1 - \eta)] \\ \gamma^*[f(\mathscr{E}_2 - \eta) - f(\mathscr{E}_1 - \eta)] & (\eta_2 - \eta)\dfrac{\partial f(\mathscr{E}_2 - \eta)}{\partial\eta} \end{array} \right\|. \tag{13.5}$$

Here $\mathscr{E}$ is the kinetic energy of an electron, $\mathscr{E}_{1,2}(\mathscr{E}) = \mathscr{E} \pm \hbar\omega_s/2$, $\eta = (\eta_1 + \eta_2)/2$ is the equilibrium chemical potential, $f(\mathscr{E})$ is the Fermi distribution function and γ is a complex parameter. This parameter can be found by calculating the trace of eq. (13.4) over configurational quantum numbers with formula (13.5) and by taking the fact that $\hat{W}(\rho') = 0$. When the trace is calculated, the term $\hat{W}_s$ reduces to a constant, multiplied by γ: thus the spin relaxation time τ_s naturally appears. As a result

$$\frac{\partial\gamma}{\partial t} + \mathrm{i}\omega_s\gamma + \frac{\gamma}{\tau_s} = \mathrm{i}2^{-1/2}\frac{e}{c\hbar}\langle V_-\rangle\tilde{\boldsymbol{A}}(t), \tag{13.6}$$

where V_- is the matrix element of the velocity $\boldsymbol{V}_-(\hat{\boldsymbol{K}})$,

$$\langle V_-\rangle = \frac{\mathrm{tr}\{V_-[f(\mathscr{E}_2 - \eta) - f(\mathscr{E}_1 - \eta)]\}}{\mathrm{tr}\{f(\mathscr{E}_2 - \eta) - f(\mathscr{E}_1 - \eta)\}}. \tag{13.7}$$

The solution of eq. (13.6) permits us to calculate the current and the conductivity tensor

$$\sigma_{jl}(\omega) = \frac{e^2}{\hbar\omega}\frac{\langle V_+\rangle_j\langle V_-\rangle_l}{\mathrm{i}(\omega_s - \omega) + \tau_s^{-1}}(n_2 - n_1), \tag{13.8}$$

where n_1 and n_2 are equilibrium electron concentrations with different spin orientations.

Formula (13.8) shows that the spin line is described by the Lorentzian of a small width τ_s^{-1}. An important peculiarity is that the numerator of (13.8) involves averages of the velocity matrix elements (but not averages of their squares, cf. (13.2)). These averages in many cases must turn to zero, then the narrow line must be absent. This is the main difference in the effect of collisional averaging in EPR and in EDSR. In EPR the matrix element is practically independent of the configurational quantum numbers and the averaging leads only to motional narrowing of the band. In contrast, in EDSR the matrix element, as a rule, strongly depends on the configurational quantum numbers, and therefore the averaging may greatly reduce the intensity of the SR line.

So, the EDSR spectrum consists of the two overlapping bands of the widths $\sim\tau^{-1}$ and $\sim\tau_s^{-1}$. Of course, it is assumed here that the collisional broadening is much larger than the inhomogeneous broadening, caused by the dependence of ω_s on configurational quantum numbers and weakened as a result of the motional narrowing. At $\omega\tau \gg 1$ one can observe the broad band and the narrow line on its background. At $\omega\tau \lesssim 1$ the broad band must be practically invisible on the background of the cyclotron absorption and one can observe only the narrow line whose intensity at arbitrary $\omega\tau$ is determined by formula (13.8). However, this formula holds only at the conventional constraint $\bar{\mathscr{E}}\tau \gg \hbar$, where $\bar{\mathscr{E}}$ is the mean energy of carriers.

To understand in which cases $\langle V_- \rangle \neq 0$ and what determines its value, it is instructive to consider some concrete examples. Two cases are possible where V is $\hat{\boldsymbol{K}}$-independent. First, the SO interaction can be represented by the k-linear terms in the dispersion law (section 5). Secondly, it can be represented by the same terms but multiplied by H (section 8). Then the overall intensity is concentrated in the narrow line (Rashba 1964a, Boiko 1964).

For the SO interaction Hamiltonians of higher orders in k two cases are possible. If $\mathscr{H}_{so}$ is even with respect to $\boldsymbol{k}$, the velocity is odd with respect to $\boldsymbol{k}$ and $\langle V_\pm \rangle = 0$; hence the SR line is missing. An example of this case is the k^4-terms in the electron Hamiltonian for InSb. If $\mathscr{H}_{so}$ is odd with respect to $\boldsymbol{k}$, then $\langle V_\pm \rangle \neq 0$, its value being dependent on the specific symmetry and on the magnitude of H. For the k^3-terms in the InSb spectrum (Mel'nikov and Rashba 1971)

$$\langle V_\pm \rangle \propto \langle \hat{K}_X^2 + \hat{K}_Y^2 - 2K_Z^2 \rangle. \tag{13.9}$$

At $\hbar\omega_c \ll \bar{\mathscr{E}}$ the leading terms are cancelled, the matrix element diminishes by the factor $\sim\hbar\omega_c/\bar{\mathscr{E}}$ and the entire absorption almost occurs in the broad band. At $\hbar\omega_c \sim \bar{\mathscr{E}}$ the absorptions in the band and in the line have comparable intensities. Since the angular indicatrix of the matrix elements of V does not depend on configurational quantum numbers (section 6), the EDSR angular indicatrices for the line and for the band are the same.

Unfortunately, the EDSR spectrum described in this section, formed by the

superposition of two bands of different widths, has not so far been observed experimentally.

14. EDSR induced by lattice imperfections

There is experimental evidence of the fact that lattice imperfections induce new EDSR mechanisms. In this section we shall consider them and also give certain models of such mechanisms. This interesting aspect of the problem is still the least developed in the COR theory.

The theory presented in section 6, based on the Hamiltonian $\mathscr{H}_{so} \propto k^3$, does not describe the experimental data of Bell (1962) for EDSR in n-type InSb under the conditions $\omega\tau < 1$. First, the observed EDSR intensity is unexpectedly high. Actually, it follows from the experimental results that I_{EDSR} is by many orders higher than I_{EPR} at $\tilde{E} \sim \tilde{H}$. At the same time, according to Dobrowolska et al. (1983) (cf. section 7), these intensities at $\omega\tau \gg 1$ differ by less than two orders. But at a strong inequality of the relaxation times ($\tau_s \gg \tau$) and at a strong scattering ($\omega\tau < 1$), i.e., under the conditions of the experiment carried out by Bell (1962), the SR line intensity should be additionally suppressed by the factor $\sim \hbar\omega_s/\eta$ (section 13). The same conclusion ensues from the too large value of the ratio $I_{EDSR}/I_{CR} \sim 10^{-5}$–$10^{-4}$, which could be estimated from fig. 16. In the second place, the observed absorption was isotropic and the same in both circular polarizations. The formulas of section 6 yield polarization-dependent, strongly anisotropic absorption. The theory in section 9 does not account for the experimental facts either. This controversy points to the fact that in highly doped crystals (the experiment by Bell was performed under the conditions $\eta\tau \lesssim \hbar$) the role of impurities in COR is modified: their influence is not reduced to the scattering of carriers, giving rise to level broadening and to the averaging of transition matrix elements. Inducing transformation of the energy spectrum, they give rise to the appearance of new COR mechanisms and, consequently, make a new contribution to the COR oscillator strength, a contribution that becomes dominant in certain conditions.

Although these experimental data are not yet properly understood, we can nevertheless mention certain mechanisms which may, in principle, be responsible for the observed effect. For example, the impurity potential $V(\boldsymbol{r})$ generates an 'anomalous' velocity (Blount 1962) which in n-type InSb has the structure $\boldsymbol{v} \propto \boldsymbol{\sigma} \times V\nabla V(\boldsymbol{r})$. Furthermore, impurity centres produce the strain, calling forth new terms in the dispersion law: in n-type InSn they are linear in k (cf. section 5).

The second experiment displaying a new EDSR mechanism concerns not the conduction electrons but the electrons bound in As donors in Ge. Gershenzon et al. (1970) discovered that in compensated samples the intensity and the width of the SR spectrum rapidly increases at decreasing T. By moving a sample within a

waveguide it was proved that the new spectrum is an EDSR spectrum. The data are given in fig. 17. The intensity of the EDSR spectrum is so high that when the sample is moved towards the antinode of the field $\tilde{H}$, EDSR is about 70 times more prevalent than EPR due to the finite size of the sample ($T = 1.7$ K). Such a high intensity of EDSR on impurities was all the more unexpected because EDSR was not observed in experiments on band electrons in Ge, and the theoretical estimates (Boiko 1962) predicted a relatively low EDSR intensity (section 8). For bound electrons one can expect EDSR to be weakened by the factor $(\hbar\omega_s/\mathscr{E}_1)^2 \sim 10^{-5}$ (section 10).

The treatment of these data proposed by Mel'nikov and Rashba (1971) is grounded on the following basic facts: (*i*) the Ge spectrum is a multivalley spectrum; (*ii*) parameters of the valleys are strongly anisotropic; and (*iii*) the random electric field $\boldsymbol{E}(\boldsymbol{r})$ of charged impurities leads to the mixing of wave functions belonging to different valleys. If we assume that the field $\boldsymbol{E}$ is homogeneous within the centre, then for the spin Hamiltonian of the ground state of the donor centre in Ge the following expression is valid:

$$H_{\text{eff}} = \tfrac{1}{2} g \mu_B (\boldsymbol{\sigma H}) + \frac{2\mu_B}{9\Delta}(g_\parallel - g_\perp)(P_\parallel - P_\perp)\,[(\boldsymbol{HE})(\boldsymbol{\sigma E}) - \sum_i H_i E_i^2 \sigma_i], \tag{14.1}$$

where

$$P_{ij}^v = \sum_{n>1} \frac{(d_i)_{1n}^v (d_j)_{n1}^v}{\mathscr{E}_n - (\mathscr{E}_1 - \Delta)}. \tag{14.2}$$

Here n numbers the quantum levels of the centre in the one-valley approximation, $\mathscr{E}_n$ is the energy of the levels, v numbers the valleys, Δ is the valley–orbit splitting, d is the dipole moment of the transition, the quantities P_{ij}^v have the meaning of polarizabilities, and $P_\parallel$, $P_\perp$ and $g_\parallel$, $g_\perp$ are values of the tensorial components of P and g in the main axes of electron ellipsoids. Formula (14.1) holds if the Zeeman and Stark energies are small compared to Δ. It is clear from (14.1) that the product $(g_\parallel - g_\perp)(P_\parallel - P_\perp)$ has the meaning of the SO coupling constant. If charged impurities are arrayed chaotically, there follows from (14.1) a formula for the conductivity tensor per donor:

$$\sigma_{ij}(\omega) = \sigma_0 \int_0^\infty x^3 \varphi(x)\,\mathrm{d}x \int \mathrm{d}\Omega_e (M_{i-} - M_{j+}) \times \delta\left(\omega - \omega_s - \omega_s a x^2 [(\boldsymbol{eh})^2 - \sum_{i'} e_{i'}^2 h_{i'}^2]\right). \tag{14.3}$$

It is written down in the basis of the crystallographic axes. Here

$$\sigma_0 = \frac{2E_0^2H^2}{81\hbar\Delta^2}\mu_B^2(g_\parallel - g_\perp)^2(P_\parallel - P_\perp)^2\omega\tanh(\omega/2T),$$

$$E_0 = 4\pi e(n_i/30)^{2/3}, \qquad \varphi(x) = \int_0^\infty k\sin(kx)\exp(-k^{3/2})\mathrm{d}k,$$

$$a = \frac{4}{9\Delta}\frac{g_\parallel - g_\perp}{g}(P_\parallel - P_\perp)E_0^2, \qquad g = \tfrac{1}{3}(g_\parallel + 2g_\perp),$$

$$M_{ij} = h_ie_j + (\boldsymbol{he} - 2h_ie_j)\delta_{ij}, \qquad M_{j\pm} = 2^{-1/2}(M_{jX} \pm iM_{jY}), \tag{14.4}$$

$\boldsymbol{e}$ and $\boldsymbol{h}$ are unit vectors of the electric and magnetic fields, respectively (integration (14.3) is performed over the orientation of $\boldsymbol{e}$), and n_i is the charged impurity concentration.

Although the model is very simplified, the conclusions are in good, at least qualitative, agreement with the experiment. The uniaxial strain, transforming the spectrum into a one-valley spectrum, does away with the EDSR band (Gershenzon et al. 1976). The EDSR band has wide wings, decreasing as $|\omega - \omega_s|^{-3/4}$ (cf. fig. 17a). At $\omega \to \omega_s$ σ_{ij} logarithmically diverges, therefore on the background of the broad band, narrow peaks are seen (fig. 17a). The characteristic width of the curve has the magnitude $|\omega - \omega_s| \sim a\omega_s$, i.e., it increases with increasing frequency. The absorption intensity is σ_0-proportional, i.e., it increases with increasing H. The width of the curve depends on the orientation of $\boldsymbol{H}$: it is minimal at $\boldsymbol{H}\|[001]$ (according to (14.3) it is even zero). All the three conclusions are in qualitative agreement with the data of Gershenzon et al. (1976). Numerical estimates show that $I_{EDSR} > I_{EPR}$ at $n_i \gtrsim 10^{15}\,\mathrm{cm}^{-3}$, which also agrees with the experiment. The decrease in the ratio I_{EDSR}/I_{EPR} with increasing T, observed in the experiment, is probably accounted for by hopping conductivity, i.e., the mechanism discarded by the theory.

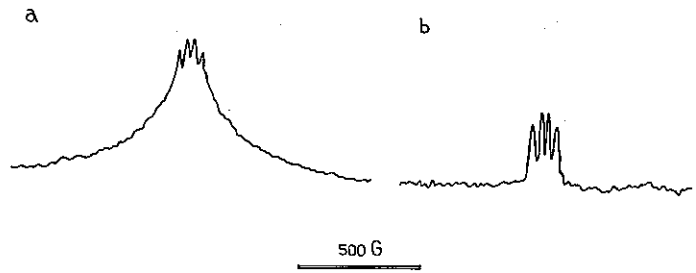

Fig. 17. SR spectrum of Ge:As. (a) EDSR in a compensated sample, (b) four-component EPR spectrum in a noncompensated sample. For either sample $N_d - N_a = 3.2 \times 10^{15}\,\mathrm{cm}^{-3}$. For the first sample the compensation factor is $K = 0.5$, $T = 4.2\,\mathrm{K}$, $\upsilon = 10\,\mathrm{MHz}$ (Gershenzon et al. 1970).

Note also that inhomogeneity of the field $\boldsymbol{H}$ may also give rise to COR, since the Zeeman Hamiltonian $g\mu_B(\boldsymbol{\sigma}\boldsymbol{H}(\boldsymbol{r}))/2$ involves both $\boldsymbol{\sigma}$ and $\boldsymbol{r}$. In particular, it has been shown (Pekar and Rashba 1964) that this mechanism may operate in magnetic materials due to the interaction of an electron spin with the spin and orbit variables of other electrons. Now it is becoming clear that a similar mechanism is efficient in semimagnetic semiconductors and that it is realized via the exchange interaction of an electron with magnetic ions.

Since this interaction simultaneously involves $\boldsymbol{r}$ and $\boldsymbol{\sigma}$, it allows electric-dipole spin transitions analogously to the SO interaction. Conformably to parameters of $Cd_{1-x}Mn_xSe$ (cf. section 10) the intensities of both processes may compete. The exchange mechanism has a number of peculiarities. Since the spins of an electron and of an ion change simultaneously (the flip–flop process), the transition frequency is shifted by the Zeeman frequency of the ion. For this reason electric-dipole transition bands may have a doublet structure (SO and exchange components). Since spins of impurities play the role of a magnetic field, the electric-dipole transition between components of the Kramers doublet, forbidden by (10.1), is allowed, and therefore the matrix element of the transition is nonzero already in the zeroth order in H. The resonance is allowed in all polarizations and the angular dependence of the intensity is close to isotropic. These results were obtained by Rubo et al. (1988, 1989).

An allied COR mechanism for semiconducting alloys of inhomogeneous composition was proposed by Leibler (1978). In this case, in formula (1.3) there emerges an extra term for $\mathscr{H}_{so}$, containing a quasielectric field, proportional to the gradient of the composition. This term apparently makes an extra contribution to the COR intensity.

15. Conclusion

We intended in this survey to elucidate the main problems pertaining to combined resonance in solids, mainly in semiconductors, and to shed light on the latest research in this field.

COR was the first phenomenon to reveal the presence of a strong coupling between an electron spin and an a.c. electric field in crystals. This coupling gives rise to a number of new phenomena, discovered later: spin-flip Raman scattering (Yafet 1966, Slusher et al. 1967) (see chapter 5 of this volume by Häfele) spin resonances of nonlinear susceptibility (Nguyen and Bridges 1972, Brueck and Mooradian 1973), and other higher-order processes.

For perfect crystals a complete description of COR is achieved on the basis of the appropriately derived EMA Hamiltonian. General symmetry requirements and numerical values of the parameters, which are specific for concrete crystals and vary in wide ranges, completely determine the Hamiltonian. Accordingly, for different crystals different COR mechanisms may dominate. Moreover, the

intensities of different COR bands in one crystal may be controlled by different mechanisms. The two main mechanisms are: (*i*) the inversion asymmetry mechanism inherent in crystals without the inversion centre, and (*ii*) the mechanism usually (and not quite adequately) termed as 'nonparabolicity'. At present, all the most interesting situations (k-linear and k^3-inversion asymmetric terms, nonparabolicity) have been observed in experiments and the succession of these mechanisms has been followed as the strain affecting the symmetry of the crystal was increased.

Thanks to its high intensity and to the considerable amount of bands in its spectrum, COR is a mighty tool for studying the band structure of semiconductors. Apart from determining the basic parameters of the spectrum, COR is used for many specific purposes (such as determining the energy dependence of the g-factor, measuring the SO splitting of bands in the vicinity of the symmetry points, finding the deformation potentials and constants of the coupling of electrons to optical phonons, and so on). Experimental studies of angular indicatrices of the COR band intensities (which for a variety of systems must exhibit a universal behaviour) should allow to check the reliability of the assignment of COR bands.

At present, spin-flip Raman scattering, the physical mechanism on which the operation of tunable lasers is based, is of practical significance. For possible applications of COR to quantum electronics (Rashba 1964b), heterostructures with spin injection look quite promising.

Of particular interest is COR in nonperfect crystals. Theoretical predictions relevant to peculiarities in the behaviour of COR on electrons bound to impurities, particularly resonance enhancement of the COR intensity, have lately received convincing confirmation in experiments on semimagnetic semiconductors. The most fascinating aspect of the problem is the search for new COR mechanisms induced by imperfections, the mechanisms nonexistent in perfect crystals. Such imperfections may be randomly positioned: impurities as well as heterojunctions and dislocations. Recent progress made in discovering EDSR on 2D and 1D electrons in heterojunctions and dislocations is especially encouraging. These achievements prove that COR is becoming an efficient tool for studying defects in crystal lattices. COR may also be applicable for the purpose of determining the magnitude of random electric fields and strains in disordered crystals.

COR can be regarded from two points of view. First, as a method of measuring parameters of crystals, and secondly, as a phenomenon which is in itself an interesting subject of study. As far as the second aspect is concerned, the most intriguing and impressive results may be expected in COR studies on nonperfect crystals.

Acknowledgements

We are grateful to all the authors who kindly gave their consent to their figures being reproduced in this review. We are particularly thankful to Professor R.L. Aggarval, Dr. J.C. Hensel, Professor D.G. Seiler and Professor J.K. Furdyna for providing us with the originals of the figures.

Addendum A. Transformation of the reference system and of the Hamiltonian

It is convenient to perform the calculation of the quantum level arrangement, classification of states and determination of transition intensities in the reference system A′, associated with the magnetic field $\boldsymbol{H}$. In this system the axis $Z \parallel \boldsymbol{H}$ and classification of wave functions of the spherically symmetric part of the Hamiltonian can be carried out in terms of the angular momentum projection m. Therefore it is handy to use circular coodinates in the A′ system:

$$R = (R_{\mathrm{I}}, R_0, R_1),$$
$$R_{\mathrm{I}} = 2^{-1/2}(X - \mathrm{i}Y), \quad R_0 = Z, \quad R_1 = 2^{-1/2}(X + \mathrm{i}Y). \tag{A.1}$$

In the A system, associated with the crystallographic axes, we shall use Cartesian coordinates:

$$\boldsymbol{r} = \{x_i\}, \qquad x_i = x, y, z. \tag{A.2}$$

To avoid confusion, the vectors defined by their coordinates in the A system will be labelled with lower case letters, whereas those defined by the coordinates in the A′ system will be labelled with capital letters.

Transformation of the tensor corresponding to the angular momentum J from the A system into the A′ system is carried out in a standard manner with the aid of the matrix $\boldsymbol{S}_J(\theta, \phi)$, which belongs to the irreducible representation D_J. Here θ and ϕ are the polar and azimuthal angles of the vector $\boldsymbol{H}$ in the A system.

Spinors are transformed by means of the $\boldsymbol{S}_{1/2}(\theta, \phi)$ matrix constituted from the Cauley–Klein parameters (Landau and Lifshitz 1974):

$$\boldsymbol{S}_{1/2}(\theta, \phi) = \begin{Vmatrix} \alpha & \beta \\ \gamma & \delta \end{Vmatrix}$$
$$= \begin{Vmatrix} \cos\frac{\theta}{2}\exp\left[\frac{\mathrm{i}}{2}\left(\phi + \frac{\pi}{2}\right)\right] & \sin\frac{\theta}{2}\exp\left[\frac{\mathrm{i}}{2}\left(\frac{\pi}{2} - \phi\right)\right] \\ -\sin\frac{\theta}{2}\exp\left[\frac{\mathrm{i}}{2}\left(\phi - \frac{\pi}{2}\right)\right] & \cos\frac{\theta}{2}\exp\left[-\frac{\mathrm{i}}{2}\left(\frac{\pi}{2} + \phi\right)\right] \end{Vmatrix}. \tag{A.3}$$

To transform the vectors defined in the canonical basis, one can employ the matrix $\boldsymbol{S}_1(\theta, \phi)$ (since its explicit form will not be needed below, we shall not write it out). However, since vectors in the A and A′ systems are defined in two different bases, namely, Cartesian and circular, it is more convenient to represent the switchover from $\boldsymbol{r}$ to $\boldsymbol{R}$ by means of the linear transformation

$$\boldsymbol{r} = \boldsymbol{B}\boldsymbol{R}, \qquad r_i = B_{i\alpha} R_\alpha, \tag{A.4}$$

with the unitary matrix $\boldsymbol{B}$,

$$\boldsymbol{B} = \|B_{i\alpha}\| = \begin{Vmatrix} 2^{-1/2}(\delta^2 - \gamma^2) & \beta\delta - \alpha\gamma & 2^{-1/2}(\alpha^2 - \beta^2) \\ \mathrm{i}2^{-1/2}(\gamma^2 + \delta^2) & \mathrm{i}(\alpha\gamma + \beta\delta) & -\mathrm{i}2^{-1/2}(\alpha^2 + \beta^2) \\ 2^{1/2}\gamma\delta & \alpha\delta + \beta\gamma & -2^{1/2}\alpha\beta \end{Vmatrix}$$

$$= \begin{Vmatrix} -2^{-1/2}(\sin\phi + \mathrm{i}\cos\theta\cos\phi) & \sin\theta\cos\phi & -2^{-1/2}(\sin\phi - \mathrm{i}\cos\theta\cos\phi) \\ 2^{-1/2}(\cos\phi - \mathrm{i}\cos\theta\sin\phi) & \sin\theta\sin\phi & 2^{-1/2}(\cos\phi + \mathrm{i}\cos\theta\sin\phi) \\ \mathrm{i}2^{-1/2}\sin\theta & \cos\theta & -\mathrm{i}2^{-1/2}\sin\theta \end{Vmatrix}. \tag{A.5}$$

Cartesian coordinates are designated in (A.4) and henceforth indicated by Latin subscripts, circular coordinates by Greek subscripts, it is implied that the summation over α is being performed.

By virtue of the unitarity of $\boldsymbol{B}$, its columns are orthogonal, and the vectors $\boldsymbol{B}_i = (B_{i\bar{1}}, B_{i0}, B_{i1})$, defined by their components in the A system, are related to each other as

$$\boldsymbol{B}_j \times \boldsymbol{B}_{j'} = \mathrm{i}\boldsymbol{B}^*_{j''}, \tag{A.6}$$

the subscripts j, j' and j'' constitute a cyclic permutation. This formula helps to simplify a number of expressions. So, for instance, for the Hamiltonian (6.2) formula (3.15) involves products of four elements of the $\boldsymbol{B}$ matrix. Still, it permits transformation to the form of (6.4) where the coefficients $B_{(\alpha\beta\gamma)}$, involving products of only three matrix elements, enter.

The next problem is to transform the EMA Hamiltonian from the A to the A′ system. Let us confine ourselves to the case where the irreducible representation D, corresponding to the band under study, coincides with the representation D_f of the rotation group for all elements of the group $g \in \mathrm{G}_k$ (for a more general case, see, Bir and Pikus 1972). If $g \in \mathrm{G}_k$ is an improper element, it should be simply replaced by the element $g\hat{I}$ ($\hat{I}$ is the inversion operator) of the group of proper rotations; therefore henceforth we shall not distinguish between g and $g\hat{I}$.

Under these conditions, matrices of the angular momentum J (whose rank coincides with the dimension of the irreducible representation) can be chosen as basis matrices via which the Hamiltonian $\mathscr{H}$ may be written. When the Hamiltonian $\mathscr{H}$ transforms from A to A', matrices of the momentum J are transformed as

$$\boldsymbol{S}_J \hat{J}_i \boldsymbol{S}_J^{-1} = \boldsymbol{B}(\theta, \phi)\hat{J}_i = B_{i\alpha}\hat{J}_\alpha. \tag{A.7}$$

This formula has a simple meaning: during rotation, components of the pseudovector $\hat{\boldsymbol{J}}$ are transformed as components of the vector $\boldsymbol{r}$. To transform the Hamiltonian $\mathscr{H}$ from A to A', it is required to perform both the transformation (A.7) and the transformation from $\boldsymbol{k}$ to $\boldsymbol{K}$ by analogy with formula (A.4).

If the g-factor is isotropic, the Zeeman energy is proportional to $(\hat{\boldsymbol{J}}\boldsymbol{H})$ and the transformation (A.7) diagonalizes it. One can confirm this by taking into account that $B_{i\alpha} = B^*_{i\bar{\alpha}} = (\boldsymbol{B}^+)_{\bar{\alpha}i}$:

$$(\hat{\boldsymbol{J}}\boldsymbol{H}) \Rightarrow (\boldsymbol{S}_J \hat{\boldsymbol{J}} \boldsymbol{S}_J^{-1}, \boldsymbol{H})$$
$$= B_{i\alpha}B_{i\beta}\hat{J}_\alpha H_\beta = \hat{J}_\alpha H_{\bar{\alpha}} = \hat{J}_0 H = \hat{J}_Z H. \tag{A.8}$$

If the g-factor is anisotropic, the Zeeman energy is diagonalized, as, for instance, in the paper by Rashba and Sheka (1961c).

Similarly, one can check commutation relations in the A' system:

$$[\hat{K}_\alpha, R_{\bar{\beta}}] = (\boldsymbol{B}^{-1})_{\alpha j}(\boldsymbol{B}^{-1})_{\bar{\beta}_j}, [\hat{k}_j, r_{j'}] = -i(B^{-1})_{\alpha j}B_{j\beta} = -i\delta_{\alpha\beta}. \tag{A.9}$$

Addendum B: Kane model

The Kane Hamiltonian (Kane 1957) has proved to be rather efficient for describing electron properties of cubic InSb-type semiconductors with a narrow direct forbidden gap. In the Kane model there are three adjacent bands: the conduction band, valence band (consisting of the light hole and heavy hole bands) and spin split-off band. The conduction band has s-type symmetry and the other bands emerge from the splitting of the original p-type band due to the SO interaction. Eight basis functions φ_l with $\boldsymbol{k} = 0$, corresponding to the s- and p-states (table 2), are taken as the basis in the $\boldsymbol{kp}$ method (Luttinger and Kohn 1955). The choice is made in such a manner that φ_1 and φ_2 are transformed over the $D_{1/2}$ rotation group representation and correspond to the conduction band, the functions φ_3–φ_6 are transformed over the $D_{3/2}$ representation (valence band) and φ_7 and φ_8 are transformed over the $D_{1/2}$ representation (spin split-off band). Interaction of these terms is taken into account exactly via matrix elements $\langle\varphi_{l'}|\boldsymbol{kp}|\varphi_l\rangle$. As a result, we obtain the 8×8 EMA Hamiltonian which should be treated as the zero approximation Hamiltonian $\mathscr{H}_0$. It involves diagonal terms and nondiagonal terms Pk_j (the terms $\hbar\boldsymbol{k}^2/2m_0$ on the diagonal

Table 2
Kane Hamiltonian (simplified)

0	0	$-P\hat{k}_+$	$\sqrt{2/3}P\hat{k}_z$	$\frac{P}{\sqrt{3}}\hat{k}_-$	0	$\frac{P}{\sqrt{3}}\hat{k}_z$	$\sqrt{2/3}P\hat{k}_-$	$\varphi_1 = -\mathrm{is}\uparrow$	$C_1\psi_{m-1/2}$
0	0	0	$-\frac{P}{\sqrt{3}}\hat{k}_+$	$\sqrt{2/3}P\hat{k}_z$	$P\hat{k}_-$	$\sqrt{2/3}P\hat{k}_+$	$-\frac{P}{\sqrt{3}}\hat{k}_z$	$\varphi_2 = -\mathrm{is}\downarrow$	$C_2\psi_{m+1/2}$
$-P\hat{k}_+^+$	0	$-E_G$	$\frac{C}{\sqrt{2}}\hat{k}_+$	$-C\hat{k}_z$	$\sqrt{3/2}C\hat{k}_-$	0	0	$\varphi_3 = -\frac{1}{\sqrt{2}}(x+\mathrm{i}y)\uparrow$	$C_3\psi_{m-3/2}$
$\sqrt{2/3}P\hat{k}_z^+$	$-\frac{P}{\sqrt{3}}\hat{k}_+^+$	$\frac{C}{\sqrt{2}}\hat{k}_-$	$-E_G$	$-\sqrt{3/2}C\hat{k}_+$	$C\hat{k}_z$	0	0	$\varphi_4 = \sqrt{2/3}z\uparrow - \frac{1}{\sqrt{6}}(x+\mathrm{i}y)\downarrow$	$C_4\psi_{m-1/2}$
$\frac{P}{\sqrt{3}}\hat{k}_-^+$	$\sqrt{2/3}P\hat{k}_z^+$	$-C\hat{k}_z$	$-\sqrt{3/2}C\hat{k}_-$	$-E_G$	$\frac{C}{\sqrt{2}}\hat{k}_+$	0	0	$\varphi_5 = \frac{1}{\sqrt{6}}(x-\mathrm{i}y)\uparrow + \sqrt{2/3}z\downarrow$	$C_5\psi_{m+1/2}$
0	$P\hat{k}_-^+$	$\sqrt{3/2}C\hat{k}_+$	$C\hat{k}_z$	$\frac{C}{\sqrt{2}}\hat{k}_-$	$-E_G$	0	0	$\varphi_6 = \frac{1}{\sqrt{2}}(x-\mathrm{i}y)\downarrow$	$C_6\psi_{m+3/2}$
$\frac{P}{\sqrt{3}}\hat{k}_z^+$	$\sqrt{2/3}P\hat{k}_-^+$	0	0	0	0	$-E_G-\Delta$	0	$\varphi_7 = \frac{1}{\sqrt{3}}[z\uparrow + (x+\mathrm{i}y)\downarrow]$	$C_7\psi_{m-1/2}$
$\sqrt{2/3}P\hat{k}_-^+$	$-\frac{P}{\sqrt{3}}\hat{k}_z^+$	0	0	0	0	0	$-E_G-\Delta$	$\varphi_8 = \frac{1}{\sqrt{3}}[(x-\mathrm{i}y)\uparrow - z\downarrow]$	$C_8\psi_{m+1/2}$

The right-hand side of the table gives a simplified notation of the Kane 8 × 8 Hamiltonian. The bottom of the conduction band is chosen as the origin for the energy. E_G is the width of the forbidden band, and Δ is the SO splitting. The second column on the right-hand side gives the basis functions φ_i. The extreme right-hand side column gives the components of the wave function Ψ_m of the spherically symmetric part of the EMA Hamiltonian. In the A′ system m plays the role of AQM, and the ψ functions depend exclusively on the azimuthal angle, whereas the factors C depend on other variables. The following designations are used: $\hat{k} = \hat{k}_j + \mathrm{i}(G/P)(\hat{k}_{j'}k_{j''} + \hat{k}_{j''}k_{j'}) + \mathrm{i}(C_2/P)\varepsilon_{j'j''}$ (j, j' and j'' constitute a cyclic permutation), $\hat{k}_\pm = (\hat{k}_x \pm \mathrm{i}\hat{k}_y)/\sqrt{2}$ for the Cartesian $\hat{k}_j$, $\hat{k}_j$ and circular $\hat{k}_\alpha$, $\hat{k}_\alpha$ coordinates in the A system.

are dropped as irrelevant). The Hamiltonian $\mathscr{H}_0$ is spherically symmetric (see below). It makes it possible to express via the parameter P the value of m^* for electrons on the bottom of the band and the dependence $m^*(\mathscr{E})$ (Kane 1957)

$$\frac{1}{m^*(\mathscr{E})} = \frac{2}{\hbar^2} \frac{2\Delta + 3(E_G + \mathscr{E})}{3(E_G + \mathscr{E})(E_G + \Delta + \mathscr{E})} P^2. \tag{B.1}$$

A similar formula is easily derived for light holes. And if one introduces the field $\boldsymbol{H}$ by means of the replacement $\boldsymbol{k} \to \hat{\boldsymbol{k}}$, one gets an expression for the g-factor of electrons (Roth et al. 1959):

$$g(\mathscr{E}) = -\frac{4m_0}{\hbar^2} \frac{\Delta}{3(E_G + \mathscr{E})(E_G + \Delta + \mathscr{E})} P^2. \tag{B.2}$$

Here the contribution $g = 2$, corresponding to a free electron in a vacuum, is omitted. Since P has an atomic order of magnitude $P = 10\,\text{eV Å} \sim 1$ a.u., in crystals with a narrow forbidden gap $E_G \sim (0.1\text{–}0.3)\,\text{eV}$ $m^* \ll m_0$ is small and $|g| \gg 1$ is large. It is very important that $m^*(E)$ and $g(E)$ change a good deal on the scale $\mathscr{E} \sim E_G$, the spherical symmetry of the spectra of electrons and light holes being retained with high accuracy in the entire region. This strong dependence of the spectrum on $\mathscr{E}$ is termed nonparabolicity. However heavy holes cannot be described by the Hamiltonian $\mathscr{H}_0$: their effective mass in this approximation is infinite. $\mathscr{H}_0$ has the same form for crystals with the inversion centre and for crystals without the inversion centre.

Eigenfunctions of $\mathscr{H}_0$ are characterized by the angular quasimomentum m (section 4). In table 2 Ψ_m is represented as a column: the subscript of the ψ_μ function in each line equals the value AQM, which should be attributed to the respective component of Ψ_m.

The next step is to take into account more distant bands. For this purpose it is necessary to project approximately the total Hamiltonian onto the subspace $\{\varphi_1\}$. In the Luttinger–Kohn formalism such a projection is performed as a unitary transformation. As a result, new terms emerge in the 8×8 Hamiltonian. Most of them do not possess spherical symmetry and among them there are higher order terms in k compared to $\mathscr{H}_0$. In particular, there are terms which render the mass of heavy holes finite and are responsible for band warping, reducing their band symmetry from spherical to cubic. Among them there are terms which enter into the Hamiltonian of a crystal irrespective of whether or not the crystal possesses inversion symmetry. We shall denote them as $\mathscr{H}_w$; it is these terms that are mainly responsible for the warping of heavy hole bands (this is a 'quasi-Ge' spectrum). Alongside these terms, there are also $\mathscr{H}_{as}$ arising due to inversion asymmetry which are specific for crystals of the $A_{III}B_V$-type. The most complete form of the Kane Hamiltonian studied so far is that written out by Weiler et al. (1978). Table 2 includes only two types of such inversion asymmetric terms, namely, those which play a major role in COR (Rashba and Sheka 1961b, Cardona et al. 1986a, 1987). First, there are the k-linear terms,

contained in the central 4×4 square and determined by the invariant (Pidgeon and Groves 1969):

$$\mathscr{H}_C = -\frac{2}{\sqrt{3}} C(\boldsymbol{\kappa}(\hat{\boldsymbol{J}})\boldsymbol{k}), \qquad \kappa_i(\hat{\boldsymbol{J}}) = \hat{J}_{i'}\hat{J}_i\hat{J}_{i'} - \hat{J}_{i''}\hat{J}_i\hat{J}_{i''}, \tag{B.3}$$

here $\hat{J}_i$ are matrices of the $J = 3/2$ angular momentum. They may prove to be important for COR in the valence band for low carrier concentrations. Secondly, there are the k-quadratic terms, entering in the Hamiltonian with the constant G. This constant is nonrelativistic, and therefore the corresponding terms are not small. The constant δ_3, which determines the COR intensity in the conduction band, is expressed via G (Rashba and Sheka 1961b):

$$\delta_3 = -4GP\Delta/3E_G(E_G + \Delta). \tag{B.4}$$

As a rule, $\mathscr{H}_{as}$ makes a relatively small contribution to the shape of the bands.

From the viewpoint of this article, the terms $\mathscr{H}_w$ and $\mathscr{H}_{as}$ are important because at $\boldsymbol{H} \neq 0$ they allow a lot of transitions which are forbidden for the Hamiltonian $\mathscr{H}_0$. These are CR harmonics, spin-flip transitions and CFR. For the latter two groups of transitions (i.e., spin transitions) $\mathscr{H}_{as}$ is of major importance.

Here we shall make use of the explicit form of the two terms of the Hamiltonian $\mathscr{H}_{as}$ (shown in table 2) to illustrate the general property of matrix elements dealt with in section 4. This property is that the operator $\mathscr{H}' = \mathscr{H}_w + \mathscr{H}_{as}$, breaking spherical symmetry, consists of the sum of the operators $\mathscr{H}'_\zeta$ such that their matrix elements obey the relation:

$$\langle \Psi_{m'} | \mathscr{H}'_\zeta | \Psi_m \rangle \propto \mathscr{B}^{(\zeta)}_{m-m'}(\theta, \phi). \tag{B.5}$$

$\mathscr{B}^{(\zeta)}_{m-m'}$ are functions of the angles θ and ϕ, determining the orientation of $\boldsymbol{H}$, universal in the sense that they are independent of the parameters of the Hamiltonian. The quantum numbers m and m' enter in them only as a difference $m - m'$ (Sheka and Zaslavskaya 1969).

Division of $\mathscr{H}'$ into separate terms $\mathscr{H}'_\zeta$, obeying the condition (B.5), is not a trivial task. So, different matrix elements of the same term $\mathscr{H}'_\zeta$ may involve different powers of k, differing from one another even by parity. For instance, in the simplified Kane model given in table 2, all matrix elements responsible for the absence of spherical symmetry (of the type of Ck and Gk^2; the latter being contained in $\hat{k}_j$) form one term $\mathscr{H}'_\zeta = \mathscr{H}_{as}$. One of the methods, which may be recommended for dividing $\mathscr{H}'$ into separate terms $\mathscr{H}'_\zeta$, is to project $\mathscr{H}'$ onto the 2×2 subspace corresponding to the conduction band. Then all invariants entering in $\mathscr{H}'$, which in projection will generate equivalent terms in the 2×2 Hamiltonian, should be included in one $\mathscr{H}'_\zeta$. This procedure simultaneously allows us to establish the correlation between each $\mathscr{H}'_\zeta$ and the appropriate term of (4.9) and thus to find the value of the superscript l, corresponding to $\mathscr{H}'_\zeta$. In our case $\zeta = l = 3$, which ensues from formulas (6.1), (6.2) and (B.4) as well as

from the generalization of (B.4) if the contribution from the invariant $\mathscr{H}_C$ (B.3) is incorporated (Rashba and Sheka 1961b). Similarly, of the terms of the order k^2 one can single out the invariant $\mathscr{H}_w$, corresponding to the valence band warping (table 2 does not contain it). In projecting onto the 2×2 conduction band subspace (Ogg 1966) it becomes evident that in this case $\zeta = l = 4$; angular diagrams were found by Sheka and Zaslavskaya (1969). The analysis of the resultant 2×2 Hamiltonians and evaluation of the indicatrices are performed as in the situations considered in sections 5 and 6 of this chapter.

The basis $\{\varphi_l\}$ is a joint basis for the three bands, which is why the functions φ_l are transformed over the $D = D_{1/2} + D_{3/2} + D_{1/2}$ representation. Accordingly, the matrix $\boldsymbol{S}$, transforming $\mathscr{H}$ from A to A′, equals

$$\boldsymbol{S}(\theta, \phi) = \begin{Vmatrix} \boldsymbol{S}_{1/2}(\theta, \phi) & 0 & 0 \\ 0 & \boldsymbol{S}_{3/2}(\theta, \phi) & 0 \\ 0 & 0 & \boldsymbol{S}_{1/2}(\theta, \phi) \end{Vmatrix}. \tag{B.6}$$

At the transformation $\mathscr{H} \Rightarrow \boldsymbol{S}\mathscr{H}\boldsymbol{S}^{-1}$, the matrix elements, proportional to the components of $P\hat{\boldsymbol{k}}$, are transformed as

$$P\hat{k}_j \Rightarrow P(\boldsymbol{B}^+ \boldsymbol{k})_\alpha = P\hat{K}_\alpha. \tag{B.7}$$

The origin of the $\boldsymbol{B}^+$ matrix in (B.7) can be understood if we transform $(\hat{\boldsymbol{J}}\hat{\boldsymbol{k}})$ using (A.7): $(\hat{\boldsymbol{J}}\hat{\boldsymbol{k}}) \Rightarrow (\boldsymbol{B}\hat{\boldsymbol{J}}, \hat{\boldsymbol{k}}) = (\hat{\boldsymbol{J}}, \boldsymbol{B}^+\hat{\boldsymbol{k}})$. To get the ultimate result one must bear in mind that $\hat{\boldsymbol{k}} = \boldsymbol{B}\hat{\boldsymbol{K}}$ (cf. (A.4)) and also the unitarity of $\boldsymbol{B}$. The relation (B.7) ensures the spherical symmetry of $\mathscr{H}_0$:

$$\mathscr{H}_0(\hat{\boldsymbol{k}}) = \boldsymbol{S}^{-1}\mathscr{H}_0(\boldsymbol{B}^{-1}\hat{\boldsymbol{k}})\boldsymbol{S} = \boldsymbol{S}^{-1}\mathscr{H}_0(\hat{\boldsymbol{K}})\boldsymbol{S}. \tag{B.8}$$

The terms of the $\hat{k}_i\hat{k}_j$-type in $\mathscr{H}'$, proportional to G, after the transformation $\boldsymbol{S}$ and the switchover to $\hat{K}_\alpha\hat{K}_\beta$ acquire the coefficients proportional to the products of three elements of the $\boldsymbol{B}$ matrix: one element comes from the $\boldsymbol{B}^+$ matrix similarly to (B.7) and two elements appear at the switchover from $\hat{k}$ to $\hat{K}$. These products are grouped into coefficients of the $B_{(\alpha\beta\gamma)}$-type entering in (6.10). The simplest way to find them is to expand the products $\hat{K}_\alpha\hat{K}_\beta$ in the operators

$$\mathscr{A}_{\pm 2} = K_\pm^2, \quad \mathscr{A}_{\pm 1} = \{\hat{K}_0, \hat{K}_\pm\}, \qquad \mathscr{A}_0 = \{\hat{K}_+, \hat{K}_-\} - 2\hat{K}_0^2. \tag{B.9}$$

The curly brackets $\{\ldots\}$ mark an anticommutator. In terms of these operators it is convenient to write, analogously to (B.7), the transformation of the terms of the operator $\mathscr{H}'$ involving $\hat{k}_j$ (table 2):

$$\hat{k}_j \Rightarrow \hat{\mathscr{K}}_\alpha = k_\alpha + (G/P) \sum_{\beta=-2}^{2} b_{\alpha\beta} B_{\alpha-\beta} \mathscr{A}_\beta. \tag{B.10}$$

Here $b_{0,\pm 1} = -2$, whereas $b_{\alpha\beta} = 1$ in the other cases. The functions $\mathscr{B}_\alpha(\theta, \phi)$ equal

$$\mathscr{B}_0 = -\mathrm{i}\tfrac{3}{4} \sin 2\phi \sin\theta \sin 2\theta, \tag{B.11}$$

$$\mathscr{B}_1 = -\mathrm{i}2^{-3/2}[\cos 2\phi \sin 2\theta - \mathrm{i} \sin 2\phi \sin\theta(2\cos^2\theta - \sin^2\theta)], \tag{B.12}$$

$$\mathscr{B}_2 = \cos 2\phi \cos 2\theta - \mathrm{i}\tfrac{1}{2} \sin 2\phi \cos\theta(2\cos^2\theta - \sin^2\theta), \tag{B.13}$$

$$\mathscr{B}_3 = 3 \times 2^{-3/2}[\sin 2\phi \sin\theta(1 + \cos^2\theta) + \mathrm{i} \cos 2\phi \sin 2\theta], \tag{B.14}$$

$$\mathscr{B}_{-\alpha} = -\mathscr{B}_\alpha^*. \tag{B.15}$$

If we employ the explicit form of the coefficients $B_{(\alpha\beta\gamma)}$, found by Rashba and Sheka (1961a), it is easy to verify that*

$$\mathscr{B}_0 = -B_{(\bar{1}11)}, \quad \mathscr{B}_1 = -\tfrac{1}{3}B_{(000)}, \quad \mathscr{B}_2 = B_{(\bar{1}00)}, \quad \mathscr{B}_3 = 2B_{(\bar{1}\bar{1}0)}. \tag{B.16}$$

At the transformation $\mathrm{A} \to \mathrm{A}'$, matrix elements of the operator $\mathscr{H}_C$ (B.3) acquire coefficients, including products of four elements of the $\boldsymbol{B}$ matrix: three of them stem from transformation of the matrices $\boldsymbol{\kappa}(\hat{\boldsymbol{J}})$ in quite a similar way as in (B.7), and one stems from the switchover to $\hat{K}$. By means of (A.6) and (B.16) they reduce to $B_{(\alpha\beta\gamma)}$ and $\mathscr{B}_\alpha$. The explicit form of matrix elements of $\mathscr{H}_C$ in the A′ system is:

$$\begin{aligned}
&\mathscr{H}_{33} = -(3^{1/2}/2)C(\mathscr{B}_{\bar{1}}\hat{K}_1 - \mathscr{B}_1\hat{K}_{\bar{1}}), \qquad H_{44} = -H_{55} = 3H_{66} = -3H_{33},\\
&\mathscr{H}_{34} = 2^{-1/2}C(\mathscr{B}_{\bar{2}}\hat{K}_1 + \mathscr{B}_{\bar{1}}\hat{K}_0 - 2\mathscr{B}_0\hat{K}_{\bar{1}}), \qquad H_{56} = H_{34},\\
&\mathscr{H}_{35} = \tfrac{1}{2}C(\mathscr{B}_{\bar{3}}\hat{K}_1 - 2\mathscr{B}_{\bar{2}}\hat{K}_0 - 5\mathscr{B}_{\bar{1}}\hat{K}_{\bar{1}}), \qquad H_{46} = -H_{35},\\
&\mathscr{H}_{36} = (3/2)^{1/2}C(-\mathscr{B}_{\bar{3}}\hat{K}_0 + \mathscr{B}_{\bar{2}}\hat{K}_{\bar{1}}),\\
&\mathscr{H}_{ij} = (\mathscr{H}^+)_{ji}.
\end{aligned} \tag{B.17}$$

Now we have come to the key point in the verification of (B.5). So it is necessary to consider the action of the operators $\mathscr{A}_\alpha$ upon separate components of the Ψ_m functions, treated in terms of the perturbation theory over $\mathscr{H}'$ as eigenfunctions of the spherically symmetric Hamiltonian $\mathscr{H}_0$. Let us take two examples.

If $\mathscr{H}_0$ is a Hamiltonian of a free electron in the field $\boldsymbol{H}$, then the lines of Ψ_m are eigenfunctions of the Landau oscillator (using the Landau gauge). The values of N in different lines correlate with each other in the way shown in table 2. They differ from m by a half-integer, so in this case AQM with an accuracy of up to a half-integer has the meaning of the Landau quantum number. The operators $\mathscr{A}_\alpha$ and $\hat{K}_\alpha$ transform ψ_N with an accuracy up to a numerical factor as

$$\mathscr{A}_\alpha\psi_N \Rightarrow \psi_{N+\alpha}, \qquad \hat{K}_\alpha\psi_N \Rightarrow \psi_{N+\alpha}, \tag{B.18}$$

*Note that in the paper by Rashba and Sheka (1961a) the subscripts (123) correspond to the subscripts ($\bar{1}10$) in this review.

i.e., they act as the step-up and step-down operators. Now we can explicitly calculate the action of $\mathscr{H}'$ on an arbitrary eigenvector $\Psi_m^{(t)}$: at a given m the index $t = 1 \ldots 8$. Application of table 2 and of formulas (B.10), (B.17) and (B.18) yields

$$\mathscr{H}' \Psi_m^{(t)} = \sum_{\alpha=-3}^{3} \sum_{t'} \Gamma_{mtt'}^{(\alpha)} \mathscr{B}_{-\alpha}(\theta, \phi) \Psi_{m+\alpha}^{(t')}. \tag{B.19}$$

The numerical coefficients $\Gamma_{mtt'}^{(\alpha)}$ are θ- and ϕ-independent due to the spherical symmetry of $\mathscr{H}_0$. Since ψ_N with different N are orthogonal, it follows from (B.19) that (B.5) is fulfilled, irrespective of the values of the indices t.

The second example concerns a spherically symmetric impurity centre in the field $\boldsymbol{H}$ (Sheka and Zaslavskaya 1969). In this case, it is handy to employ the axially symmetric gauge in order to use the axial symmetry inherent in the problem. In this case m can be defined as a genuine angular momentum (section 4). Singling out the azimuthal angle φ one can represent the lth component of the $\Psi_m^{(t)}$ function as

$$\psi_{mt,l}(r, \vartheta, \varphi) = \chi_{mt,l}(r, \vartheta) \exp(\mathrm{i}\mu_{ml}\varphi) \tag{B.20}$$

where (r, ϑ, φ) are polar coordinates in the A′ system. The action of the operators $\mathscr{A}_\alpha$ and $\hat{K}_\alpha$ upon $\psi_{mt,l}$ reduces, similarly to (B.19), to the replacement

$$\mu_{ml} \Rightarrow \mu_{ml} + \alpha \tag{B.21}$$

and to a complicated modification of the form of the $\chi_{mt,l}$ functions; the details of this modification are irrelevant. Acting in the same way as at the derivation of (B.19), we arrive at

$$\mathscr{H}' \Psi_m^{(t)} = \sum_{\alpha=-3}^{3} \mathscr{B}_{-\alpha}(\theta, \phi) \bar{\Psi}_{m+\alpha}^{(t)}. \tag{B.22}$$

This formula can be checked by inspection. It is important that all components of the $\Psi_{m+\alpha}^{(t)}$ function contain φ only via the exponential factor, in a similar way to (B.20). Yet, μ_{ml} is replaced in it by $\mu_{ml} + \alpha$ in accordance with (B.21). The explicit form of the r-, ϑ-dependent factor does not affect the result. It is of importance only in that, by virtue of the spherical symmetry of the problem, this factor does not depend on θ and ϕ. Therefore from (B.22) the result (B.5) ensues. To get this result, it suffices to use the orthogonality condition at integration over φ in each line.

At the derivation of (B.19) and (B.22), the C- and G-proportional terms in $\mathscr{H}_{as}$ have been used above (table 2). However, verification shows that these formulas are satisfied if all the terms included in the Kane Hamiltonian by Weiler et al. (1978) are taken into account in $\mathscr{H}_{as}$. That is why the result (B.5) is largely general. However, it holds only if lower-order EMA terms, inducing certain transitions, are taken into account. For instance, if we consider, alongside the invariant (B.3), the invariant $\sum_i \kappa_i(\hat{J}) \hat{k}_i^3$, this gives rise to the appearance of a new angular dependence but the respective terms will have small numerical

coefficients. It appears that the most important distortions of angular dependences, determined by the functions $\mathscr{B}_\alpha$, occur for holes due to the term $\mathscr{H}_w$.

In the above, the matrix elements of $\mathscr{H}'$ have been calculated. However, the probability of transitions is determined by the velocity operator $\boldsymbol{v}$. If we work in the A' system, matrix elements of the operator $(V_{so})_\tau = i[\mathscr{H}', R_\tau]/\hbar$ (section 4) differ from (B.5) only by a change in the subscript of the difference $(m - m') \Rightarrow (m - m' + \tau)$. The same result is obtained if we calculate total V_τ according to formula (3.8). Note here that in the Kane model the operator $\hat{\boldsymbol{R}}$ must be different from $\boldsymbol{R}\hat{I}$ ($\hat{I}$ is a unit 8×8 matrix) due to the corrections resulting from the Luttinger–Kane procedure (Luttinger and Kohn 1955) and caused by the influence of more distant bands (analogous to $\boldsymbol{r}_{so}$ in (3.8b)). Verification shows that these corrections to the velocity have the same symmetry as the terms originating from $\mathscr{H}'$, and that these corrections are small.

To summarize, one could write down formulas for the coordinate $\boldsymbol{R}$ and the velocity $\boldsymbol{V}$, analogously to (B.19) and (B.22); so, an analogue of (B.22) for the velocity has the form

$$V_\tau \Psi_m = \sum_{\alpha=-3}^{3} \mathscr{B}_{-\alpha}(\theta, \phi) \bar{\bar{\Psi}}_{m+\alpha+\tau}. \tag{B.23}$$

List of abbreviations

CR	cyclotron resonance	CRI	cyclotron-resonance inactive
SR	spin resonance	EMA	effective mass approximation
EPR	electron paramagnetic resonance	SO	spin orbit
COR	combined resonance	AQM	angular quasimomentum
EDSR	electric-dipole spin resonance	a.u.	atomic units
CFR	combinational frequency resonance	MOS	metal-oxide-semiconductor
CRA	cyclotron-resonance active		

References

Abrikosov, A.A., and L.A. Fal'kovskii, 1962, Zh. Eksp. Teor. Fiz. **43**, 1089 (Sov. Phys-JETP **16**, 769).

Appold, G., H. Pascher, R. Ebert, U. Steigenbergen and M. von Ortenberg, 1978, Phys. Status Solidi B **86**, 557.

Aronov, A.G., G.E. Pikus and A.N. Titkov, 1983, Zh. Eksp. Teor. Fiz. **84**, 1170 (Sov. Phys-JETP **57**, 680).

Babich, V.M., N.P. Baran, A.A. Bugaj, A.A. Konchitz and B.D. Shanina, 1988, Zh. Eksp. Teor. Fiz. **94**, 319 (Sov. Phys.-JETP **67**, 1697).

Balkanski, M., and J. Cloizeaux, 1960, J. Phys. et Radium **21**, 825.

Bangert, E., 1981, L. N. Phys. (Springer-Verlag, Berlin) **152**, 216.

Bell, R.L., 1962, Phys. Rev. Lett. **9**, 52.

Bell, R.L., and K.T. Rogers, 1966, Phys. Rev. **152**, 746.
Bir, G.L., and G.E. Pikus, 1959, Fiz. Tverd. Tela **1**, 1642.
Bir, G.L., and G.E. Pikus, 1961, Fiz. Tverd. Tela **3**, 3050 (1962, Sov. Phys.-Solid State **3**, 2221).
Bir, G.L., and G.E. Pikus, 1972, Symmetry and Strain-Induced Effects in Semiconductors (Nauka, Moscow, English translated, 1974, Halsted Press, New York).
Bir, G.L., E.I. Butikov and G.E. Pikus, 1963, J. Phys. Chem. Solids **24**, 1475.
Bloembergen, N., 1961, Sci. **133**, 1363.
Blount, E.I., 1962, Solid State Phys., eds F. Seitz and D. Turnbull (Academic Press, New York) **13**, 305.
Bodnar, J., 1978, in: Phys. Narrow-Gap Semicond., eds J. Rauluszkiewicz, M. Gorska and E. Kaczmarek (Elsevier, Amsterdam; PWN, Warsaw) p. 311.
Boiko, I.I., 1962, Fiz. Tverd. Tela **4**, 2128 (Sov. Phys.-Solid State **4**, 1558).
Boiko, I.I., 1964, Ukr. Fiz. Zh. **9**, 1256.
Bowers, R., and Y. Yafet, 1959, Phys. Rev. **115**, 1165.
Braun, M., and U. Rössler, 1985, J. Phys. C: Solid State Phys. **18**, 3365.
Brueck, S.R.J., and A. Mooradian, 1973, Opt. Commun. **8**, 263.
Burgiel, J.C., and L.C. Hebel, 1965, Phys. Rev. A **140**, 925.
Bychkov, Yu.A., and E.I. Rashba, 1984, Pis'ma Zh. Eksp. Teor. Fiz. **39**, 66 (Sov. Phys.-JETP Lett. **39**, 78).
Bychkov, Yu.A., and E.I. Rashba, 1985, in: Proc. 17th Int. Conf. Phys. Semicond., San Francisco, 1984, eds J.D. Chadi and W.A. Harrison (Springer-Verlag, New York) p. 321.
Cardona, M., N.E. Christensen and G. Fasol, 1986a, Phys. Rev. Lett. **56**, 2831.
Cardona, M., N.E. Christensen, M. Dobrowolska, J.K. Furdyna and S. Rodriguez, 1986b, Solid State Commun. **60**, 17.
Cardona, M., N.E. Christensen and G. Fasol, 1987, in: Proc. 18th Int. Conf. Phys. Semicond., Stockholm, 1986, p. 1133.
Casella, R.C., 1960, Phys. Rev. Lett. **5**, 371.
Chen, Y.-F., M. Dobrowolska and J.K. Furdyna, 1985a, Phys. Rev. B **31**, 7989.
Chen, Y.-F., M. Dobrowolska, J.K. Furdyna and S. Rodriguez, 1985b, Phys. Rev. B **32**, 890.
Cohen, M.H., and E.I. Blount, 1960, Philos. Mag. **5**, 115.
Curie, P., 1894, J. Phys., 3 serie **3**, 393.
Därr, A., J.P. Kotthaus and T. Ando, 1976, in: Proc. 13th Int. Conf. Phys. Semicond., Rome, 1976, ed. F.G. Fumi (Marves, Rome) p. 774.
Das, B., D.C. Miller, S. Datta, R. Reifenberger, W.P. Hong, P.K. Bhattacharya, J. Singh and M. Jaffe, 1989, Phys. Rev. B **39**, 1411.
Dickey, D.H., and D.M. Larsen, 1968, Phys. Rev. Lett. **20**, 65.
Dietl, T., 1983, J. Magn. Magn. Mater. **38**, 34.
Dobers, M., K. von Klitzing and G. Weimann, 1988, Phys. Rev. B **38**, 5453.
Dobrowolska, M., H.D. Drew, J.K. Furdyna, T. Ichiguchi, A. Witowski and P.A. Wolff, 1982, Phys. Rev. Lett. **49**, 845.
Dobrowolska, M., Y. Chen, J.K. Furdyna and S. Rodriguez, 1983, Phys. Rev. Lett. **51**, 134.
Dobrowolska, M., A. Witowski, J.K. Furdyna, T. Ichiguchi, H.D. Drew and P.A. Wolff, 1984, Phys. Rev. B **29**, 6652.
Dorozhkin, S.I., and E.B. Ol'shanetskii, 1987, Pis'ma Zh. Eksp. Teor. Fiz. **46**, 399 (Sov. Phys.-JETP Lett. **46**, 000).
Edelstein, V.M., 1983, Solid State Commun. **45**, 515.
Elliott, R.J., 1954, Phys. Rev. **96**, 280.
Erhardt, W., W. Staghuhn, P. Byszewski, M. von Ortenberg, G. Landwehr, G. Weimann, L. van Bockstal, P. Janssen, F. Herlach and J. Witters, 1986, Surf. Sci. **170**, 581.
Fantner, E.J., H. Pascher, G. Bauer, R. Danzer and A. Lopez-Otero, 1980, J. Phys. Soc. Jpn. **49**, Suppl. A, 741.
Gatos, H.C., and M.C. Levine, 1960, J. Phys. Chem. Solids **14**, 169.

Gershenzon, E.M., N.M. Pevin and M.S. Fogel'son, 1970, Pis'ma Zh. Eksp. Teor. Fiz. **12**, 201 (Sov. Phys.-JETP Lett. **12**, 139).
Gershenzon, E.M., N.M. Pevin, I.T. Semenov and M.S. Fogel'son, 1976, Fiz. Tekh. Polupr. **10**, 175 (Sov. Phys.-Semicond. **10**, 104).
Glinchuk, M.D., V.G. Grachev, M.F. Deigen, A.B. Roitsin and L.A. Suslin, 1981, Electric Effects in Radiospectroscopy (in Russian), Nauka, Moscow.
Golin, S., 1968, Phys. Rev. **166**, 643.
Golubev, V.G., and V.I. Ivanov-Omskii, 1977, Pis'ma Zh. Tekh. Fiz. **3**, 1212 (Sov. Tech. Phys. Lett. **3**, 501).
Gopalan, S., J.K. Furdyna and S. Rodriguez, 1985, Phys. Rev. B **32**, 903.
Gopalan, S., S. Rodriguez, J. Mycielski, A. Witowski, M. Grynberg and A. Wittlin, 1986, Phys. Rev. B **34**, 5466.
Grisar, R., H. Wachernig, G. Bauer, S. Hayashi, E. Amzallag, J. Wlasak and W. Zawadzki, 1976, in: Proc. 13th Int. Conf. Phys. Semicond., Rome, 1976, ed. F.G. Fumi (Marves, Rome) p. 1265.
Gurgenishvili, G.E., 1963, Fiz. Tverd. Tela **5**, 2070 (Sov. Phys.-Solid State **5**, 1510).
Hensel, J.C., 1968, Phys. Rev. Lett. **21**, 983.
Hermann, C., and C. Weisbuch, 1977, Phys. Rev. B **15**, 823.
Ivchenko, E.L., and A.V. Sel'kin, 1979, Zh. Eksp. Teor. Fiz. **76**, 1837 (Sov. Phys.-JETP **49**, 933).
Jagannath, C., and R.L. Aggarwal, 1985, Phys. Rev. B **32**, 2243.
Johnson, E.J., and D.M. Larsen, 1966, Phys. Rev. Lett. **16**, 655.
Kacman, P., and W. Zawadzki, 1976, Solid State Commun. **18**, 945.
Kalashnikov, V.P., 1974, Teor. Matem. Fiz. **18**, 108.
Kane, E.O., 1957, J. Phys. Chem. Solids **1**, 249.
Kohn, W., 1957, in: Solid State Phys., eds F. Seitz and D. Turnbull (Academic Press, New York) **5**, 257.
Koshelev, A.E., V.Ya. Kravchenko and D.E. Khmel'nitskii, 1988, Fiz. Tverd. Tela **30**, 433.
Kriechbaum, M., R. Meisels, F. Kuchar and E. Fantner, 1983, in: Proc. 16th Int. Conf. Phys. Semicond., Montpellier, 1982, ed. M. Averous (North-Holland, Amsterdam) p. 444.
Kuchar, F., R. Meisels, R.A. Stradling and S.P. Najda, 1984, Solid State Commun. **52**, 487.
Kveder, V.V., Yu.A. Osip'yan and A.I. Shalynin, 1984, Pis'ma Zh. Eksp. Teor. Fiz. **40**, 10 (Sov. Phys.-JETP Lett. **40**, 729).
Kveder, V.V., V.Ya. Kravchenko, T.R. Mchedlidze, Yu.A. Osip'yan, D.E. Khmel'nitskii and A.I. Shalynin, 1986, Pis'ma Zh. Eksp. Teor. Fiz. **43**, 202 (Sov. Phys.-JETP Lett. **43**, 255).
Kveder, V.V., A.E. Koshelev, T.R. Mchedlidze, Yu.A. Osip'yan and A.I. Shalynin, 1989, Zh. Eksp. Teor. Fiz. **95**, 183 (Sov. Phys.-JETP **68**, 104).
La Rocca, G.C., N. Kim and S. Rodriguez, 1988a, Phys. Rev. B **38**, 7595.
La Rocca, G.C., N. Kim and S. Rodriguez, 1988b, Solid State Commun. **67**, 693.
Landau, L.D., and E.M. Lifshitz, 1974, Quantum Mechanics, Nauka (English translated, 3rd edition, Pergamon Press, 1977).
Lax, B., J.G. Mavroides, H.J. Zeiger and R.J. Keyes, 1961, Phys. Rev. **122**, 31.
Leibler, L., 1978, Phys. Status Solidi B **85**, 611.
Lin-Chung, P.J., and B.W. Henvis, 1975, Phys. Rev. B **12**, 630.
Littler, C.L., D.G. Seiler, R. Kaplan and R.J. Wagner, 1983, Phys. Rev. B **27**, 7473.
Lommer, G., F. Malcher and U. Rössler, 1985, Phys. Rev. B **32**, 6965.
Ludwig, G.W., and F.S. Ham, 1962, Phys. Rev. Lett. **8**, 210.
Luo, J., H. Munekata, F.F. Fang and P.J. Stiles, 1988, Phys. Rev. B **38**, 10142.
Luttinger, J.M., 1956, Phys. Rev. **102**, 1030.
Luttinger, J.M., and W. Kohn, 1955, Phys. Rev. **97**, 869.
Malcher, F., G. Lommer and U. Rössler, 1986, Superlattices and Microstructures **2**, 267.
McClure, J.W., and K.H. Choi, 1977, Solid State Commun. **21**, 1015.
McCombe, B.D., 1969, Phys. Rev. **181**, 1206.
McCombe, B.D., and R. Kaplan, 1968, Phys. Rev. Lett. **21**, 756.

McCombe, B.D., and R.J. Wagner, 1971, Phys. Rev. B **4**, 1285.
McCombe, B.D., S.G. Bishop and R. Kaplan, 1967, Phys. Rev. Lett. **18**, 748.
McCombe, B.D., R.J. Wagner and G.A. Prinz, 1970a, Solid State Commun. **8**, 1687.
McCombe, B.D., R.J. Wagner and G.A. Prinz, 1970b, Phys. Rev. Lett. **25**, 87.
McCombe, B.D., R.J. Wagner and J.S. Lannin, 1974, in: Proc. 12th Int. Conf. Phys. Semicond., Stuttgart, 1974 (B.G. Teubner, Stuttgart) p. 1176.
Mel'nikov, V.I., and E.I. Rashba, 1971, Zh. Eksp. Teor. Fiz. **61**, 2530 (1972, Sov. Phys.-JETP **34**, 1353).
Merkt, U., M. Horst, T. Evelbauer and J.P. Kotthaus, 1986, Phys. Rev. **34**, 7234.
Mims, W.B., 1976, The Linear Electric Field Effect in Paramagnetic Resonance (Clarendon Press, Oxford).
Nguyen, V.T., and T.J. Bridges, 1972, Phys. Rev. Lett. **29**, 359.
O'Dell, T.H., 1970, The Electrodynamics of Magnetoelectric Media (North-Holland, Amsterdam).
Ogg, N.R., 1966, Proc. Phys. Soc. **89**, 431.
Ohta, K., 1969, Phys. Rev. **184**, 721.
Pascher, H., 1981, L. N. Phys. (Springer-Verlag, Berlin) **152**, 202.
Pastor, K., M. Jaczynski and J.K. Furdyna, 1981, Phys. Rev. B **24**, 7313.
Pekar, S.I., and E.I. Rashba, 1964, Zh. Eksp. Teor. Fiz. **47**, 1927 (1965, Sov. Phys.-JETP **20**, 1295).
Pevtsov, A.B., and A.V. Sel'kin, 1983, Fiz. Tverd. Tela **25**, 157 (Sov. Phys.-Solid State **25**, 85).
Pidgeon, C.R., and R.N. Brown, 1966, Phys. Rev. **146**, 575.
Pidgeon, C.R., and S.H. Groves, 1969, Phys. Rev. **186**, 824.
Ranvaud, R., H.-R. Trebin, U. Rössler and F.H. Pollak, 1979, Phys. Rev. B **20**, 701.
Rashba, E.I., 1960, Fiz. Tv. Tela **2**, 1224 (Sov. Phys.-Solid State **2**, 1109).
Rashba, E.I., 1961, in: Proc. Int. Conf. Phys. Semicond., Prague, 1960 (Publ. House of the Czechosl. Acad. Sci., Prague) p. 45.
Rashba, E.I., 1964a, Usp. Fiz. Nauk **84**, 557 (1965, Sov. Phys.-Usp. **7**, 823).
Rashba, E.I., 1964b, Fiz. Tverd. Tela **6**, 3178 (1965, Sov. Phys.-Solid State **6**, 2538).
Rashba, E.I., 1979, J. Magn. Magn. Mater. **11**, 63.
Rashba, E.I., and V.I. Sheka, 1959, Fiz. Tverd. Tela, selected papers, Vol. 2, 162.
Rashba, E.I., and V.I. Sheka, 1961a, Fiz. Tverd. Tela **3**, 1735 (Sov. Phys.-Solid State **3**, 1257).
Rashba, E.I., and V.I. Sheka, 1961b, Fiz. Tverd. Tela **3**, 1863 (Sov. Phys.-Solid State **3**, 1357).
Rashba, E.I., and V.I. Sheka, 1961c, Fiz. Tverd. Tela **3**, 2369 (Sov. Phys.-Solid State **3**, 1718).
Rashba, E.I., and V.I. Sheka, 1964a, Fiz. Tverd. Tela **6**, 141 (Sov. Phys.-Solid State **6**, 114).
Rashba, E.I., and V.I. Sheka, 1964b, Fiz. Tverd. Tela **6**, 576 (Sov. Phys.-Solid State **6**, 451).
Roitsin, A.B., 1971, Usp. Fiz. Nauk, **105**, 677 (1972, Sov. Phys.-Usp. **14**, 766).
Romestain, R., S. Geschwind and G.E. Devlin, 1977, Phys. Rev. Lett. **39**, 1583.
Rössler, U., 1984, Solid State Commun. **49**, 943.
Roth, L.M., B. Lax and S. Zwerdling, 1959, Phys. Rev. **114**, 90.
Rubo, Yu. G., L.S. Khasan, V.I. Sheka and A.S. Ioselevich, 1988, Pis'ma Zh. Eksp. Teor. Fiz. **48**, 30 (Sov. Phys.-JETP Lett. **48**, 30).
Rubo, Yu.G., L.S. Khasan, V.I. Sheka and E.V. Mozdor, 1989, Zh. Eksp. Teor. Fiz. **95**, 1180 (Sov. Phys.-JETP **68**, 1087).
Schaber, H., and R.E. Doezema, 1979a, Solid State Commun. **31**, 197.
Schaber, H., and R.E. Doezema, 1979b, Phys. Rev. B **20**, 5257.
Seiler, D.G., W.M. Becker and L.M. Roth, 1970, Phys. Rev. B **1**, 764.
Sheka, V.I., 1964, Fiz. Tverd. Tela **6**, 3099 (Sov. Phys.-Solid State **10**, 2470).
Sheka, V.I., and L.S. Khazan, 1985, Pis'ma Zh. Eksp. Teor. Fiz. **41**, 61 (Sov. Phys.-JETP Lett. **41**, 72).
Sheka, V.I., and I.G. Zaslavskaya, 1969, Ukr. Fiz. Zh. **14**, 1825.
Singh, M., and P.R. Wallace, 1983, Physica B **117 & 118**, 441.
Slusher, R.E., C.K.N. Patel and P.A. Fleury, 1967, Phys. Rev. Lett. **18**, 77.
Smith, G.E., J.K. Galt and F.R. Merritt, 1960, Phys. Rev. Lett. **4**, 276.

Stein, D., K. von Klitzing and G. Weimann, 1983, Phys. Rev. Lett. **51**, 130.
Stepniewski, R., 1986, Solid State Commun. **58**, 19.
Stepniewski, R., and M. Grynberg, 1985, Acta Phys. Pol. A **67**, 373.
Störmer, H.L., 1988, Materials of the Soviet-American Seminar: Electronic Properties of two-dimensional systems (Moscow, 1988), unpublished.
Sugihara, K., 1975, J. Phys. Soc. Jpn. **38**, 1061.
Thiclemann, J., M. von Ortenberg, F.A.P. Blom and K. Strobel, 1981, L. N. Phys. (Springer-Verlag, Berlin) **152**, 207.
Trebin, H.-R., U. Rössler and R. Ranvaud, 1979, Phys. Rev. B **20**, 686.
Tuchendler, J., M. Grynberg, Y. Couder, H. Thome and R. Le Toullec, 1973, Phys. Rev. B **8**, 3884.
Verdun, H.R., and H.D. Drew, 1976, Phys. Rev. B **14**, 1370.
Weiler, M.H., 1982, Solid State Commun. **44**, 287.
Weiler, M.H., R.L. Aggarwal and B. Lax, 1978, Phys. Rev. B **17**, 3269.
Wigner, E.P., 1959, Group Theory and its Application to the Quantum Mechanics of Atomic Spectra (Academic Press, New York).
Witowski, A., K. Pastor and J.K. Furdyna, 1982, Phys. Rev. B **26**, 931.
Wlasak, J., 1986, J. Phys. C: Solid State Phys. **19**, 4143.
Wolff, P.A., 1964, J. Phys. Chem. Solids **25**, 1057.
Yafet, Y., 1963, in: Solid State Phys., eds F. Seitz and D. Turnbull (Academic Press, New York) **14**, 1.
Yafet, Y., 1966, Phys. Rev. **152**, 858.
Zavoisky, E.K., 1945, J. Phys. USSR **9**, 245.
Zawadzki, W., and J. Wlasak, 1976, J. Phys. C: Solid State Phys. **9**, L663.
Zawadzki, W., P. Pfeffer and H. Sigg, 1985, Solid State Commun. **53**, 777.